

In the IOCCG Report Series:

1. *Minimum Requirements for an Operational Ocean-Colour Sensor for the Open Ocean (1998).*
2. *Status and Plans for Satellite Ocean-Colour Missions: Considerations for Complementary Missions (1999).*
3. *Remote Sensing of Ocean Colour in Coastal, and Other Optically-Complex, Waters (2000).*
4. *Guide to the Creation and Use of Ocean-Colour, Level-3, Binned Data Products (2004).*
5. *Remote Sensing of Inherent Optical Properties: Fundamentals, Tests of Algorithms, and Applications (2006).*
6. *Ocean-Colour Data Merging (2007).*
7. *Why Ocean Colour? The Societal Benefits of Ocean-Colour Technology (2008).*
8. *Remote Sensing in Fisheries and Aquaculture (2009).*
9. *Partition of the Ocean into Ecological Provinces: Role of Ocean-Colour Radiometry (2009).*
10. *Atmospheric Correction for Remotely-Sensed Ocean-Colour Products (2010).*
11. *Bio-Optical Sensors on Argo Floats (this volume).*

The printing of this report was sponsored and carried out by the Joint Research Centre (JRC), European Commission, which is gratefully acknowledged.

# Reports and Monographs of the International Ocean-Colour Coordinating Group

An Affiliated Program of the Scientific Committee on Oceanic Research (SCOR)  
An Associated Member of the Committee on Earth Observation Satellites (CEOS)

IOCCG Report Number 11, 2011

## Bio-Optical Sensors on Argo Floats

Edited by:

Hervé Claustre, Laboratoire d'Océanographie de Villefranche, Villefranche-sur-mer, France)

Report of an IOCCG working group on Bio-optical Sensors on Argo Floats, chaired by Hervé Claustre, and based on contributions from (in alphabetical order):

Stewart Bernard	CSIR - NRE, South Africa
Jean-François Berthon	Joint Research Centre - European Commission
Jim Bishop	Lawrence Berkeley National Laboratory, USA
Emmanuel Boss	University of Maine, USA
Hervé Claustre	Laboratoire d'Océanographie de Villefranche, France
Christine Coatanoan	Coriolis Data Center, France
Fabrizio D'Ortenzio	Laboratoire d'Océanographie de Villefranche, France
Ken Johnson	Monterey Bay Aquarium Research Institute, USA
Aneesh Lotliker	INCOIS, India
Oswaldo Ulloa	Universidad de Concepción, Chile

Series Editor: Venetia Stuart

Correct citation for this publication:

*IOCCG (2011). Bio-Optical Sensors on Argo Floats. Claustre, H. (ed.), Reports of the International Ocean-Colour Coordinating Group, No. 11, IOCCG, Dartmouth, Canada.*

The International Ocean-Colour Coordinating Group (IOCCG) is an international group of experts in the field of satellite ocean colour, acting as a liaison and communication channel between users, managers and agencies in the ocean-colour arena.

The IOCCG is sponsored by the Canadian Space Agency (CSA), Centre National d'Etudes Spatiales (CNES, France), Department of Fisheries and Oceans (Bedford Institute of Oceanography, Canada), European Space Agency (ESA), National Institute for Space Research (INPE, Brazil), Indian Space Research Organisation (ISRO), Japan Aerospace Exploration Agency (JAXA), Joint Research Centre (JRC, EC), Korea Ocean Research and Development Institute (KORDI), National Aeronautics and Space Administration (NASA, USA), National Centre for Earth Observation (NCEO, UK), National Oceanic and Atmospheric Administration (NOAA, USA), and Second Institute of Oceanography (SIO), China.

<http://www.ioccg.org>

Published by the International Ocean-Colour Coordinating Group,  
P.O. Box 1006, Dartmouth, Nova Scotia, B2Y 4A2, Canada.

ISSN: 1098-6030

©IOCCG 2011

Printed by the Joint Research Centre (JRC), European Commission

# Contents

---

<b>Executive Summary</b>	<b>1</b>
<b>1 Introduction: The Development of Bio-Optical Profiling Floats in the Context of Remote Sensing</b>	<b>5</b>
1.1 Marine Biogeochemistry Observations Before Bio-Optical Floats . . . . .	5
1.2 Developing Synergies Between Observations by Ocean Remote Sensing and Bio-Optical Floats . . . . .	7
1.3 Mandate of the BIO-Argo Working Group . . . . .	8
<b>2 Scientific Objectives</b>	<b>11</b>
2.1 Validation of Ocean-Colour Radiometric Products and Improvement of Bio-Optical Algorithms . . . . .	11
2.1.1 Ocean-colour radiometry products . . . . .	11
2.1.2 Calibration and validation ("CALVAL") . . . . .	12
2.1.3 Potential advantages of a VAL-float Network . . . . .	13
2.1.4 Refining bio-optical algorithms . . . . .	14
2.2 Implementation of New, Explorative Observational Strategies in Marine Biogeochemistry . . . . .	15
2.2.1 Inter-annual and seasonal changes in biogeochemical properties	15
2.2.2 Resolving events not detected through classical sampling strategies . . . . .	16
2.2.3 The diel scale: an important scale for bio-optical and biogeochemical processes . . . . .	18
2.2.4 Heating rate of the upper ocean . . . . .	18
2.3 Ocean Modelling and Data Assimilation . . . . .	19
<b>3 Key Bio-Optical Properties Amenable to Measurement by Floats</b>	<b>23</b>
3.1 Downward Irradiance, Upwelling Radiance . . . . .	23
3.1.1 Basics . . . . .	23
3.1.2 Derived bio-optical or biogeochemical products . . . . .	24
3.2 Backscattering Coefficient . . . . .	25
3.2.1 Basics . . . . .	25
3.2.2 Derived bio-optical or biogeochemical products . . . . .	26
3.3 Beam Attenuation Coefficient . . . . .	27
3.3.1 Basics . . . . .	27
3.3.2 Derivation of bio-optical or biogeochemical products . . . . .	27
3.4 Chlorophyll-a Fluorescence . . . . .	30

3.4.1	Basics . . . . .	30
3.4.2	Derivation of bio-optical and biogeochemical products . . . . .	31
3.5	Other Measurements . . . . .	33
3.5.1	Birefringent photons . . . . .	33
3.5.2	Coloured dissolved organic material . . . . .	34
3.5.3	Absorption and scattering coefficients . . . . .	36
<b>4</b>	<b>Sensor Requirements</b>	<b>37</b>
4.1	Radiometers . . . . .	37
4.2	Scattering Sensors . . . . .	38
4.2.1	Back-scattering meter . . . . .	38
4.2.2	Turbidity sensor . . . . .	39
4.3	Transmissometers . . . . .	39
4.4	Chla Fluorometers . . . . .	40
4.5	Birefringence Sensors . . . . .	42
4.6	Other Sensors . . . . .	42
4.6.1	Oxygen sensors . . . . .	42
4.6.2	Optical nitrate sensors . . . . .	43
4.6.3	CDOM fluorescence sensors . . . . .	43
<b>5</b>	<b>The Different Types of Floats and Missions</b>	<b>45</b>
5.1	The VAL Mission . . . . .	45
5.1.1	General objectives . . . . .	45
5.1.2	Measurements and specific requirements with respect to mission objectives . . . . .	45
5.1.3	Mission description and constraints . . . . .	49
5.2	The BIO-Argo Mission . . . . .	50
5.2.1	General objectives . . . . .	50
5.2.2	Measurements and specific requirements . . . . .	51
5.2.3	Mission description and constraints . . . . .	51
5.2.4	The BIO-Argo float in the context of Argo-related activities . . . . .	51
5.3	The Carbon-Explorer Float Mission . . . . .	52
5.3.1	General objectives . . . . .	52
5.3.2	Measurements and specific requirements . . . . .	53
5.3.3	Mission description and constraints . . . . .	53
<b>6</b>	<b>Technical Issues</b>	<b>55</b>
6.1	Life-Time, Bio-Fouling Deployment Issues . . . . .	55
6.2	Communication . . . . .	56
6.3	Energy Constraints . . . . .	57

<b>7</b>	<b>Data Management Issues</b>	<b>59</b>
7.1	Quality Control . . . . .	59
7.1.1	General philosophy . . . . .	59
7.1.2	BIO-Argo mission . . . . .	60
7.1.3	The VAL mission . . . . .	62
7.1.4	Carbon-Explorer mission . . . . .	64
7.2	Archiving and Data Distribution . . . . .	64
7.2.1	Standardization of the format . . . . .	64
7.2.2	Data status . . . . .	66
7.3	Matching Float and OCR Satellite Measurements . . . . .	68
<b>8</b>	<b>Towards the Implementation of Float Arrays</b>	<b>71</b>
8.1	VAL-floats: Preparatory Phase Before an Operational Array . . . . .	71
8.2	BIO-Argo Floats: Pilot and Regional Studies Before Global Dissemination	72
	<b>Acknowledgements</b>	<b>74</b>
	<b>Appendices</b>	
<b>A</b>	<b>Symbols and Acronyms</b>	<b>75</b>
<b>B</b>	<b>Example of Quality Control for Chla Fluorescence</b>	<b>77</b>
B.1	Real Time Mode . . . . .	77
B.2	Adjusted Mode . . . . .	78
B.3	Delayed Mode . . . . .	80
B.3.1	Radiometry-based correction . . . . .	80
B.3.2	HPLC correction . . . . .	80
B.3.3	Satellite correction . . . . .	80
	<b>References</b>	<b>83</b>



## Executive Summary

---

In the past two decades, thanks to the advent of satellite ocean-colour radiometry (OCR), biogeochemical processes at the ocean surface have begun to be documented on unprecedented spatial (~1 km to the global ocean) and temporal scales (~1 day and longer). These observation techniques, however, have their own inherent limitations. Firstly, remotely-sensed products are not direct measurements but quantities derived through models. *In situ* data are thus essential to validate the inversion algorithms. Secondly, as satellites only "see" the upper surface layer, the extension of the surface properties to the deeper layers requires extensive *in situ* measurements. Therefore, it is necessary to increase the *in situ* observation density associated with measurements from space. This is essential for refining bio-optical algorithms, implementing new and explorative strategies in marine biogeochemistry, as well as supporting biogeochemical-modelling activities (in association with the development of biogeochemical data assimilation techniques).

The profiling floats of the Argo array were initially designed for physical oceanography and hydrography. They now also represent a promising technology for future observations in ocean biogeochemistry and bio-optics. Indeed, new generations of optical and biological miniature, low-power consumption sensors have been developed and deployed on similar floats. The promising results already obtained through these local demonstration experiments have paved the way for the design of future global observational strategies relying on these bio-optical floats and on their synergetic and integrated use with ocean-colour radiometry (OCR).

The general objective of the IOCCG working group was to provide recommendations and establish a framework for the future development of a cost-effective, bio-optical float network corresponding to the needs and expectations of the scientific community. In this context, our recommendations are necessarily broad; they range from the identification of key bio-optical measurements to be implemented on floats to the real-time management of the data flux resulting from the deployment of a "fleet of floats". Each chapter of this report is dedicated to an essential building block necessary towards developing the goal of implementing a bio-optical profiling float network. In particular, and with respect to specificities of the scientific objectives as well as the capability (and associated cost) of the technology, the working group recommends three main categories of floats to be developed and associated missions to be subsequently implemented i.e. the VAL, BIO-Argo and Carbon-Explorer floats and missions.



## The VAL-Float and Mission

The primary objective of a VAL-float will be to acquire accurate and frequent profiles of radiometric and associated biogeochemical data contemporaneous to satellite ocean-colour overpasses. These floats will be operated as part of an array that will allow satellite sea truths to be acquired globally. Given the very specific objectives of a VAL mission, and the considerable differences to the standard Argo physics-oriented mission, it is envisaged that this array will be operated independently of Argo, and will be funded by space agencies in direct support of OCR missions. Standardized measurement protocols and associated data processing will be developed. This is essential to guarantee, in conjunction with the increasing number of validation matchups, the consistency and the overall quality of validation databases.

The technology (sensor, float, transmission) is available and has already been tested. The VAL-float requires an optimal integration of the various elements, especially the radiometers, with respect to the required highest-quality measurements. Currently, there are on-going developments aimed at building VAL-floats by integrating a suite of  $E_d$  and  $L_u$  sensors, as well as a suite of IOP and other biogeochemical sensors onto various types of floats. The prototypes of these floats are being tested in close proximity to the permanent MOBY (Hawaii) and BOUSSOLE (Western Mediterranean Sea) optical moorings, which are the appropriate sites to conduct these float performance evaluations. After this on-going preparatory phase, the implementation of an operational VAL-float array will be envisaged. A dedicated VAL-float array will have to be developed independently of the Argo program. Over a 5 year-term, an array of 50 ( $10 \text{ year}^{-1}$ ) floats deployed in various trophic areas (covering the range of [Chla] detected by ocean-colour satellites) is a reasonable target. Prior to development, specific locations and periods for maximizing the efficiency with respect to VAL activities will have to be identified. The total annual cost is estimated to be  $\sim \$1\text{M}$ , including two full time people for data management.

## The BIO-Argo Float and Mission

The rationale for the development of such a float is to provide the biogeochemical community with an unprecedented amount of (real-time) vertical profiles of some biogeochemical and bio-optical measurements. Obviously, this large bio-optical database would also satisfy some of the requirements of OCR satellite validation. This objective would be achieved by developing a generic, cheap, low-consumption bio-optical/bio-geochemical payload that would be disseminated through the Argo network and would take advantage of existing infrastructure. Besides providing data in specific time periods (e.g. winter, high latitudes) and/or locations (e.g. Southern Ocean) that are chronically under-sampled, the dense and continuous data acquisition from a BIO-Argo network would support (beside satellite validation) various scientific or operational topics to be tackled. These scientific applications

are potentially diverse and (non exhaustively) concern the extension of the satellite signal to the ocean interior, the validation of global biogeochemical and bio-optical models, the extraction of biogeochemical/bio-optical trends relevant to climate change (from the dense databases generated), or, more simply, the identification of processes in the ocean interior currently not amenable to sampling by ocean-colour radiometry or by traditional ship-based sampling strategies.

Rather than immediately targeting the development of a global network, the working group recommended the development of pilot studies in some biogeochemically-relevant "hotspots", as a first step. These pilot studies would serve as test cases for evaluating the design of a BIO-Argo array and its efficiency (in particular with respect to data density, management and dissemination). Among these regional hotspots, the North Pacific, the North Atlantic sub-polar gyre and Oxygen Minimum zones associated with upwelling areas, are potential target areas. For all these areas, the potential link and synergy with OCR is obvious. Presently, the biogeochemical community is organizing itself at an international level to design these pilot studies. The currently-funded floats could begin to contribute to a BIO-Argo program. Within 3-4 years, the community will benefit from a return of experience from these pilot studies to envisage a more global dissemination. In the meantime, and to prepare for this next step, it is highly recommended that the biogeochemical and bio-optical community strengthen ties with the Argo program, with the objective to develop a well-identified biogeochemical component, fully integrated within Argo. Targeting that 20% of the Argo array that would be equipped with biogeochemical sensors, the yearly cost of this development, as well as the associated data management, is estimated to be ~\$3M.

### **The Carbon-Explorer Float and Mission**

The Carbon-Explorer float is designed for the autonomous measurement of the most complete set of variables and fluxes related to the carbon cycle on time scales relevant to biological carbon productivity and carbon export processes. More specifically, the floats will measure proxies of POC and PIC and their diurnal variations, as well a proxy of carbon sinking rates. The scientific outcomes of the Carbon-Explorer float and mission will provide some of the required variables to validate GCM-coupled global biogeochemical models, to provide an estimate of Net Community Productivity for the entire photic zone. The Carbon-Explorer mission will also contribute to the validation of Level 3 satellite products (POC, PIC, NCP, export) for ocean-colour sensors as well as characterize the diurnal variability of the light field experienced by phytoplankton. The prototype phase of the Carbon-Explorer has been completed and it is now awaiting use by the broader community. The complete suite of up-to-date (and sometimes prototype) sensors as well as the possibility to sample at high frequency (e.g. diel cycle), make it especially suitable for specific process or targeted studies. In its present state, it is not considered to be amenable

to large global dissemination.

Finally, the working group emphasizes to the need for designing a data management system that allows for quality-controlled data distribution in real-time as well as in delayed mode. The scientific success of any float network and the subsequent appropriation of these new technologies by the community will depend heavily on the establishment of such a data management system. For this implementation, the IOCCG working group recommends that all the procedures which have already been implemented by the Argo program and which have demonstrated efficient data dissemination, be followed.

# Introduction: The Development of Bio-Optical Profiling Floats in the Context of Remote Sensing

---

## 1.1 Marine Biogeochemistry Observations Before Bio-Optical Floats

Oceanic physical forcing impacts ecosystem structure, elemental cycling and standing stocks of living resources. Because climate change will very likely affect the intensity and frequency of physical forcing, an associated response is expected in oceanic biogeochemistry. The physical forcing occurs over a continuum of spatial (sub-meso, meso, basin, global) and temporal (diurnal, seasonal, decadal) scales. Our present observational capabilities of biogeochemical oceanic properties represent a major limitation to our understanding of the coupling between physical forcing and the biogeochemical response. Biogeochemical processes are chronically undersampled as they are essentially investigated through ship-based platforms (e.g. CTD-rosette sampling and subsequent analysis of water samples). These sampling strategies cannot resolve the large range of temporal and spatial scales needed to establish climatologies of biogeochemical properties. This limitation in our observation capability constrains our present understanding of the functioning of the oceans and also our capability for modelling/predicting their future evolution. It is essential to increase our capability of measuring biogeochemical properties: new observational strategies are thus critical for the future. These should allow for high-density measurements to be performed for resolving the present poorly-described processes, while global observations would be more constrained.

In the past two decades, biogeochemical processes at the ocean surface have begun to be documented on unprecedented spatial (from 1 km to the global ocean) and temporal scales (in the order of 1 day and longer), due to the advent of satellite ocean-colour radiometry (OCR). Satellite OCR is now a unique tool through which biogeochemists have access to synoptic scale measurements of the surface Chlorophyll-a concentration, [Chla], an essential climate variable that can be linked to physical variables of similar resolution (sea surface temperature and height). More recently, thanks to new analytical or empirical algorithms, other fundamental biogeochemical quantities have expanded to include the absorption coefficients of coloured detrital material (Siegel et al., 2002b; Morel and Gentili, 2009), the

backscattering coefficient  $b_b$ , a proxy of particulate organic carbon concentration ([POC]), indices of particle size (Loisel et al., 2006; Kostadinov et al., 2009) or phytoplankton community composition (Uitz et al., 2006; Alvain et al., 2005). A two-band water leaving radiance - iterative scattering cross-section algorithm has been developed by Balch et al. (2005) for particulate inorganic carbon concentration, [PIC]. These observation techniques, however, also have their own inherent limitations. First, remotely-sensed products are not direct measurements but quantities derived through models. *In situ* data are thus essential to validate the inversion algorithms, especially those providing new products for which validation remains a critical issue. Secondly, as satellites only "see" the upper 20% of the euphotic zone<sup>1</sup>, the extension of the surface properties to the deeper layers requires extensive *in situ* measurements. There is thus a strong requirement to increase the *in situ* observation density associated with measurements from space. Indeed, this represents a great opportunity to increase the benefit of remote sensing of ocean colour as a tool for global biogeochemical observations and subsequent modelling. In addition, at any given time, nearly 70% of the Earth's surface is covered by clouds, resulting in poor temporal satellite OCR coverage with a frequency of once a month or even less in some regions of the ocean.

In the late 90's the physical oceanographic community designed and then implemented the Argo program (Roemmich et al., 1999), the aim of which was to develop an array of vertically-profiling floats to measure temperature and salinity in the ocean's upper 1000 to 2000 m, throughout the world's oceans. After a decade of operation, this program has succeeded in attaining its initial objective of 3,000 floats actively profiling (once every 10 days) and providing data with improved accuracy that are used by a large array of agencies and researchers (e.g. Freeland et al., 2010). With more than 100,000 Temperature-Salinity (TS) profiles during 2008 alone, the Argo array accounts for 95% of all the vertical profiles ever measured. The achievement of Argo is even more obvious with regards to the remote regions of the ocean. For example, Argo is producing more profile data south of 30°S during a single austral winter than in the entire pre-Argo history of oceanography (Roemmich et al. 2009).

The profiling floats of the Argo array were initially designed for physical oceanography and hydrography. They now also represent a promising technology for future observations in oceanic biogeochemistry. Indeed, new generations of chemical, optical and biological miniature, low-power consumption sensors have been developed and deployed on similar floats. Integrated on these new platforms, they allow repeated high-resolution observations of certain bio-variables presently derived from satellite observations e.g. [Chl<sub>a</sub>],  $b_{bp}$ , [POC], primary productivity and fluorescence (Bishop et al., 2002; Boss et al., 2008a; Bishop and Wood, 2009; Whitmire et al. 2009).

---

<sup>1</sup>The euphotic zone is defined as the layer between the surface and the depth where the light level of PAR is 1% of its value at the surface.

Other fundamental biogeochemical variables ( $O_2$ ,  $NO_3$ ) have also been measured by these platforms (Kortzinger et al., 2004; Riser and Johnson, 2008; Johnson et al., 2010). It is thus timely to envisage the design of future observational strategies relying on the combined use of remote sensing and bio-optical/bio-geochemical floats.

## 1.2 Developing Synergies Between Observations by Ocean Remote Sensing and Bio-Optical Floats

Remote sensing of the ocean surface covers spatial scales ranging from kilometers to the global scale and temporal scales ranging from days to the decadal scale (Figure 1.1). Profiling floats sample the water column between the surface and 2 km (up to 1 m resolution) covering horizontal spatial scales from  $\sim 1$  km to  $\sim 1000$  km, and temporal scales from a day to several years. Interestingly, the intersection between the spatio-temporal domains covered by both remote sensing and profiling floats (Figure 1.1) encompasses the mesoscale processes and the seasonal cycle of mixed layer dynamics and its impact on biomass cycles. Studying these is pivotal for improving our understanding of the impact of physical forcing on ocean biology and the biogeochemical cycle of elements, in particular of carbon. Although considered as essential, these processes have been poorly studied to date, because of the lack of appropriate observational strategies. Obviously, the design of observational strategies based on the combined use of both remote approaches would be essential for improving our knowledge of these fundamental oceanic processes.

The potential of combining Argo float technology with ocean-colour observations can be demonstrated with "simple" TS floats. For example, in the most oligotrophic waters in the vicinity of Easter Island in the South Pacific Gyre, a seasonality in surface [Chla] is observed with winter values exceeding the summer minimal values ( $0.02 \text{ mg m}^{-3}$ ) by a factor of  $\sim 3$  (Figure 1.2). The analysis of the TS data from an Argo float deployed in this area at the same period shows a cycle in mixed layer depth. One interpretation of this data is that winter mixing erodes the deep nutricline, allowing phytoplankton growth limitation to be alleviated resulting in the subsequent increase in biomass in these clear waters (Morel et al., 2010). Another interpretation, not necessarily contradictory with the first one, is that low average irradiance within the deepening mixed layer in winter induces phytoplankton photo-adaptation, i.e. more Chlorophyll-a per cell (McClain et al., 2004 ; Morel et al., 2010). Thanks to two independent datasets (SeaWiFS and Argo) openly available in quasi real time, an analysis of the tight coupling between physical forcing and biological response is now possible (e.g. Figure 1.2). It illustrates the potential to develop the synergetic association of remote platforms (space borne and *in situ*). This synergy is essential in the investigation, at the appropriate scales, of the role of oceanic biological and biogeochemical processes in the context of the increase of

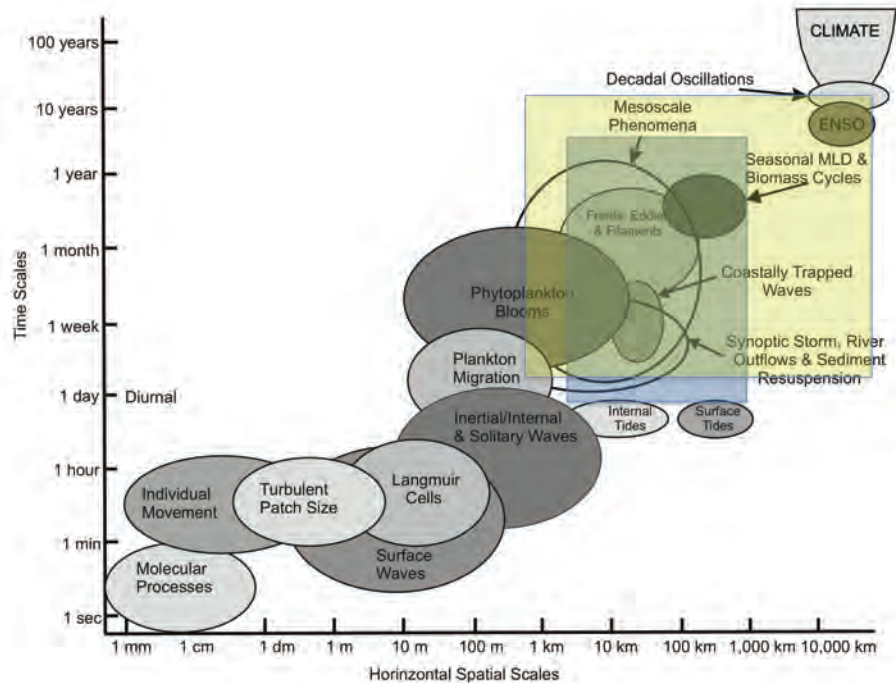


**Figure 1.1** The spatio-temporal domain relevant to major physical and biological processes in the context of observations by remote sensing (shaded yellow) and profiling floats (shaded blue). The intersection between both spatio-temporal domains identifies the scales of oceanic processes that can be scrutinized using both remote (space and *in situ*) approaches. For the open ocean, it encompasses processes that are essential for our understanding of the impact of physical forcing on the biogeochemical cycle of carbon. Adapted from Dickey (2003).

anthropogenic CO<sub>2</sub> and, more generally, of global change.

The calibration and validation of remotely-sensed satellite data is another area that would benefit strongly from the development and deployment of bio-optical floats. On the one hand, this technology would permit measurements in remote oceanic areas that are not easily accessible by ship. On the other hand, dense and homogenous (with respect to data treatment) databases of surface oceanic properties measured by ocean-colour satellites would be established.

### 1.3 Mandate of the BIO-Argo Working Group

In the future, an intensification of *in situ* measurements by bio-optical profiling floats is expected that will foster our understanding of ocean bio-optical and biogeochemical properties (Claustre et al., 2010a). Bio-optical floats will undoubtedly become the corner stone of future open-ocean observation systems dedicated to biogeochemistry and ecosystems that will largely be based on automated and remote

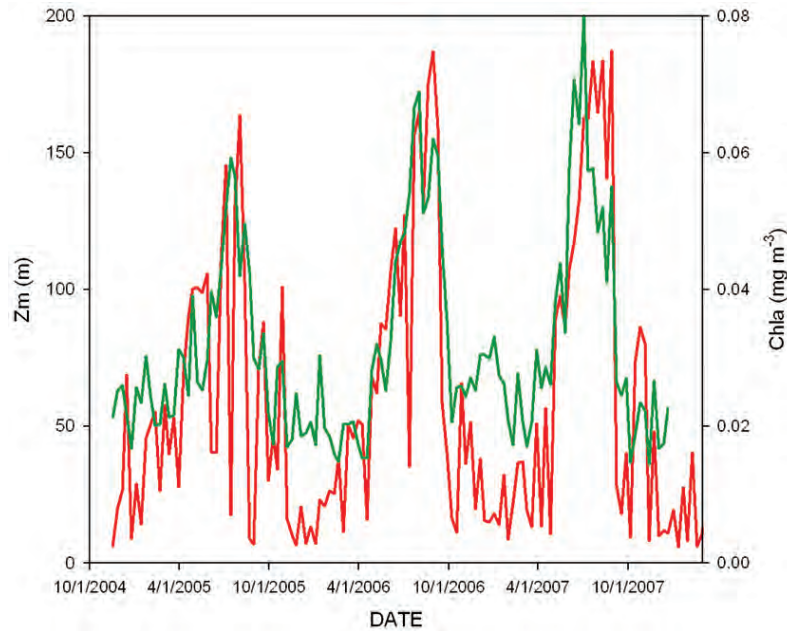


**Figure 1.2** Dynamics of algal biomass as a function of physical forcing in the center of the South Pacific Gyre (vicinity of Easter Island). The surface Chlorophyll-*a* concentration (green line), as quantified by SeaWiFS, is tightly linked to the thickness of the mixed layer (red line),  $Z_m$ , as recorded by a TS Argo float (WMO # 3000302). Adapted from Morel et al. (2010).

techniques (Claustre et al., 2010b). Combined with satellite OCR, bio-optical float arrays will permit, specifically, the creation of unique bio-optical 3D/4D climatologies, linking surface (remotely detected) properties to their vertical distribution (measured by autonomous platforms), and thus facilitating novel investigations.

The general objective of the IOCCG BIO-Argo working group is thus to elaborate recommendations for a framework for the future development of a cost-effective, bio-optical float network corresponding to the needs and expectations of the scientific community. In this context, our recommendations will necessarily be broad; they range from the identification of key bio-optical measurements to be implemented on floats, to the real-time management of the data flux resulting from the deployment of a "fleet of floats". Each chapter of this report is dedicated to an essential element leading towards the goal of implementing a bio-optical profiling float network. The following topics are discussed in the Chapters listed below:

- ❖ Chapter 2 reviews the scientific objectives that could be tackled through the development of such networks, by allowing some of the gaps in the present spatio-temporal resolution of bio-optical variables to be progressively filled.
- ❖ Chapter 3 identifies the optical and bio-optical properties that are now amenable to remote and autonomous measurement through the use of optical sensors mounted on floats.



- ❖ Chapter 4 addresses the question of sensor requirements, in particular with respect to measurements performed from floats.
- ❖ Chapter 5 proposes and argues for the development of dedicated float missions corresponding to specific scientific objectives and relying on specific optical sensor suites, as well as on specific modes of float operation.
- ❖ Chapter 6 identifies technological issues that need to be addressed for the various bio-optical float missions to become even more cost-effective
- ❖ Chapter 7 covers all aspects of data treatment ranging from the development of various quality control procedures (from real-time to delayed mode) to the architecture required for favoring easy access to data.
- ❖ Chapter 8 reviews the necessary steps and experience required before the operational implementation of different types of float networks can become a reality.

### Scientific Objectives

---

#### 2.1 Validation of Ocean-Colour Radiometric Products and Improvement of Bio-Optical Algorithms

##### 2.1.1 Ocean-colour radiometry products

The primary radiometric quantity derived from ocean-colour measurements is a radiance emerging from the sea surface,  $L_w$  (see Appendix A for list of symbols and abbreviations) at different wavelengths. Its derivation requires the application of an atmospheric correction procedure aimed at extracting the light having penetrated the sea surface and interacted with the water content from the remotely-sensed “top-of-atmosphere” signal. The atmospheric models used for such corrections contribute to the total uncertainty associated with the retrieval of  $L_w$ . Another important element contributing to this uncertainty is the sensor calibration drift. For further applications,  $L_w$  is transformed, with additional uncertainties, into “normalized water leaving radiance”,  $nL_w$ , to remove the dependence on viewing geometry and water bidirectional effects.

From the spectral characteristics of  $nL_w$ , secondary products are derived using a variety of algorithms, ranging from the purely empirical to the semi-analytical category. The most commonly derived ocean-colour product is [Chla], a proxy for phytoplankton biomass. Other products are diverse and include, in particular: the backscattering coefficient of particles at 555 nm ( $b_p(555)$ ), a proxy for [POC] (Stramski et al., 1999; Loisel et al., 2001); the absorption coefficient of non-pigmented particles and coloured dissolved organic matter ( $a_{CDM}$ ) (Maritorena et al., 2002); the spectral dependence of the backscattering coefficient, an indicator for the particle size distribution (Loisel et al., 2006); [PIC] (Balch et al., 2005) and phytoplankton carbon (Behrenfeld et al., 2005). Nevertheless, the extraction of such biogeochemical variables from ocean-colour data is an under-constrained problem: the number of variables expected is larger than the number of available optical variables (radiances). Consequently, this implies that uncertainties or ambiguities affect the extraction of these products. In this context, it is critical that additional *in situ* data are acquired for the validation of these new products.

### 2.1.2 Calibration and validation ("CALVAL")

To fulfill the requirement for accuracy in remotely-sensed products over the duration of a satellite mission (e.g. the top-of-atmosphere radiance, the water leaving radiance), the calibration of the sensor must be monitored constantly (the "CAL" program of any satellite mission). Apart from techniques involving onboard calibration, the main method consists of comparing *in situ* measured and satellite retrieved  $nL_w(\lambda)$ . Such a procedure combines the performance of the sensor and of the atmospheric correction algorithm and leads to the derivation of adjustment gains, or "vicarious" calibration coefficients. Obviously, *in situ* sampling must be contemporaneous with the satellite overpass and the accuracy associated with the measured water-leaving radiance must be optimal. For example, the SeaWiFS project aimed at retrieving the water-leaving radiance with an accuracy objective of 5% (Mueller and Austin, 1992). Assuming the uncertainty of *in situ* and SeaWiFS water-leaving radiances have the same weight and are independent (thus adding in quadrature), this objective requires both quantities to be measured with a 3.5% accuracy. Note that further data processing making use of the "recalibrated" signal has to include the same atmospheric correction algorithm.

Similarly, the quantitative comparison between *in situ* measurements and contemporaneous "match-up" satellite products ([Chla], [POC], Apparent Optical Properties (AOP) such as  $nL_w(\lambda)$ ,  $K_d(\lambda)$  or  $R_{rs}(\lambda)$  and Inherent Optical Properties (IOP) such as  $a(\lambda)$  or  $b_b(\lambda)$ ), is a way to estimate the uncertainties affecting the satellite products. This validation of the satellite products retrieval ("VAL" program) requires that uncertainties affecting *in situ* measurements themselves are well quantified, as well as the spatial and temporal scale mismatches between satellite and *in situ* measurements. In this case, the validation procedure incorporates sensor performance, atmospheric correction and the marine algorithm. A VAL program also requires accurate, frequent and globally-distributed *in situ* measurements. The SeaWiFS project required the agreement between *in situ* measurements and satellite derived products to be within 5% and 35% for water leaving radiance and [Chla], respectively (Mueller and Austin, 1992). Again, by attributing half of the uncertainty budget to the *in situ* measurements, the latter should be performed with accuracies of 3.5% and 25%, respectively. For validation purposes, the radiometric accuracy objective can be relaxed and a value of 5% is generally aimed for, and is feasible (at least for the blue and green wavelengths) if rigorous protocols are adopted for above- and below-surface measurements from oceanographic ships or specialized buoys or towers (Hooker et al., 2004; Zibordi et al., 2004; Antoine et al. 2008).

Whereas selection criteria considerably restrict the number of available radiometric *in situ* measurements for vicarious calibration of space sensors, *in situ* optical and biogeochemical measurements for the validation of ocean-colour products are commonly determined from moving ships or fixed buoys or platforms using recommended protocols. On the one hand, fixed buoys/platforms, allowing "continuous"

measurements, fulfill the request of "high frequency" thus increasing the probability of getting "good" satellite match-ups. On the other hand, they provide a very limited geographical coverage (and generally do not address the distribution of properties over the vertical axis) achievable as part of oceanographic cruises, with equally high cost, but over much shorter duration. Nevertheless, whatever the sampling system used at sea, differences of orders of magnitude between the satellite spatial resolution (typically 0.1 - 1 km<sup>2</sup>) and *in situ* resolution (typically 1 - 10 m<sup>2</sup>) are an additional source of uncertainty. However, for a particular environment, a scale analysis can be performed so that match-up numbers can be maximized without significant, application dependent, sacrifice in accuracy (see Section 7.3).

### 2.1.3 Potential advantages of a VAL-float Network

The potential advantages of using float technology are numerous for ocean-colour VAL activities. Firstly, the individual platform cost is low. Secondly, the repetition of high-frequency measurements will enhance the probability of match-up satellite records. Indeed, repeated measurements of surface quantities can be expected every day around solar noon for each float. Thirdly, the global distribution of such floats will allow the validation of satellite products to be obtained in a variety of atmospheric conditions and trophic areas all year round. In particular, polar and sub-polar zones or oceanic gyres, which are presently under-sampled by traditional CALVAL activities (Figure 2.1), would highly benefit from such a network. Finally, a large-scale network of VAL floats, complemented by a similar network of BIO-Argo floats, for some variables (see later), will allow an increase in the dynamic range and the number of data points available for validation, and will form a significant addition to existing data bases, such as the NOMAD data set (Werdell and Bailey, 2005). The subsequent availability of numerous data points from the implementation of such networks will compensate, at least partly, for the possible difficulties to reach the requested low levels of uncertainty in radiometric products from float measurements.

Similarly, it is anticipated that sensor calibration as well as data processing procedures will be unique and standardized for all floats. This will undoubtedly lead to a reduction in the uncertainty currently found in radiometric datasets gathered from a variety of instruments, and processing measurements carried out during various ship campaigns. Access to the vertical dimension of the radiometric quantity will facilitate, in some environments, the extrapolation of the signal to the surface. Flexibility is indeed conserved for the selection of the extrapolation layer with respect to fixed-depth measurements. Finally, the capacity to transmit, process and distribute data in near real-time will permit the development of an adaptive sampling strategy to allow an optimization of the sampling. For example, additional sampling of particularly cloudy areas could be performed when clear sky conditions are identified in quasi-real time.

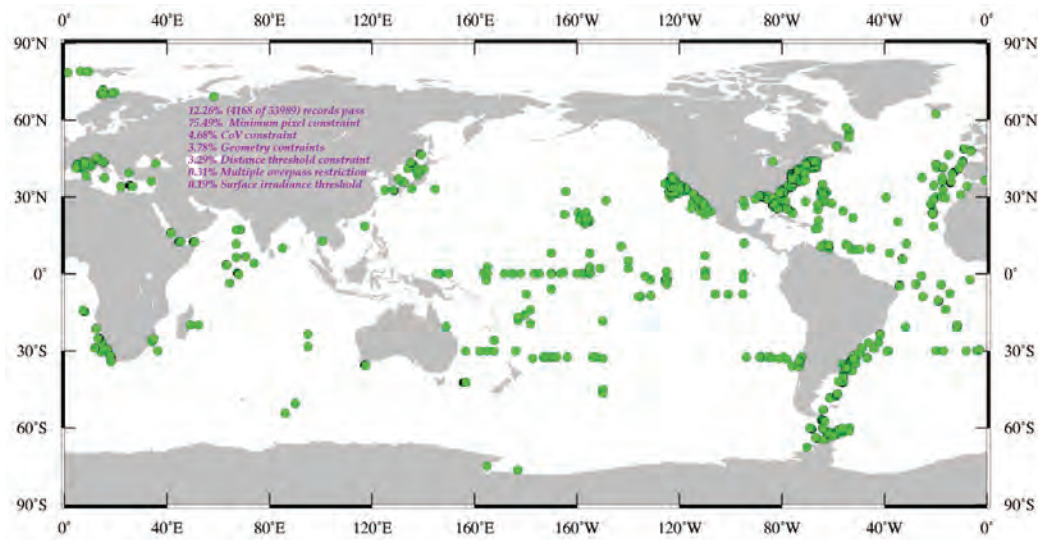


**Figure 2.1** SeaWiFS match-ups (simultaneous  $nL_w$  and [Chla] measurements) in the NASA SeaBass database (22 August 2008).

#### 2.1.4 Refining bio-optical algorithms

There is an increasing body of evidence that, in open ocean waters, significant deviations can be found between the average laws linking the optical status of a water body (through the measurement of its AOP) and the concentration as well as the composition of optically-significant substances such as [Chla] and coloured dissolved organic matter (CDOM), particularly in oligotrophic areas which represent 60% of the global ocean. For example, for the same surface [Chla], there are marked differences in reflectance spectra for Mediterranean and South Pacific waters (Morel et al., 2007a). In other words, the accuracy of the retrieval of relevant bio-optical and biogeochemical variables may be biased for regions of the ocean which are under-represented in the global data base (e.g. Claustre and Maritorena, 2003 and Figure 2.1). Again, the mitigation of such potential bias reinforces the necessity for intensifying measurements in these regions and therefore an array of VAL and BIO-Argo floats (see Chapter 8) is essential. These new databases would possibly allow the development and validation of regional empirical bio-optical algorithms sometimes required for certain atypical areas like the Mediterranean Sea (D’Ortenzio et al., 2002; Bricaud et al., 2002; Morel et al., 2007b) or in polar latitudes (Sathyendranath et al., 2001).

An expansion of validation data sets offered by a float network would also serve the refinement of semi-analytical algorithms across a variety of oceanic regimes. Such algorithms, more sophisticated than empirical approaches (see summary in IOCCG Report 5), exploit the ability to model, inversely, the relationship between IOPs and AOPs. VAL floats, carrying both AOP and IOP sensors, are of particular value

for this emerging algorithm class, as they will offer independent and simultaneous measurements of both algorithm input and output from the same platform.

## 2.2 Implementation of New, Explorative Observational Strategies in Marine Biogeochemistry

Profiling floats operate over a continuum of temporal scales ranging from daily to seasonal and even inter-annual time scales. The implementation of bio-optical and biogeochemical sensors on such floats thus opens the possibility of conducting a wide range of explorative studies dedicated to important biogeochemical processes at critical scales, which have been out of reach until present. Some of the potential applications based on such floats are outlined in detail hereafter. It should be pointed out that some basic measurements, essential for ocean-colour VAL, will be also measured as part of these investigations. The contribution to VAL activities will thus remain a systematic and important output of all of these biogeochemical investigations.

### 2.2.1 Inter-annual and seasonal changes in biogeochemical properties

#### 2.2.1.1 Net community production in high latitude areas

For high latitudes, which are not easy to investigate using classical ship-based investigations, a better understanding of the processes that control seasonal primary production is required to evaluate the possible impacts of climate change on carbon sinks in these key areas. The Sverdrup hypothesis (Sverdrup, 1953) suggests that the spring bloom occurs when the depth of the mixed layer becomes shallower than the critical depth, i.e. where production equals losses due to respiration, sinking and any other loss terms. These processes have been explored at regional scales (e.g. North Atlantic) using satellite remote-sensing data to determine chlorophyll concentration and mixed-layer depths interpolated from ocean climatologies (Siegel et al., 2002a). Floats equipped with nitrate and optical sensors would allow us to explore and study these processes more deeply by providing direct observations on mixed layer depth, rates of net community production inferred from nitrate uptake rates (Wong et al., 1998; MacCready and Quay, 2001; Rubin, 2003) and from observation of biomass accumulation derived from optical measurements (Boss and Behrenfeld, 2010). Most importantly, "continuous" biogeochemical time series over the vertical would allow investigation of the causes of inter-annual variability in production processes and carbon sinks. Such variability has recently been shown to be extremely high in high latitude areas (Corbiere et al., 2007; Metzl et al., 2010).

### **2.2.1.2 Respiration of sinking carbon in response to changes in Net Community Production**

Equally important to the role of production in the carbon cycle is the export toward the deep sea. Bio-optical sensors implemented on profiling floats clearly show biomass export into the mesopelagic layer (200 - 1000 m) (Bishop et al., 2004; Boss et al., 2008a; Bishop and Wood, 2009). Oxygen sensors on profiling floats can provide a novel perspective of the effects of this carbon export on respiration rates in the upper mesopelagic layer (Martz et al., 2008). Optical methods detect particulate concentration and flux variability to kilometer-plus depths. These observations can be used to study inter-annual variations in carbon production and export in regions where comparisons to sediment trap data are available. These comparisons would thereafter provide the groundwork for future autonomous observations of carbon export, based on optical observations and oxygen respiration rates throughout the world ocean.

## **2.2.2 Resolving events not detected through classical sampling strategies**

### **2.2.2.1 Episodic events**

Late summer phytoplankton blooms near the Hawaii ocean time-series (HOT) station seem to occur recurrently, although they are poorly sampled by monthly shipboard cruises, so that the mechanisms driving them are not well understood (White et al., 2007). Large increases in dissolved oxygen are observed by profiling floats when late summer blooms occur at HOT (Riser and Johnson, 2008). Observations from a network of floats equipped with bio-optical and chemical sensors would provide important constraints on the mechanisms that trigger such blooms, and more generally, the mechanisms that drive events of high primary production and carbon export in the North Pacific.

Mineral aerosols (dust), lofted from arid regions and transported over long distances in the atmosphere before deposition onto the surface, are hypothesized to be a major source of iron to the ocean. With the deployment of two Carbon-Explorer floats (optics and telemetry-enhanced Argo floats) in the North Pacific in April 2001, Bishop et al. (2002) documented for the first time the enhancement of marine productivity after an Asian dust storm, but found that episodes of dust-iron-enhanced marine productivity lasted only two weeks, much shorter than commonly believed. The pair of floats confirmed a doubling of POC while SeaWiFS data showed (a) that the dust storm effects were large scale, and (b) that there was only a 20% enhancement of chlorophyll, hence an improved photosynthetic efficiency.

Prior to the Carbon-Explorer, no ship expedition in the world's ocean had captured a time series of the biological response to dust deposition. Dust storms crossing over the north Pacific occur on average once every three years. The April

2001 Gobi Desert dust event that was observed was one of the biggest dust storms crossing the North Pacific in decades. Simply stated, by "being there" for an entire year there was a one in three chance of observing a dust storm.

Deep winter mixing near the Bermuda Atlantic time-series study (BATS) entrains nitrate into the euphotic zone. Again, the magnitude and duration of these events are not well sampled by the monthly time series. For example, winter increases in nitrate were not observed during several years of monthly sampling and whether this is the result of coarse sampling is unknown. As a result, the influence of winter mixing on sustaining new production is not fully appreciated. Profiling floats are well suited to sample these events on a regular basis, and hence to quantify the contribution of nutrient input from winter mixing to new production each year near BATS.

Paired Carbon-Explorer deployments in the Antarctic circumpolar current (Bishop and Wood, 2009) provided a first documentation of the effect of transient wintertime shallow stratification of 400 m-deep mixed layers onto phytoplankton bloom dynamics and particle export to the deep mesopelagic zone. These observations support an emergent and easily-testable hypothesis that water columns exhibiting transient winter stratification represent a much more favorable light environment for phytoplankton, thus leading to earlier food web development and more efficient deep particle export. Bishop and Wood (2009) point to the importance of transient wintertime stratification in setting the conditions that would permit the development of a bloom-quenching grazing community.

#### **2.2.2.2 Impact of eddies**

Recent observations from a mooring (Conte et al., 2003) and profiling float (Boss et al., 2008a) suggest that some eddies, barely visible in remote-sensing data, might be responsible for a large fraction of the particulate flux to depth. At both HOT and BATS locations, it is difficult to reconcile annual dissolved inorganic carbon draw-down with nitrate fluxes into the euphotic zone (Karl et al., 2003). Near BATS, observations from moorings, satellites and ships indicate that eddies may contribute to net community production and draw-down of dissolved inorganic carbon (DIC) by elevating the flux of nutrients into the euphotic zone (McGillicuddy et al., 1999; McNeil et al., 1999; Siegel et al., 1999). There are, however, few direct observations of these processes. Evidently, an array of profiling floats with oxygen, nitrate and bio-optical sensors would provide a much richer data set to assess what fraction of net community production is supported by eddy events available to upwelled nutrients.



### 2.2.3 The diel scale: an important scale for bio-optical and biogeochemical processes

Photosynthesis, the main process that injects organic carbon into the upper ocean, typically occurs at diel scales. Yet this fundamental scale for biological processes is generally neglected by observational studies because it is extremely time consuming and is generally incompatible with classical ship-based sampling strategies. The diurnal cycle of certain *in situ* optical properties is nevertheless a clearly established phenomenon (Siegel et al., 1989; Claustre et al., 1999). These diel processes are likely at the origin of part of the ‘noise’ observed in optical databases (Stramski and Reynolds, 1993), on which the development of a number of bio-optical algorithms is dependent (see above).

Because IOPs can be inverted into variables of biogeochemical relevance, interesting information can be inferred from their variations at the diel scale. This is particularly the case for diel variations in the attenuation coefficient,  $c_p$ , a proxy of POC (Gardner et al., 1993; Bishop, 1999). In locations where one-dimensional physical processes prevail (no lateral advection, or biological scales are larger scale than advection), optically-determined POC presents conspicuous diel oscillations with an increase during the day time and a decrease at night. The magnitude of this diel increase can be considered as a proxy of net community production (Bishop et al., 2002; Bishop and Wood, 2008; Claustre et al., 2008) and is thus amenable to quantification by floats profiling several times a day. Thus these high temporal resolution *in situ* studies would be very appropriate to obtain a better understanding of diel carbon processes, some of which could ultimately be studied from space. Indeed, the deployment of geostationary satellites (e.g. GOCI from KORDI) for ocean-colour observation in the next decade will possibly allow the observation of these diurnal changes in surface optical properties. In particular, the backscattering coefficient, another proxy of POC (Loisel et al., 2001), can be now retrieved from space observation through a variety of models and would be an interesting property to be targeted for diel *in situ* studies.

### 2.2.4 Heating rate of the upper ocean

Accurately quantifying the heat deposition at the ocean surface is essential for modelling the physical processes within the upper oceanic layer. Due to the strong absorption by water molecules, the solar infrared radiation (IR), which represents ~50% of the solar radiation, is rapidly absorbed in the top (<1 m) layer. By contrast, the penetration of visible and near-ultraviolet radiation, a spectral domain where absorption by water is several orders of magnitude lower, is much deeper and depends on the content of optically-significant substances (mostly [Chl $a$ ] in open ocean waters). The euphotic zone depth,  $Z_e$  (m) (a property derived from optical measurement) is defined as the depth at which the amount of the remaining visible

radiation is equal to 1% of the surface value. In other words, 99% of the visible radiation is attenuated within the euphotic layer (0 -  $Z_e$ ). Part of this absorbed energy is transformed into chemical energy (reduced carbon) and the other part, and by far the dominant portion, is converted into heat.

In open ocean water,  $Z_e$  varies between less than 10 m (upwelling waters) to 170 m (some sub-tropical waters) (Morel and Gentili, 2004; Morel et al., 2007a). The heat deposition in open-ocean waters is tightly dependent on the bio-optical status (through [Chla]). Relatively accurate parameterizations of this deposition have been proposed for application to remotely-sensed ocean-colour scenes (Morel and Antoine, 1994). Nevertheless, such "mean" parameterizations do not take into consideration the potentially large variability linking the [Chla] to the concentration of other optically-active substances. For example, for approximately the same low surface [Chla] ( $\sim 0.03 \text{ mg m}^{-3}$ ),  $Z_e$  can vary between 170 m (South Pacific Gyre) and 80 m (Mediterranean Sea). Such differences are accounted for by the variation in the relative contribution of CDOM in both areas (high in the Mediterranean Sea, low in the South Pacific Gyre). For a proper estimation of heat deposition at a local scale, it thus remains essential to quantify directly the decrease of irradiance with depth. Bio-optical floats equipped with radiometers at appropriate wavelengths can provide the required data to estimate the radiative heat flux into the ocean.

## 2.3 Ocean Modelling and Data Assimilation

Ocean biogeochemical and ecosystem models require observations for initialization, boundary conditions and validation (Lynch et al., 2009). Climatologies of *in situ* data are frequently used for initialization purposes. Satellite ocean-colour data, usually chlorophyll concentration, is used as an important component of model validation (Doney et al., 2009), but only provides information of the state of the surface ocean. Time series data (e.g. BATS, HOTS) are often used to validate models at depth. However eddies have a strong imprint on the biogeochemical signals at these sites. Eddies are not captured in coarse resolution models, and though captured in higher resolution models, there will remain temporal inconsistencies. Thus, though very useful for model validation, especially for interannual variability, time series data alone are not sufficient for many modelling purposes. BIO-Argo floats will provide a much needed, larger scale perspective on the biogeochemistry of the upper layers of the ocean that have not been sampled sufficiently for modelling purposes in the past.

Data assimilation provides a means of using models and observations so that each strengthens the other (Brasseur et al., 2009). Data provides context and validation, and models fill in temporally and spatially where the data is insufficient. Data assimilation is well established in atmospheric studies, and indeed is essential for much of the forecasting available to us. In the last decade or two, data assimilation

has become important for estimates of ocean circulation. Currently there are many projects dedicated to ocean data assimilation (see Lee et al., 2010 for a list). Some projects are dedicated to reanalysis products using sequential techniques to provide hindcasts and forecasts of the ocean state, others use variational techniques (Wunsch, 1996; Talagrand, 1997) to optimize model parameters or forcing to provide optimized state estimates of the ocean circulation (Wunsch et al., 2010). These projects use a variety of observations, including global satellite and scattered *in situ* ocean data. In particular, Argo floats have provided an important constraint on the upper ocean physical state. As an example, Forget et al. (2008b) used an adjoint model to quantify the utility of Argo floats in constraining the volume and heat transport in the North Atlantic. These studies found that the Argo array are likely to be able to capture large scale, low frequency circulation of the ocean.

Data assimilation remains relatively new in ocean biogeochemistry itself. The expanding satellite ocean-colour and biogeochemically relevant *in situ* observations are, however, leading to increased use of these techniques (see Gregg et al., 2009 for a list of these studies). Global models assimilating satellite-derived chlorophyll suggest the utility of these approaches (Tjiputra et al., 2007; Gregg, 2008) both for reanalysis products and for model parameter optimization. More biogeochemical assimilation projects are currently underway. Though ocean colour provides an excellent global surface perspective, it cannot provide crucial information about ocean ecosystems at depth. Ship-board surveys (e.g. the Atlantic Meridional Transect, AMT) and long term observational sites (e.g. BATS, HOTS) can provide some of the sub-surface information required, but it will be the bio-optical floats that will fill many of the gaps in observation and thus will be an essential part of biogeochemical data assimilation. Adjoint modelling studies, similar to that of Forget et al. (2008a) from the biogeochemical perspective, could also be useful to help establish the numbers and placements of these floats that would provide maximum benefit.

One of the significant contributions of a bio-optical profiling float array (VAL, as well as BIO-Argo) will also be the ability to provide routine depth-resolved bio-optical and geophysical data at low cost from which the development of climatologies will be an essential outcome. These climatologies are indeed of critical importance for many diverse scientific applications that deal with, for example, bio-optical modelling of primary production (Antoine et al., 1996), the identification and understanding of long-term trends in biogeochemical properties, or the modelling of coupled ecosystem/biogeochemical cycling of elements at global scale (Lequ er  et al., 2005 and previous references).

Developing a 3D/4D biogeochemical picture of the ocean is certainly challenging but this can be likely achieved by developing synergies between the two remotely-operated techniques (space-based and *in situ*) together with the use of modelling and assimilation techniques. One prerequisite is to elaborate databases from which the relationship between vertical distribution of a certain variable and its surface signature can be established, analyzed and further modelled using appropriate

parameterization. For chlorophyll-a, methods already exist allowing the inference of the water column content from its remotely-sensed surface values (Morel and Berthon, 1989; Uitz et al., 2006; Westberry et al., 2008). However, the databases on which these empirical methods are based consist of discrete measurements and do not have the same spatio-temporal coverage (only a few thousand profiles for references mentioned above) as the hydrological databases (Levitus climatology). For example, in 2008 the Argo program collected 130,000 TS profiles. It is thus essential to increase the density of observations over the vertical for this fundamental variable. Additionally, databases of vertical profiles of other biogeochemical or bio-optical variables potentially accessible by remote sensing (e.g. backscattering coefficient, diffuse attenuation coefficient, absorption coefficient, particle size index) remain much less dense than Chla databases (but see Westberry et al., 2008). A dedicated acquisition and archiving effort for these ‘new’ variables needs to be undertaken; it is a prerequisite before the development of robust methods for the inference of these sub-surface variables in the ocean interior from satellite data.

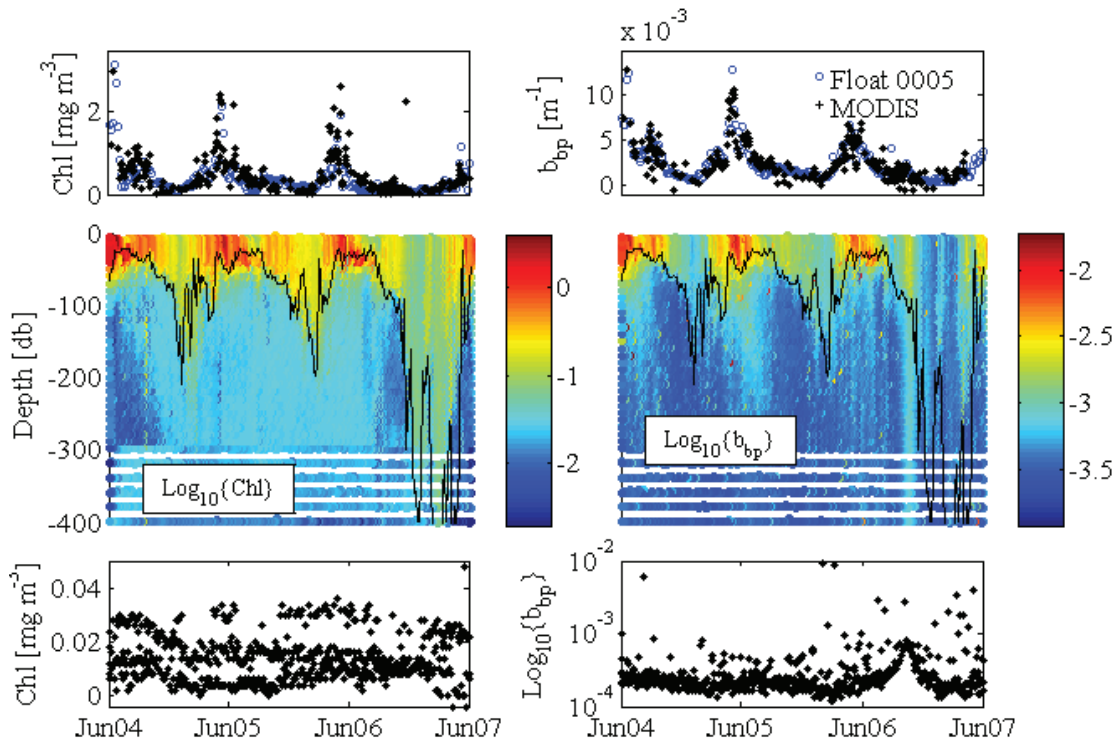


**Figure 2.2** Satellite retrievals of Chla and particulate backscattering (top panels), near-surface in-water distributions of particulate backscattering and Chla (middle panels) and Chla and backscattering values below 950 m measured by a profiling float during three years in which it roved in the North Atlantic at the end of 2006. The increase in backscattering at depth was associated with the float being trapped in an eddy. The signature of the eddy was barely discernable in surface data (from Boss et al., 2008b).

We must nevertheless be aware that *in situ* observations in the ocean interior will very likely depart from predicted values from remote sensing or from generated climatologies. It will be interesting to analyze these deviations in the context of highlighting specific biogeochemical signatures deviating from the 'mean' laws, and resulting from either specific physical or biogeochemical processes. This will likely reveal the importance of critical spatial and/or temporal scales for biogeochemical processes and will be helpful for evaluating how deep surface processes penetrate. For example, Boss et al. (2008a) did not find any evidence of the spring bloom in particle backscattering below 950 m in the North Atlantic near 50°N and 37°W while they observed a significant increase of backscattering at these depths during an eddy passage that was barely noticeable in the satellite data (Figure 2.2).

## Chapter 3

# Key Bio-Optical Properties Amenable to Measurement by Floats

---

## 3.1 Downward Irradiance, Upwelling Radiance

### 3.1.1 Basics

Radiance  $L$  at a point in space (e.g. underwater at depth  $z$ ) is the radiant flux,  $\Phi$ , at that point in a given direction per unit of solid angle per unit of projected area,  $A$ .

$$L(\theta, \varphi, z, \lambda) = d^2\Phi/d\omega dA \quad (3.1)$$

where  $dA = ds \cos\theta$  is the projected area of the element of surface  $ds$ , seen from the direction of propagation (defined by the zenith angle  $\theta$  and the azimuth angle  $\varphi$ ) onto the plane perpendicular to this direction. The radiance is spectrally dependant and has the unit of  $\text{W m}^{-2} \text{sr}^{-1} \text{nm}^{-1}$ . The upwelling radiance  $L_u(\pi, 0, z, \lambda)$  classically measured using underwater profiling radiometers, is the radiance coming from the upward vertical or "nadir" (zenith angle equal to steradians). The water leaving radiance  $L_w(\pi, 0, 0^+, \lambda)$  is the radiance leaving the sea at nadir and quantified "just above" the surface ( $0^+$ ) by taking into account refraction and reflection at the interface. Note that the water-leaving radiance  $L_w(\theta, \varphi, 0^+, \lambda)$  as derived from an ocean-colour sensor measurement after the so-called atmospheric correction, is coming from an angle and azimuth defined by the viewing angle and position of the satellite sensor (and not nadir), and that the "normalized water leaving radiance", a standard remote sensing product, is not  $L_w(\pi, 0, 0^+, \lambda)$ .

Irradiance  $E$  at a given depth,  $z$ , can be defined as the radiant flux per unit area of surface (Kirk, 1994). Irradiance has the units  $\text{W m}^{-2} \text{nm}^{-1}$ .

$$E(z, \lambda) = d\Phi/ds \quad (3.2)$$

Downward irradiance,  $E_d$  and upward irradiance,  $E_u$  represent the irradiance for the downwelling and upwelling light, respectively, of a horizontal surface.  $E_d$  is the integral of all radiance elements over the whole upper hemisphere and similarly,  $E_u$  is the integral of all radiance elements over the whole lower hemisphere.

$$E_d(z, \lambda) = \int_{\varphi=0}^{2\pi} \int_{\theta=0}^{\pi/2} L(\theta, \varphi, z, \lambda) |\cos\theta| \sin\theta d\theta d\varphi \quad (3.3)$$

$$E_u(z, \lambda) = \int_{\varphi=0}^{2\pi} \int_{\theta=\pi/2}^{\pi} L(\theta, \varphi, z, \lambda) |\cos\theta| \sin\theta d\theta d\varphi \quad (3.4)$$

A beam of photons intercepting a flat surface will produce an irradiance that is proportional to the cosine of the incident angle (Mobley, 1994). A so-called "cosine collector" used to measure the downward or upward irradiance will induce a detector response that is proportional to  $\cos\theta$  thus weighting each photon contribution according to the cosine of the incidence angle. Accurate measurements of *in situ* irradiance rely on the accurate characterization of the cosine response of the particular collector used.

### 3.1.2 Derived bio-optical or biogeochemical products

#### 3.1.2.1 Diffuse attenuation coefficient for downward irradiance, $K_d$

The spectral diffuse attenuation coefficient for downward irradiance  $K_d(\lambda)$  (in units of  $\text{m}^{-1}$ ) quantifies the exponential decrease of irradiance with depth in the water column.

$$K_d(z, \lambda) = -\frac{d \ln E_d(z, \lambda)}{dz} = -\frac{1}{E_d(z, \lambda)} \frac{dE_d(z, \lambda)}{dz} \quad (3.5)$$

In practice, an average  $K_d(\lambda)$  is computed for a defined water layer  $z_0 - z_1$  (e.g. the "euphotic layer") and is the negative of the slope of the linear relationship between  $\ln E_d(z, \lambda)$  and depth  $z$  within the  $z_0 - z_1$  interval. The underlying assumption is that the water layer  $z_0 - z_1$  is homogeneous with respect to optical properties and thus  $\ln E_d(z, \lambda)$  decreases linearly with depth  $z$ . Note that an analogous diffuse attenuation coefficient for upward irradiance  $K_u(z, \lambda)$  can be computed for the relationship between  $E_u(z, \lambda)$  and  $z$ . In addition, and although it is not generally used as a product itself, an attenuation coefficient  $K_{Lu}(z, \lambda)$  for the upwelling radiance can be computed similarly from  $L_u(z, \lambda)$  versus  $z$  measurements and is crucial for deriving the above-water  $L_w(0^+, \lambda)$  and subsequently, the remote sensing reflectance (see below). The diffuse attenuation coefficients for irradiance and radiance are "apparent optical properties" (AOP) as they depend on both the water content and the directional structure of the ambient light field.

#### 3.1.2.2 Normalized water leaving radiance, $nL_w$

To validate the satellite measured  $L_w(\theta, \varphi, 0^+, \lambda)$  by comparing it with an *in situ* measured value, a normalization process is applied to both radiances. This leads to the derivation of the "normalized water leaving radiance",  $nL_w$ , which aims to remove the effect of the illumination conditions (sun zenith, atmospheric transmittance).

$$nL_w(0^+, \lambda) = L_w(0^+, \lambda)E_s(\lambda)/E_d(0^+, \lambda) \quad (3.6)$$

where  $E_s$  is the extraterrestrial solar flux (geometry dependency omitted in this equation). Note that, since the extraterrestrial solar flux is a constant (to a high degree of accuracy),  $nL_w$  is, in fact, a function of wavelength multiplied by  $R_{rs}$  (defined below).

### 3.1.2.3 Remote sensing reflectance, $R_{rs}$

The spectral remote sensing reflectance  $R_{rs}$  (in units of  $\text{sr}^{-1}$ ) as measured (at nadir) using underwater radiometers is defined as:

$$R_{rs}(\pi, 0, \lambda) = \frac{L_w(\pi, 0, 0^+, \lambda)}{E_d(0^+, \lambda)} \quad (3.7)$$

This ratio indicates the proportion of light incident onto the sea surface that is eventually scattered back to a sensor looking at nadir. As for the radiance  $L_w$ , the remote sensing reflectance as derived from an ocean-colour sensor measurement,  $R_{rs}(\theta, \varphi, \lambda)$ , is defined by the viewing angle and position of the satellite sensor. The remote sensing reflectance is also an apparent optical property.

### 3.1.2.4 Derived secondary products

Biogeochemical products (e.g. [Chla]) or optical properties (absorption and back-scattering coefficient) can be retrieved from spectra of  $K_d(z, \lambda)$  or  $R_{rs}(\lambda)$  (for simplicity the geometry is omitted here) by using empirical or semi-analytical models (see IOCCG 2000; 2006). In particular, recent inversion algorithms have been developed to retrieve the absorption coefficient of coloured dissolved organic matter,  $a_{CDOM}(\lambda)$  (possibly combined with the absorption coefficient of particulate "detrital" matter) as well as the absorption coefficient of pigmented matter (phytoplankton),  $a_{ph}(\lambda)$ , from surface or vertical spectra of AOPs (Lee et al., 2002; Maritorena et al., 2002; Brown et al., 2004; Gordon et al., 2009). Notably, Brown et al. (2004) proposed a retrieval algorithm for these properties in the absence of a simultaneous reference irradiance measurement, which will most likely be the case for measurements performed by floats.

## 3.2 Backscattering Coefficient

### 3.2.1 Basics

In natural waters where particles are assumed to be randomly oriented, the volume scattering function (VSF;  $\beta(\theta)[\text{m}^{-1} \text{sr}^{-1}]$ ) describes the angular distribution of scattering relative to the direction of light propagation ( $\theta$ ). The scattering coefficient,  $b$



( $\text{m}^{-1}$ ), is the integration of  $\beta(\theta)$  over all  $\theta$ , while the backscattering coefficient,  $b_b$  ( $\text{m}^{-1}$ ) denotes the amount of light scattered into the back hemisphere:

$$b_b = 2\pi \int_{\pi/2}^{\pi} \beta(\theta) \sin\theta d\theta \quad (3.8)$$

The backscattering coefficient,  $b_b$ , of a water body is the sum of the backscattering coefficient of particles,  $b_{bp}$ , and of the backscattering coefficient of pure seawater,  $b_w$  i.e.  $b_{bp} + b_w$ . It should be noted that  $b_{bp}$  represents a very small fraction (0.5 - 3%) of the scattering coefficient for particles,  $b_p$ , and is also a proxy for particle abundance although it depends significantly on particle size distribution (e.g. median particle size) and particle composition (e.g. organic vs. inorganic, through differences in the index of refraction). Most importantly, the spectral reflectance of the ocean (known as ocean colour) is, to a first order, proportional to  $b_b$ . Measurements and fundamental understanding of  $b_b$  are thus required for understanding and successful application of remotely-sensed ocean colour. Note, however, that there are still unresolved questions regarding the major contributors to  $b_b$  (Morel and Ahn, 1991; Stramski and Kiefer, 1991; Stramski et al., 2004; Dall’Olmo et al., 2009; Whitmire et al., 2010).

## 3.2.2 Derived bio-optical or biogeochemical products

### 3.2.2.1 Particulate organic carbon

In recent years,  $b_{bp}$  has been found to correlate well with particulate organic carbon, POC (Stramski et al., 1999 ; Stramski et al., 2008 ; Dall’Olmo et al., 2009) as well as total suspended mass (Boss et al. 2009a) in aquatic environments. While colloids and particles smaller than  $0.2\mu\text{m}$  are believed to have negligible contribution to  $b_{bp}$  (Stramski and Wozniak, 2005) salt water has been shown to have a significant contribution to  $b_b$ , and care should be applied to account for it appropriately (Twardowski et al., 2007).

### 3.2.2.2 Size index of particulate matter

Theoretical considerations suggest that the spectral behaviour of scattering,  $b_p$  ( $\text{m}^{-1}$ ), of non-absorbing spherical and homogeneous particles (or in non-absorbing bands) could provide information on the particle size distribution (Morel, 1973). Spectral  $b_{bp}$  measurements could provide a proxy for particle size assuming that the backscattering has the same spectral dependence as scattering, or can be in some way predicted (see Huot et al., 2008), This property has been used for inferring particle size from remotely-sensed ocean-colour scenes (Loisel et al., 2006; Kostadinov et al., 2009; 2010) or from spectral  $b_{bp}$  measurements acquired by a glider (Niewiadomska et al., 2008). Optimally, the spectral measurements should be performed at bands weakly influenced by absorption (infra-red, green).

### 3.3 Beam Attenuation Coefficient

#### 3.3.1 Basics

The beam attenuation coefficient,  $c$  ( $\text{m}^{-1}$ ) describes the decrease in intensity of a plane collimated beam as it propagates through a medium. It accounts for losses both due to absorption and scattering. The attenuation coefficient is measured by a beam transmissometer, which measures the loss of photons from a narrow parallel beam passing through a known path length of seawater. The measurement of the attenuation coefficient at 660 nm was primarily dictated by the need to avoid absorption interference by dissolved organic substances which occur at shorter wavelengths (plus the practical fact that stable red LED light sources were available).

#### 3.3.2 Derivation of bio-optical or biogeochemical products

##### 3.3.2.1 Particulate organic carbon

In open ocean waters, the beam attenuation coefficient at 660 nm measured by a transmissometer, once corrected for absorption by pure water, is essentially a measurement of the attenuation coefficient by particles,  $c_p$  ( $\text{m}^{-1}$ ), because the absorption coefficient by dissolved material is negligible at this wavelength (Loisel and Morel, 1998). Furthermore, the absorption by particles (detrital and phytoplankton) is relatively small so that  $c_p$  is equivalent to the integrated particle scattering coefficient. Thus, from a theoretical point of view, the main source of variation in  $c_p$  is the numerical abundance and size (cross-section) of particles, while second order sources are the refractive index and shape of particles (Gardner et al., 1993). For a standard particle size distribution (Junge type with a -4 exponent), the homogenous and spherical particles to which the transmissometer is most sensitive lie in the 0.5-10  $\mu\text{m}$  size range (Stramski and Kiefer, 1991) which typically corresponds to the size domain of the living (pico- and nanophytoplankton, heterotrophic bacteria, pico- and nano-zooplankton) and non-living particles (detritus). In reality, particle size distributions are not log-normal and large aggregate particles contain micron-sized elements. It has been suggested (Morel, 1988) and subsequently verified (Gardner et al., 1993; Loisel and Morel, 1998; Bishop, 1999; Bishop et al., 1999; Claustre et al., 1999; Bishop and Wood, 2009) that in oceanic waters  $c_p$  is linearly related to the particulate organic carbon concentration, POC ( $\text{mg}^{-3}$ ). However, regional differences in the  $c_p$ -POC relationship have been reported. For example, a relationship with a slope of  $502 \text{ mg C m}^{-3} \text{ m}^{-1}$  was reported for the North western part of South Pacific gyre (Claustre et al., 1999) which was at least twice as large as those found for other oceanic regions (Siegel et al., 1989; Walsh et al., 1995). The basis for these differences may be both methodological and instrumental and these factors are now beginning to be understood. A part of this uncertainty might be due to shifts to instruments with wider acceptance angles (see Section 4.3). Additional

uncertainty has been ascribed to the POC blanks in bottle collected water samples (Bishop, 1999). With proper POC calibration, the relationship between  $c_p$  and POC is far more consistent and varies typically by 10% (Bishop, 1999; Bishop et al., 1999; Bishop and Wood, 2008). Exceptions in this relationship have been found in waters with the biomass occurring predominantly in  $>50 \mu\text{m}$  size fraction, such as surface waters south of the Antarctic Polar Front where  $c_p$  response to POC is 40% less sensitive (Bishop et al., 2004) but nevertheless remains highly correlated.

Bishop (1999) shows that  $c_p$  is a far better predictor of POC than total dry-weight suspended mass measured gravimetrically. Furthermore,  $c_p$  reflects the sum of POC in all particle size fractions better than in the smallest particle fraction. Comparisons of  $c_p$  and scattering coefficient (at 810 nm integrated from  $45^\circ$  to  $135^\circ$ , Seapoint Inc.) vs. POC shows good correlation in near surface waters for  $c_p$  vs. POC (Bishop and Wood, 2008) but a breakdown of the POC/scattering relationship in mesopelagic waters below the euphotic zone (Figure 3.1). With respect to POC determination from optical measurements, scattering or backscattering sensors are simpler to use (looking downward or tangentially to the flow) but are sensitive to differences in particle composition and size distribution. Transmissometers are more stable, but sensitive to accumulation of sinking material (although this can be turned into an advantage - see next section). In any case, it appears from these observations that both  $c_p$  and scattering are complementary measurements in the estimation of POC and particle properties.

### 3.3.2.2 Carbon flux index of sedimentation

Carbon flux index (CFI), derived using a float mounted transmissometer, permits assessment of sedimentation on hourly to daily timescales, for seasons to years (Bishop et al., 2004; Bishop and Wood, 2009). CFI is a systematic measure of the accumulation of particles on the upward-looking optical (detector end) window of the transmissometer sensor (WETLabs Inc., Philomath, Oregon) while the float is "parked" at depth. Before profiling starts, the raw transmission "counts" from the POC sensor are read, then the exhaust from the float's pumped CTD removes settled particles and the transmission is read again. The difference between "before" and "after" readings divided by the time that the float was parked at depth gives the CFI (counts/day). A picture of the instrument setup is found in (Bishop and Wood, 2009).

### 3.3.2.3 Net community production

Siegel et al. (1989) presented the first data of a diel cycle in  $c_p$ , in the upper layers ( $>100 \text{ m}$ ) of the oligotrophic waters of the North Pacific Gyre. Increase of particle load was observed during daytime, while a decrease of similar amplitude was observed during nighttime, leading to the conclusion that particle production

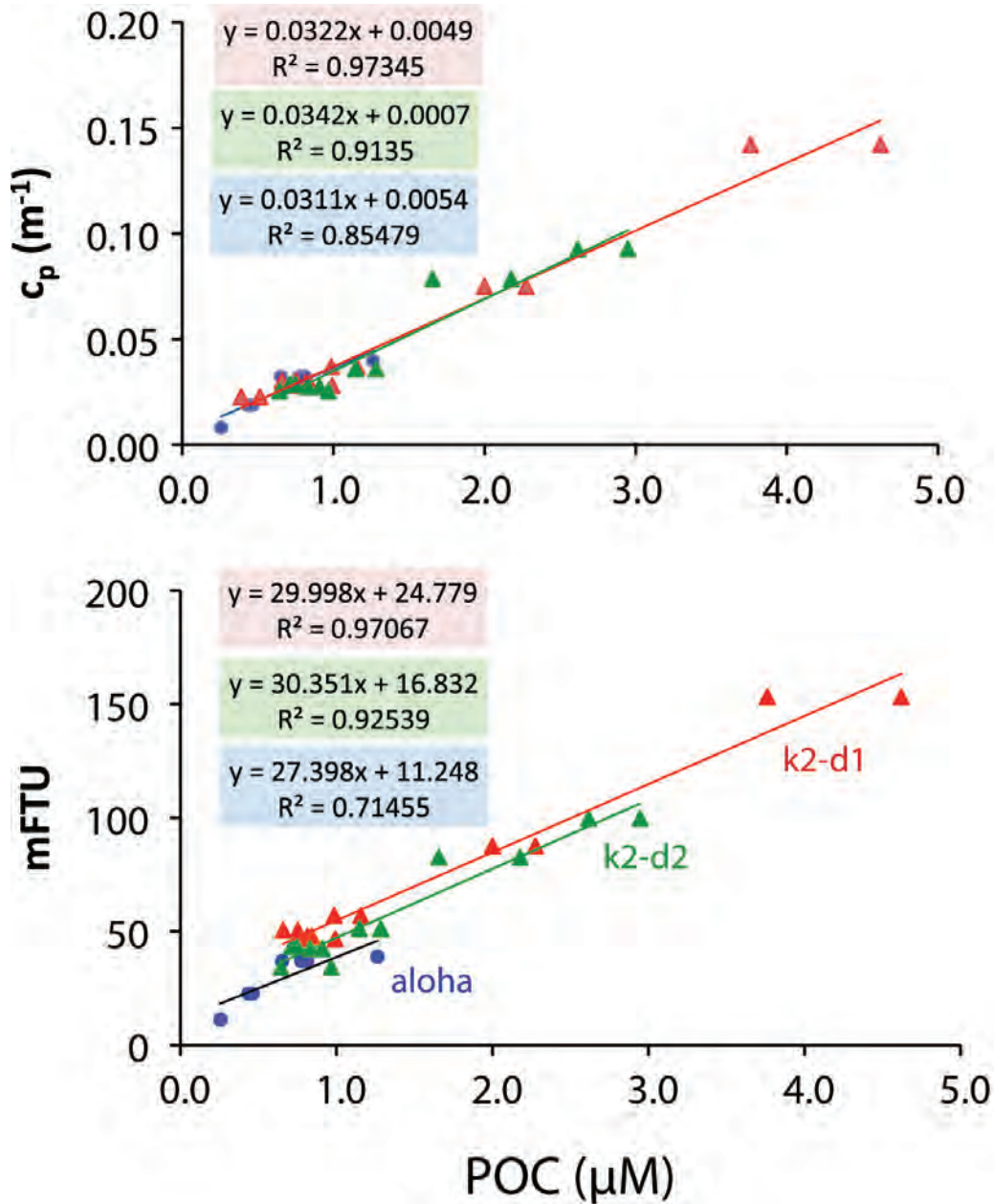


**Figure 3.1** Regressions of  $c_p$  vs. [POC] and turbidity vs. [POC] for the Oyashio current ( $47^\circ\text{N}$   $161^\circ\text{E}$ ) and station ALOHA; data for upper 250 m (Bishop and Wood, 2008). Turbidity is determined by a Seapoint scattering sensor (810 nm; 45-135 detector angle) and  $c_p$  by C-Star transmissometer (660 nm). The red (k2-d1) and green (k2-d2) data points were taken 10 days apart in the Oyashio current; blue data come from ALOHA. While both  $c_p$  and scattering predict [POC] in surface waters, scattering was sensitive to the presence of much higher quantities of particulate silicon and carbonate particles in the Oyashio current, leading to different intercepts. Use of scattering without calibration can thus over predict [POC] by as much as  $1 \mu\text{M}$ ; uncertainty of [POC] derived from  $c_p$  is  $\sim 0.1 \mu\text{M}$ .

was balanced on a daily scale. This study by Siegel was thus the starting point of subsequent studies where the diel cycle in  $c_p$  (and hence in POC), and its potential implication in terms of carbon fluxes in the upper oceanic layers, were addressed. Analyses of these diel variations were later performed either from ship-based acquisition (Cullen et al., 1992; Cullen and Lewis, 1995; Walsh et al., 1995; Claustre et al., 1999; 2008; Bishop and Wood, 2008), from mooring data (Gernez et al., 2011) or from laboratory culture (Stramski and Reynolds, 1993; Walsh et al., 1995; DuRand and Olson, 1998; Claustre et al., 2002). Diel profiling of  $c_p$  has been routine on Carbon-Explorer profiling floats (Bishop et al., 2002; 2004; Bishop and Wood, 2009) (Figure 3.2). Most of these studies were motivated by a strong interest in developing and using a non-intrusive method to measure biogeochemical rates whose estimation required ship board methods.

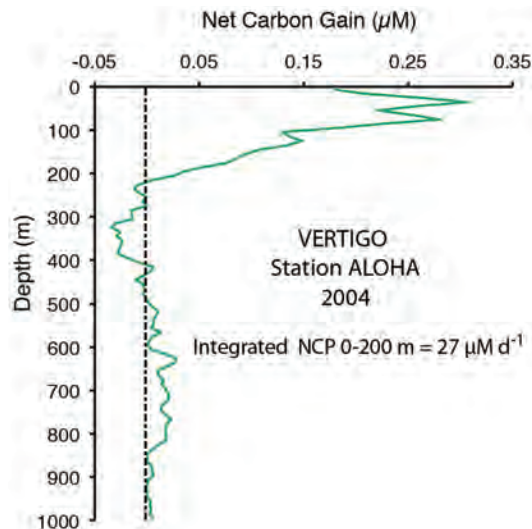


**Figure 3.2** Estimate of integrated net community production (NCP) from integration of dusk minus dawn  $c_p$  profiles at station ALOHA (Bishop and Wood, 2008). Values are in close agreement with NCP values determined using *in situ*  $C^{14}$  incubations. NCP variability near ocean station PAPA ( $50^{\circ}\text{N}$   $145^{\circ}\text{W}$ ) and at other locations has been determined using Carbon-Explorer profiling floats (Bishop et al., 2002).

## 3.4 Chlorophyll-a Fluorescence

### 3.4.1 Basics

Some of the photons absorbed by a Chla molecule in the blue part of the spectrum are re-emitted as less energetic photons in the red part of the spectrum. This rapid ( $\sim$ nanosecond) process is known as fluorescence and actually corresponds to the relaxation of the excited Chla molecule to its ground state. The light emitted through

Chla fluorescence,  $F$  (mole quanta  $\text{m}^{-3} \text{s}^{-1}$ ), can be roughly expressed through:

$$F = E[\text{Chla}]a^*\phi_f, \quad (3.9)$$

where  $E$  is the excitation irradiance (mole quanta  $\text{m}^{-2} \text{s}^{-1}$ ) (corresponding to either sun irradiance (i.e. sun-induced fluorescence) or to irradiance provided by a light source; only the latter is considered here);  $[\text{Chla}]$  is the concentration of the pigment Chlorophyll-a ( $\text{mg m}^{-3}$ );  $a^*$  is the Chla-specific absorption coefficient [ $\text{m}^2 (\text{mg Chla})^{-1}$ ] and  $\phi_f$ , the fluorescence yield [mole quanta emitted (mole quanta absorbed) $^{-1}$ ]. The *in vivo* fluorescence emission of Chla is centered at 685 nm. The excitation of the Chla molecule is triggered by the blue photons absorbed by the Chla molecule as well as by other photosynthetic accessory pigments (mostly carotenoids but also phycobiliproteins for some phytoplankton groups), which subsequently transfer their absorbed energy to the Chla molecule. As a consequence, the spectral shape of Chla excitation roughly matches the spectral domain of phytoplankton absorption.

### 3.4.2 Derivation of bio-optical and biogeochemical products

The biogeochemical product of interest here is  $[\text{Chla}]$ , the descriptor of phytoplankton biomass. Actually  $[\text{Chla}]$  is not a perfect descriptor of this biomass since photo-acclimation processes can cause the intercellular Chla content to vary with respect to cell numbers or phytoplankton carbon. Nevertheless, in the absence of any alternate proxy for phytoplankton biomass,  $[\text{Chla}]$  remains the most widely-used variable in biological oceanography. From Equation 3.9, and assuming that  $E$  is generated by a constant artificial source, fluorescence can be considered an accurate estimator of  $[\text{Chla}]$  on condition that the  $a^*\phi_f$  product is constant. In practice, this is not the case in natural waters (Babin, 2008 and references therein). The Chla-specific absorption coefficient,  $a^*$  [ $\text{m}^2 (\text{mg Chla})^{-1}$ ] has been shown to be dependant on the size structure of the phytoplankton assemblages as well as on the relative contribution of accessory pigments (carotenoids) with respect to  $[\text{Chla}]$  (Bricaud et al., 1995; 2004). At large scales,  $a^*$  covaries with  $[\text{Chla}]$  (Bricaud et al., 1995): Chla-rich waters, where large phytoplankton cells predominate, are associated with low  $a^*$  coefficients, and vice versa. The relationship between  $a^*$  and  $[\text{Chla}]$  at large scales can be approximated by a power function (Bricaud et al., 1995) but use of such global relationships at regional scales should be undertaken with caution.

The most obvious evidence of the variability in  $\phi_f$  comes from the analysis of time series of fluorescence over a period of time so short that it can be assumed that  $a^*$  does not vary significantly. It has been shown that the most important source governing  $\phi_f$  variability is the ambient irradiance. The changes can occur from very short time scales e.g. in response to cloud passage (Abbott et al., 1982) to a

response to the diel cycle (Claustre et al., 1999). During a daily cycle it is indeed well-known that, in the upper layers, fluorescence per unit chlorophyll-a systematically decreases during periods of increased irradiance with the most pronounced effect at noon. This process, known as daytime fluorescence non-photochemical quenching, results both from damage to the photosynthetic apparatus, and from certain physiological adjustments. The magnitude of daytime fluorescence quenching has also been shown to vary with seasonal variation in surface irradiance (Sackmann and Perry, 2008). With respect to developing procedures for mitigating the effect of physiological causes impacting the  $F$  vs [Chla] relationship, and for reducing the uncertainties in the estimation of [Chla], several recommendations can be made. The first recommendation is to perform profiles at night. Indeed nighttime measurements, being unaffected by fluorescence quenching, provide the most reliable estimates of [Chla] in the upper layer. This recommendation can be fulfilled by certain types of floats/missions but not with others (see Chapter 5). In particular, when irradiance profiles have to be performed as sea truths simultaneously with satellite overpass, day profiles (often around noon) are obviously required. In such cases, the combination of simultaneous irradiance and fluorescence measurements can be used to back calibrate the fluorescence sensor using appropriate bio-optical models (Xing et al., 2011).

In well-mixed conditions, all biological properties are expected to be homogeneous within the mixed layer. However, fluorescence profiles in surface layers at noon sometimes present some features departing from homogeneity and typical of fluorescence quenching (Figure 3.3). These subsets of profiles can be corrected *a posteriori* by extrapolation of deep fluorescence values (at the level of the mixed layer depth) towards the surface layer. One could also use other bio-optical properties ( $b_{bp}$ ,  $c_p$ ), if measured, to correct for quenching (Behrenfeld and Boss, 2006 Sackmann and Perry, 2008). When the float and the satellite measurements are simultaneous, the satellite [Chla] can also be used to constrain the surface [Chla], (e.g. within the first penetration depth) derived from the fluorescence profile. This correction scheme would have to be used with caution, as it implies that *in situ* measurements could not serve in such cases as sea-truths for satellite measurements.

At this stage, the above recommendations for improving the retrieval of [Chla] from fluorescence are only indicative. Future research using different methods applied to fluorescence data acquired by floats deployed at different locations may help to develop robust procedures. In any case, given the variability in observed Chla-fluorescence relationships,  $\pm 50\%$  in [Chla] accuracy should be a targeted objective for measurements performed by a fluorescence sensor mounted on a float. In the future, absorption based sensors (e.g. Davis et al., 1997), could allow us to avoid the  $\phi_f$  issue altogether.

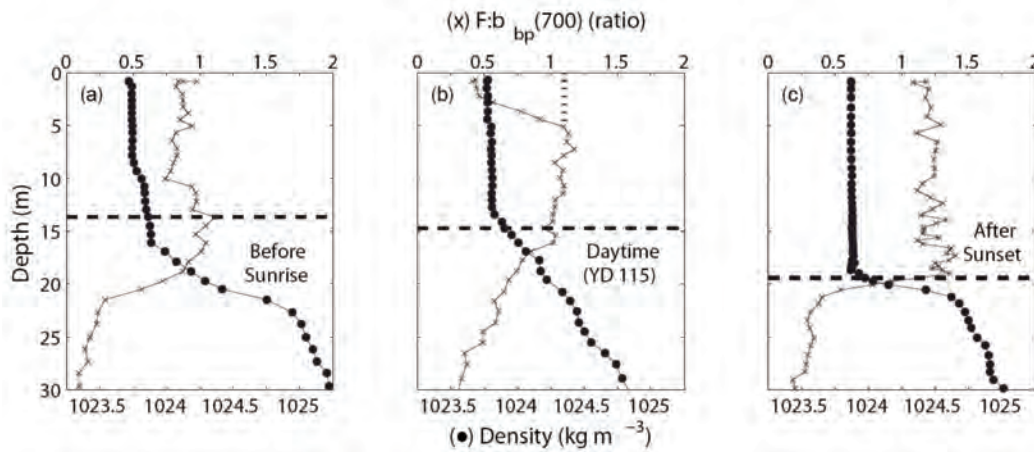


**Figure 3.3** Fluorescence quenching at noon as highlighted by the day-time variation in Chla fluorescence-to-backscattering ratio,  $F:b_{bp}(700)$  (x). Data acquired by a glider equipped with a bio-optical package in the North East Pacific. The dotted line corresponds to the basis of the mixed layer. After Sackmann and Perry (2008).

## 3.5 Other Measurements

Beside the core bio-optical measurements described above, there are other optical properties, which deserve to be measured through profiling floats. These measurements cannot yet be recommended as core measurements for various reasons, e.g. because the sensors are still in prototype phase, or their implementation on floats is challenging and still requires prior testing and validation. We nevertheless believe that performing these measurements in the near future is important with respect to a better characterization of optical and biogeochemical oceanic properties. These measurements are described in the section below.

### 3.5.1 Birefringent photons

#### 3.5.1.1 Basics

Birefringence refers to the ability of a mineral crystal to split an incident beam of linearly polarized light into two beams of unequal velocities (corresponding to two different refractive indices of the crystal), which subsequently recombine to form a beam of light that is no longer linearly polarized (Rossi, 1957).

#### 3.5.1.2 Derived bio-optical or biogeochemical products

The extreme birefringence of  $\text{CaCO}_3$  makes it appear to light up when the sample is held between crossed polarizers and viewed using transmitted light. This characteristic mineralogical property of  $\text{CaCO}_3$  is widely used as a means of identification.



Mineral particles in the ocean are dominated by calcium carbonate particles, which have an oceanic concentration range of 0.005 to 40  $\mu\text{m}$ . It has been demonstrated that a bench top spectrophotometer can be used to detect particulate inorganic carbon (PIC) (Guay and Bishop, 2002). Experiments with varying coccolith suspensions with and without dilution, by increasing amounts of non-birefringent material, have established a linear concentration response to PIC. The measurement of birefringent photons requires simultaneous measurement of transmission to correct for scattering losses, although these losses are minor in most cases.

$$B = B_{obs}/T^{0.5} \quad (3.10)$$

where  $B$  = corrected birefringence,  $B_{obs}$  = raw birefringence signal and  $T$  (%) is the measured fractional transmission (relative to particle free water) at the same wavelength. A low power (<0.5 W) PIC sensor (Figure 3.4) has been CTD-profiled to more than 2,000,000 m (surface to bottom) from ships in diverse ocean environments ranging from the poles to the equator, including oligotrophic to coastal and oxic to sub-anoxic environments (Bishop, 2009). Increasingly refined versions of the PIC sensor have been tested against calibration samples during the CLIVAR A16N expedition in the North Atlantic (Figure 3.4) and subsequent expeditions. The current fourth generation sensor has a precision of 5-10 nanomoles  $\text{l}^{-1}$  PIC in the deep ocean (Figure 3.4) and a calibration response that varies by less than a factor of two amongst diverse ocean environments.

### 3.5.2 Coloured dissolved organic material

Fluorescence sensors for CDOM are currently commercial and on some occasions, have been implemented on profiling floats. When the fluorescence CDOM measurements are combined with simultaneous radiometric measurements at 412 nm it is possible to retrieve a continuous profile of CDOM absorption (Xing et al., submitted). Preliminary results from a float equipped with such a sensor and deployed in the North Atlantic highlighted a clear change in deep FCDOM (CDOM fluorescence) when the float drifted from the Icelandic basin into the Norwegian basin. This signal in the "old" CDOM signature is likely a signature of changing water masses (Figure 3.5).

To date, the CDOM fluorometers that have been implemented onto floats (e.g. ECO from Wetlabs) generally have low signal-to-noise ratios around 5-10 counts, at best, and even less than 1 count in the top 50 m in the South Pacific Gyre (Xing et al., submitted). This relatively weak sensitivity is partly due to a non-optimal wavelength excitation/emission pair (EX370/EM460). The examination of an excitation-emission matrix (EEM) for an open ocean CDOM sample shows that this wavelength pair is located in a very low fluorescence domain, and is close to a region associated with terrestrial humics ('C' region, *sensu* Coble, 1996). This implies that the instrument is probably most useful in high-CDOM coastal areas dominated by runoff or riverine input, or more aged CDOM.

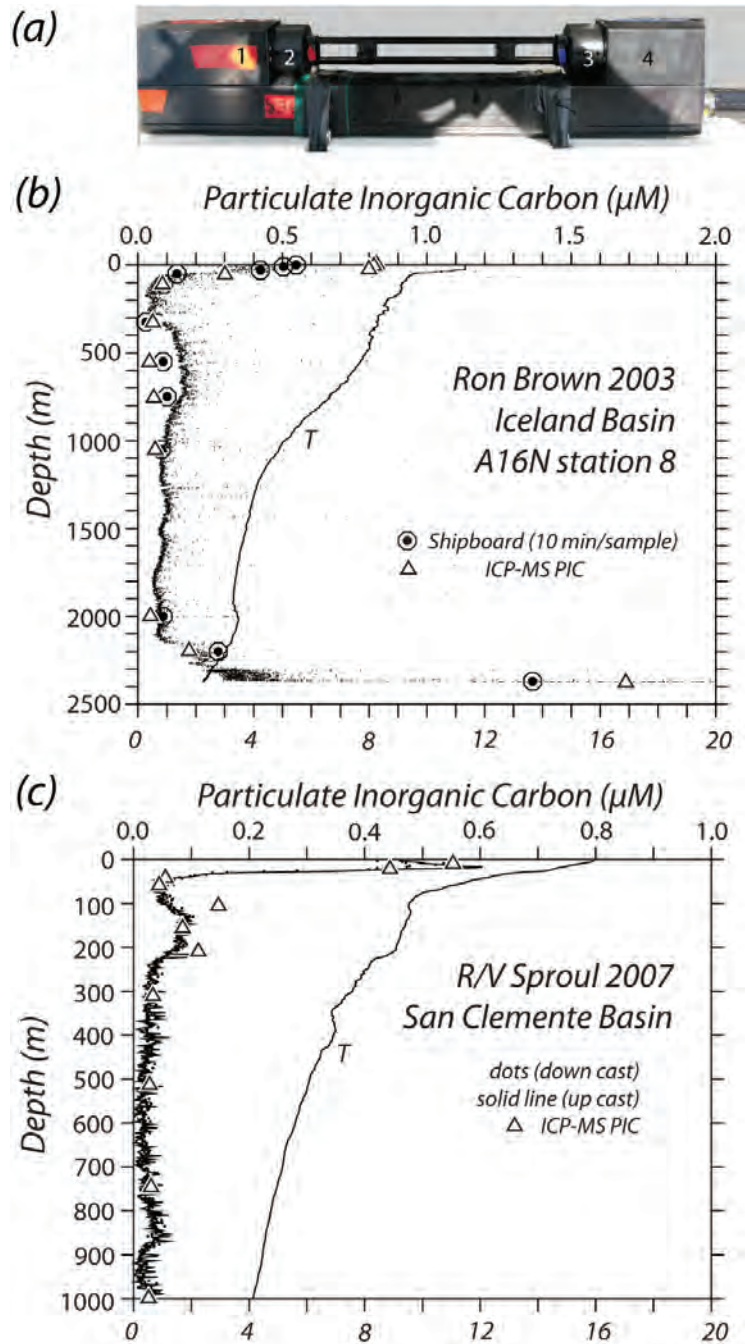


**Figure 3.4** Birefringence measurements and PIC quantification. (a) In a modification of a 25 cm pathlength WETLabs Inc. C-Star transmissometer, light from a 660 nm light emitting diode laser source (1) is filtered (2) such that it is polarized in the horizontal plane while at the same time the detector (4) on the other end of a 25 cm open water path is guarded by a second high efficiency polarizer (3) oriented to select only for vertically polarized light. In this way, the primary beam of light from the laser is blocked from passing to the detector. Suspended calcium carbonate minerals in the optical path partially depolarize the primary beam and thus give rise to a signal at the detector. (b) Optically-resolved PIC and ICP-MS measured PIC in the Icelandic Basin. (c) Optically-resolved PIC and ICP-MS measured PIC in the San Clemente basin.

From preliminary CLIVAR data, Nelson et al. (unpublished) have shown that ‘newly produced’ CDOM in the open ocean contains chromophores that are not fluorescent in the bands sampled by the ECO CDOM fluorometer. However, in the main thermocline and in the deep ocean, FCDOM from the ECO correlates well with CDOM absorption, suggesting that the chromophores at depth differ from the ones seen near the surface. In conclusion, measurements of CDOM by Argo floats have great potential, not only for bio-optical studies but also for the potential characterization of water masses.

### 3.5.3 Absorption and scattering coefficients

Absorption and scattering coefficients are routinely measured with *in situ* profiling instruments deployed from ships (e.g. "ac-9" or "ac-s" from WET Labs). However, several elements linked to the configuration and the mechanical concept of these instruments (pumping system, bio-fouling within sampling chambers, drift in pure water offset measurements) currently inhibits an operational deployment on Argo floats, although these measurements are desirable as they provide information on particle concentration, phytoplankton absorption, pigment concentration, and index of particle size distribution.

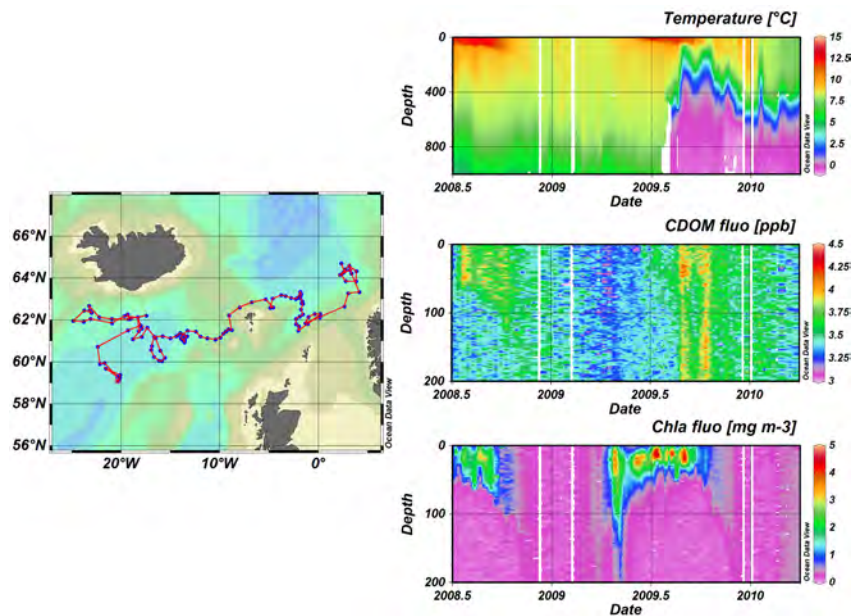


**Figure 3.5** Time-series (22 months) of a PROVOR float equipped with a bio-optical package (ECO from Wetlabs) during its travel in Icelandic and Norwegian basins. The change of water masses is highlighted by the cold deep water, typical of Norwegian basin deep waters. This change is clearly traced by an enhancement of CDOM fluorescence. A sub-surface relative maximum in CDOM is also recorded at the beginning of the observational period, associated with high [Chla] ( $\sim 2\text{-}4 \text{ mg m}^{-3}$ ) in the mixed layer (Claustre et al. unpublished data).

## Chapter 4

# Sensor Requirements

---

## 4.1 Radiometers

Only multispectral radiometry is taken into account in this section, considering the currently-available technology. Recommended sensor specifications include:

- ❖ Accuracy should remain better than 2% of the magnitude of the optical signal as a function of time relative to the pre-deployment calibration (this implies the use of high quality spectral filters);
- ❖ Dynamic range: 5 decades, minimum;
- ❖ Typical saturation value for irradiance sensor:  $500 \text{ W cm}^{-2} \text{ nm}^{-1}$  (400 - 800 nm);
- ❖ Typical saturation value for radiance sensor:  $10 \text{ W cm}^{-2} \text{ nm}^{-1} \text{ sr}^{-1}$  (400 - 800 nm);
- ❖ Acquisition frequency: 6 Hz minimum (sufficient when combined with a low profiling float velocity,  $\sim 0.1 \text{ m s}^{-1}$ );
- ❖ Spectral full-width at half-maximum (FWHM): 10 nm maximum;
- ❖ Field of view for radiance sensor:  $10^\circ$  half angle in water.

In addition, a number of other issues have to be taken into consideration.

- ❖ Immersion factors of irradiance/radiance sensors as well as cosine response for irradiance collectors should be well defined.
- ❖ Before deployment, sensors should be pressure cycled several times (at least 10) to a depth of 130% of maximum depth in planned mission. Sensors should be set such that the dark counts could be monitored through the pressure test.
- ❖ Sensors should be calibrated immediately before launch using the latest acceptable techniques. Cross calibration with other *in situ* sensors is highly recommended (e.g. with nearby moorings, with a profiler during cruises). A post-deployment calibration of all sensors is an essential requirement when the retrieval of the float is possible.
- ❖ To minimize the effect of sedimentation of particles on collectors orientated upward ( $E_d$ ) and bio-fouling on all windows, sensors could be equipped with bio-shutter systems, although this represent an additional energy consumption. This device should perhaps be restricted to VAL-floats that are operated in the

upper surface layer. Note that parking floats at depths below the euphotic zone (and associated cold water) minimizes bio-fouling, and this simple procedure should be a key consideration in mission design. This procedure is especially adapted for BIO-Argo floats.

## 4.2 Scattering Sensors

### 4.2.1 Back-scattering meter

A back-scattering meter should provide the back-scattering coefficient for particles,  $b_{bp}$ , at three wavelengths preferentially matching the radiometers wavelengths (e.g. blue, green, near-infrared). By definition total  $b_b$  estimation requires measuring light scattered on a full hemisphere. *De facto* measurements at a single plane (i.e. assuming azimuthal symmetry) and at a single angle have been found to provide  $b_b$  with an uncertainty smaller than about 10% (Boss and Pegau, 2001). This feature resulted in the development of simple flat-faced sensors for the measurements of  $b_b$  (Maffione and Dana, 1997) which are amenable for deployment on autonomous vehicles. The spectral behavior of  $b_{bp}$  has been found to exhibit features mirroring those of absorption i.e. in bands where the absorption has peaks  $b_b$  has troughs (Ahn et al., 1992). It is important that a secondary standard, e.g. a reflecting plate positioned at a fixed distance from the sensor's face in air, be developed; such a standard will provide a pre-deployment test that the sensor has not been damaged during shipping as well as a cross-check for sensors measuring  $b_b$  at different wavelengths.

Recommended back-scattering sensor specifications are as follows:

- ❖ The nominal angle has to be centered between 110 to 150 with a half-angle width smaller than 20.
- ❖ The spectral FWHM is smaller than 20 nm.
- ❖ The pathlength is smaller than 20 cm (to avoid the need for along-path attenuation correction).
- ❖ The calibration should measure dark counts as well as the scaling factor. The temperature sensitivity of these parameters (in the range 2 - 30°C) must be provided (at least tested on several sensors to determine its influence on the accuracy).
- ❖ The precision in the volume scattering function should be better than  $0.000005 \text{ m}^{-1} \text{ sr}^{-1}$ .
- ❖ The measurement range is between  $0.00001$  and  $0.005 \text{ m}^{-1} \text{ sr}^{-1}$ .
- ❖ The accuracy should be  $\pm 15\%$  throughout the range.
- ❖ NIST traceable calibration with uncertainty in scaling factor should be done.

### 4.2.2 Turbidity sensor

A turbidity sensor measuring the scattering of light over 45 to 145° at 810 nm has been shown to be reliable and repeatable on both CTD's, floats and gliders (Bishop et al., 2002; Bishop and Wood, 2008). The signals from such simple sensors are a valuable cross check on transmissometers and more complex meters described above. A (back) scattering meter or a turbidity sensor is an excellent sensor for particle concentration (Boss et al., 2009c). Near-surface POC optical proxy relationships suggest that a ±50% error in estimated POC may be expected. However, this relationship fails in deeper waters.

Recommended turbidity sensor specifications are as follows:

- ❖ The scattering measurement should be performed within 45° - 135°, preferably in the near-infrared.
- ❖ The accuracy and precision should be better than 10<sup>-3</sup> Fomazin Turbidity Units (FTU).
- ❖ The power requirements should be less than 0.1 W.

## 4.3 Transmissometers

Transmissometers have had three decades of development and have been widely deployed on ship-lowered CTDs as well as moorings, and since 2001, on profiling floats. The beam attenuation is most often estimated by measuring the loss of light energy of a collimated beam by a receiver at a fixed distance from the light source. The computation of the beam attenuation coefficient,  $c_p$ , is based on the following equation:

$$c_p = (-1/r) \ln(T/T_w) \quad (4.1)$$

where  $r$  is the beam pathlength (m),  $T_w$  (%) is transmission for particle-free 'pure' water and  $T$  (%) is the measured transmission. Measurement constraints require the detector to have a finite aperture, resulting in some of the forward scattered light not being accounted for as scattered (Pegau et al., 1995; Bishop and Wood, 2008; Boss et al., 2009b). Forward scattering is strongly dependent on the particle size (light scattered from larger particles has a larger fraction in the forward direction), and results in the particle size having an effect on the measurement (Baker and Lavelle, 1984); this effect, however, may be cancelled if the large particles are aggregates (Boss et al., 2009a).

Particle beam attenuation coefficient,  $c_p$ , has been shown to depend on the detector acceptance angle (AA) of the instrument, and can vary by as much as a factor of two (Bishop and Wood, 2008; Boss et al., 2009b) between instruments. Early instruments (1 m and 25 cm Sea Tech transmissometers: AA = 0.5°) are twice as sensitive as more modern instruments (WETLabs Inc., C-Star: AA = ~1°) due to the increased detection of forward-scattered light by the modern instruments (Bishop

and Wood, 2008). Some transmissometers also have divergent beams from source to detector thus increasing the excitation volume for forward scattered light.

This point is critical in the context of building a self-consistent, global database of the beam attenuation coefficient by implementing transmissometers on floats. Therefore it is strongly recommended that the acceptance angle of the instrument will (1) be the same for all the transmissometers that will be part of a float array; (2) be well characterized by the manufacturers to prevent any inter-instrument variability; and (3) ideally correspond to one of the nominal acceptance angles already used in previous studies ( $0.5^\circ$ ,  $0.93^\circ$  or  $1.03^\circ$  or  $1.2^\circ$  or  $1.5^\circ$ ; see Bishop and Wood, 2008; Boss et al., 2009b) allowing possible comparisons with historical data sets. Given the fact that some bio-fouling of these sensors occurs, and that beam collimation is important, it is recommended that transmissometers mounted vertically on floats be oriented with the source window looking downwards. Additionally the transmissometer specifications should be in accordance with the following recommendations:

- ❖ The central wavelength should be 650-660 nm with a spectral FWHM smaller than 20 nm;
- ❖ Standard pathlength should be 25 cm;
- ❖ The measurement should cover the  $0.005$  to  $4 \text{ m}^{-1}$  range, with a precision better than  $0.001 \text{ m}^{-1}$ , and an initial deployment accuracy of better than  $0.001 \text{ m}^{-1}$  or 5% of  $c_p$ , which ever is greater;
- ❖ Calibration: dark voltage (or counts) and transmission in air readings are to be made through float digitizing electronics prior to launch;
- ❖ Temperature sensitivity of the dark voltage and transmittance (in the range -2 to  $30^\circ\text{C}$ ) must be provided (or tested on candidate sensors to determine its influence on the accuracy);
- ❖ The power requirements should be less than 0.5 W;
- ❖ Candidate sensors should be profiled from ships' CTDs to demonstrate lack of hysteresis/temperature/pressure effects.

## 4.4 Chla Fluorometers

All Chla fluorescence sensors rely on the detection of red light emitted by water when excited by blue light. It is essential that the optical characteristics (wavelength and bandwidth) of these sensors are accurately determined and reported in a dedicated sensor specification sheet. In open ocean waters, the surface [Chla] ranges from  $0.02 \text{ mg Chla m}^{-3}$  (center of subtropical gyres) to  $\sim 20 \text{ mg Chla m}^{-3}$  (upwelling conditions). A Chla fluorescence sensor implemented on a float would thus have to cover this Chla range with a sensitivity of  $0.001 \text{ mg Chla m}^{-3}$ . Given that the conversion of the fluorescence signal to Chla is based on a linear equation with a constant denoting the dark signal, it is strongly advised that the dark signal be measured several times

prior to deployment and that its sensitivity to temperature and pressure be known.

Besides sensor specification, there is specificity in the measurements that are linked to long-term deployments. Indeed, from Equation 3.9, it appears that the long term stability of the excitation light ( $E$ ) is critical for performing reliable measurements over time (or at least a reference reading is required) because it determines the intensity of the emission. On the one hand, organic non-phytoplankton material deposited on the optical face(s) act as quenchers of the exiting light. On the other hand, bio-fouling by Chla-containing material would enhance the fluorescence signal. All these issues linked to long-term deployments have to be acknowledged, identified and possibly mitigated. Therefore, it is first recommended that the Chla fluorescence sensor should be mounted at  $90^\circ$  with respect to the float axis, or looking downwards to avoid sedimentation of material. Furthermore, parking floats at a depth below the euphotic zone and in cold environments is a simple and key procedure for mitigating the possible effect of bio-fouling over long term measurements. Finally, recording fluorescence at depth (for example at parking depth) is essential to identify any drifts in the signal that would be linked to these sources of contamination and to develop appropriate correction schemes, if needed. Recent results (Boss et al., 2008a) suggest that profiling to 1,000 m every 5 days is sufficient to avoid significant drift in the measurements for over 3 years (see Figure 4.1, also Figure 2.2).

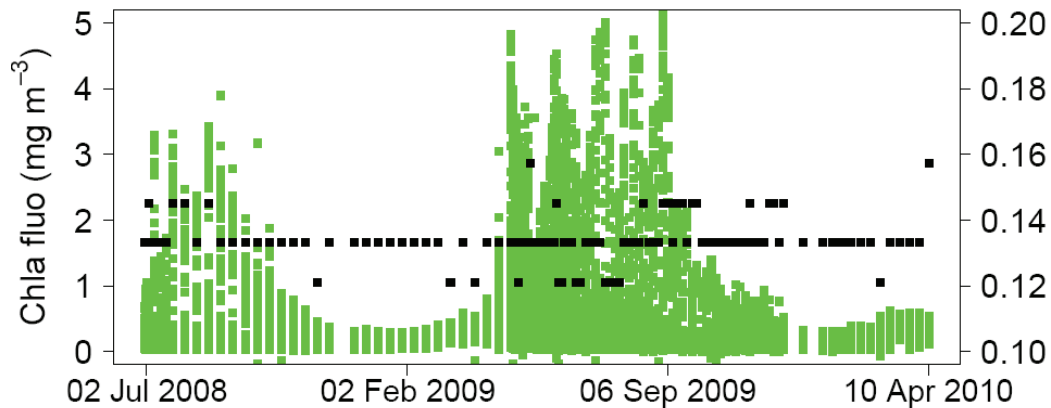


**Figure 4.1** Twenty two-month time-series of deep Chla fluorescence (black squares, scale on the right side) acquired by a PROVOR float equipped with a bio-optical package (ECO from Wetlabs) during its travel in the Icelandic and Norwegian basins. Most of the time, these measurements (average of 5 min acquisition) were performed at 1,000 m, just prior to float ascent. In some cases, the bathymetry was less than 1,000 m (e.g. when the float was in the transition zone between both basins) so that the float hit the bottom. The dynamics of [Chla] in the upper water column is presented (green squares) on a separate scale. After Claustre et al. (unpublished results).

To ensure the consistency of Chla measurements performed by various sensors (from single or different manufacturers) and hence to guarantee the consistency of



the forthcoming global float-based Chla database, a reference material (e.g. fluorescent and temporally-stable material embedded in a specific matrix or gel) should be available for quality control of sensors over time. A first record of this reference material should be performed following factory calibration. A second measurement should be performed immediately before the float deployment allowing a characterization of the sensor response. These records together with sensor specification should be included in the metadata transmitted to the data center (see Chapter 7). Optimally, and whenever possible, [Chla] should be determined (ideally with the HPLC technique) for selected water samples taken at the time of the float deployment (this information should also be included in the metadata of the float).

## 4.5 Birefringence Sensors

The recommended sensor specifications are as follows:

- ❖ The central wavelength should be 650-660 nm with a spectral FWHM smaller than 20 nm;
- ❖ The out of band/stray light energy is less than  $1.5 \times 10^{-7}$  of primary beam energy;
- ❖ The polarizer crossing efficiency is greater than 50,000:1 at central wavelength;
- ❖ Full scale response (digital/analog)  $1 \times 10^{-5}$  of primary beam energy;
- ❖ Receiver acceptance angle is similar to transmissometer;
- ❖ Beam collimation is similar to transmissometer;
- ❖ Pathlength same as transmissometer (typically 25 cm);
- ❖ The digital/analog accuracy/precision is better than 1:4096 (12 bits minimum);
- ❖ The stability (T -2° to 30°C) is better than 0.05% of full scale reading;
- ❖ The linearity, established using neutral density filters, is characterized by a coefficient of determination  $r^2$  greater than 0.9999;
- ❖ The power requirements are less than 0.5 W;
- ❖ The calibration, using neutral optical density filters (e.g. OD 4.3 - OD 7), should confirm the linearity and sensitivity stray light, and dark current readings of the birefringence sensor.

## 4.6 Other Sensors

### 4.6.1 Oxygen sensors

The scientific potential for oxygen sensors deployed on floats has been demonstrated by Kortzinger et al. (2004), Riser and Johnson (2008), and Martz et al. (2008), amongst others. Gruber et al. (2007) have synthesized much of this data and explored the potential for deploying oxygen sensors in large numbers. Although some

technical developments are still desirable, particularly with regard to improvements in initial sensor calibration, oxygen sensors appear to be ready for deployment throughout the ocean in large numbers.

#### 4.6.2 Optical nitrate sensors

Deployments of profiling floats equipped with the *in situ* ultraviolet spectrophotometer (ISUS) optical nitrate sensor (Johnson and Coletti, 2002) began in 2007. These sensors have been operated successfully for nearly one year on profiling floats. The nitrate sensor is capable of low power operation. The current ISUS design requires only 40 joules for a single nitrate measurement beginning with the instrument in a low power state. If 60 nitrate measurements are collected from 1,000 m to the surface, then the ISUS would account for about 15% of the total float energy budget (including communications, sensors, pumps, and battery self-discharge). The overall power budget for a Webb Research Apex float with Iridium communications implies that the float should have the capacity for 280 profiles from 1,000 m with 60 observations of nitrate and oxygen per profile and 500 observations of CTD. These floats would operate for nearly four years at a five-day time cycle.

#### 4.6.3 CDOM fluorescence sensors

More dedicated research is required to assess the significance of the CDOM fluorescence signal before operational deployments could provide scientifically relevant measurements. In particular, a device that might be more sensitive to 'marine humics' and would be closer to the so-called 'M' region (Coble, 1996) (EX312/EM400) is highly desirable, or perhaps one that is sensitive in the region where aromatic amino acids fluoresce (EX275/EM310-350). Currently, the state of the art technology does not seem to be capable of utilizing these wavelengths in a convenient low-consumption package similar to the ECO fluorometers.

The factory calibration of CDOM fluorometers is generally based on quinine sulfate equivalent. It is currently the most community accepted calibration procedure although obviously not practical optical metrics. There is thus also a research area (admittedly not specific to float measurements) to better exploit CDOM fluorescence signal and its significance in the future (see for example Xing et al., submitted).



## Chapter 5

# The Different Types of Floats and Missions

---

Three main types of floats and associated missions are described in this section. The VAL-floats will be totally dedicated to validation activities. The BIO-Argo floats will support biogeochemical studies as well as validation activities. They will be developed and deployed in the context of Argo-related activities and thus will adhere strictly to Argo rules. The Carbon-Explorer floats will have more flexibility with respect to the diversity of measurements as well as temporal resolution of sampling; these floats will be dedicated primarily to detailed biogeochemical investigations.

The various missions and their associated constraints are described for each float in the following section. The generic description of the core measurements (see Table 5.1), sometimes shared by the different types of floats, can be found in Chapter 3 while the sensor specific requirements and constraints are detailed in Chapter 4. Here, the measurement and sensor specifications with respect to the float and missions are discussed.

## 5.1 The VAL Mission

### 5.1.1 General objectives

The primary objective of a VAL-float is to acquire accurate and frequent profiles of radiometric and associated biogeochemical data contemporaneous to ocean-colour satellite overpasses. These floats will be operated as part of an array that will allow satellite sea truths to be acquired globally. Given the very specific objectives of the VAL mission and the considerable differences from the standard Argo physics-oriented mission, this array will be operated independently. Standardized measurement protocols and associated data processing will be developed which is essential to guarantee the consistency and the overall quality of validation databases, in conjunction with the increasing number of validation match-ups.

### 5.1.2 Measurements and specific requirements with respect to mission objectives

For the purpose of validation, associating radiometric measurements with biogeochemical ones is mandatory. The VAL-float will thus have the measurements listed in Sections 5.1.2.1 to 5.1.2.3 performed as a priority (see also Table 5.1).

**Table 5.1** The primary variables and their derived products associated with the three types of floats. "X" refers to a mandatory measurement for a specific float, while "(X)" signifies an important but optional measurement. This list does not take into consideration other measurements not related to ocean colour (e.g. NO<sub>3</sub>, O<sub>2</sub>), but that are highly recommended companion measurements for specific floats.

Primary measurement	Derived product	VAL	BIO-Argo	Carbon-Explorer
Temperature (°C)		X	X	X
Conductivity (S m <sup>-1</sup> )	Salinity	X	X	X
$L_u(\lambda)$ (W m <sup>-2</sup> sr <sup>-1</sup> nm <sup>-1</sup> )	$K_{Lu}(\lambda)$ (m <sup>-1</sup> ) $nL_w(\lambda)$ ( $\mu$ W cm <sup>-2</sup> nm <sup>-1</sup> sr <sup>-1</sup> ) $R_{rs}(\lambda)$ (sr <sup>-1</sup> )	X		
$E_d(\lambda)$ (W m <sup>-2</sup> nm <sup>-1</sup> )	$K_d(\lambda)$ (m <sup>-1</sup> ), $R_{rs}(\lambda)$ (sr <sup>-1</sup> )	X	(X)	
$b_{bp}(\lambda)$ (m <sup>-1</sup> )	[POC] (mg POC m <sup>-3</sup> ) Size index (r.u.)	X	X	(X) (X)
PAR (mole quanta m <sup>-2</sup> d <sup>-1</sup> )	$K_d$ (PAR) (m <sup>-1</sup> )	X	(X)	
$c_p(660)$ (m <sup>-1</sup> )	[POC] (mg POC m <sup>-3</sup> ) Carbon Flux Index (r.u.) Net Community Production (mg POC m <sup>-2</sup> d <sup>-1</sup> )		(X)	X X X
Turbidity (810 nm, FTU)	[POC] (mg POC m <sup>-3</sup> )	(X)	(X)	X
Chla fluorescence (mole Quanta m <sup>-2</sup> s <sup>-1</sup> )	[Chla] (mg Chla m <sup>-3</sup> )	X	X	X
CDOM fluorescence (mole Quanta m <sup>-2</sup> s <sup>-1</sup> )		(X)	(X)	(X)
Birefringent photons	[PIC] (mg PIC m <sup>-3</sup> )			X

### 5.1.2.1 Downward irradiance $E_d(\lambda)$ and upwelling radiance $L_u(\lambda)$

Multispectral radiometers are required with a minimum set of wavelengths that match the standard channels available on current and near-future satellite sensors, e.g. 412, 443, 490 nm for the blue, 555 nm for the green, 665 nm for the red, and, as a secondary requirement, 750 and 870 nm for the near-infrared in case the hypothesis of null water leaving radiance at these wavelengths needs to be tested<sup>1</sup>. Correct placement and orientation are essential for passive radiometric sensors measuring both the upward or downward light field. First, the sensor field of view must be free of any direct shadowing structure (e.g. antenna, cable, body of the float, etc). This is a more stringent requirement for irradiance sensors measuring the irradiance over the complete upward hemisphere ( $E_d$ ).

Secondly, the instrument housing induces a 'self-shading' effect by casting a

<sup>1</sup>Considering the float profiling speed ( $\sim 0.1$  m s<sup>-1</sup>), hyperspectral radiometry could become a valid (although costly) alternative in the near future

shadow and thus decreasing the amount of upward scattered light within a certain water volume. Such an effect is a function of the size of the instrument (here the float) and of the absorbing characteristics of the medium. It can induce errors greater than 50% for  $L_u$ . Although it is minimized in oceanic waters (except for wavelengths in the red and near-infrared parts of the spectrum where absorption by seawater itself is relevant) it cannot be neglected, as the diameter of a float itself (typically 20 cm) is relevant. The instrument self-shadowing effect can be corrected (Gordon and Ding, 1992; Zibordi and Ferrari, 1995; Mueller and Austin, 1995) with the help of ancillary variables measured simultaneously on the float (e.g. [Chla]) and allowing an estimation of the absorption in the medium.

Classical positions, although not free from float self-shading, are the center-bottom for  $L_u$  sensors and the centre top for  $E_d$  sensors. The latter may not be compatible with current Argo float configurations, as the float antenna placed on top could directly shadow several of the  $E_d$  collectors. Therefore,  $E_d$  and  $L_u$  sensors could be positioned at the end of light arms extending away from the float. As an example, preliminary Monte-Carlo simulations (Lemayrie, pers. comm.) show that errors due to self-shading are considerably reduced with respect to bottom/top positions for  $L_u$  if the sensor is on the sunlit side of the float (Figure 5.1). Tilt and compass sensors would thus be necessary to monitor the orientation of the float with respect to sun and to evaluate more precisely the importance of shadows (see the elevated errors for the sensors positioned on the "bad side" of the float with respect to the sun, Figure 5.1).

As an alternative to the compass, two  $E_d$  and two  $L_u$  sensors could be mounted on arms on each side of the float (Figure 5.2b). Such a configuration will guarantee that, for clear sky conditions, the  $L_u$  or  $E_d$  sensor will always be in the best position with respect to the sun. During overcast days, a cross comparison of both sensors will be possible allowing any drift or sensor evolution performances to be addressed. This possibility appears very useful with respect to controlling or developing correction procedures for ensuring the consistency of measurements over the long term. Having the sensors mounted on external arms positioned at the top of the float ("PROVOR side top" on Figure 5.2b) is the recommended solution for VAL-activities. Note that such sophisticated configurations, including external arms, are probably not applicable to BIO-Argo floats, for which the deployment procedure must be as simple as possible to be executed by non specialists. In this case the classical top/bottom position for  $E_d/L_u$  sensors will probably have to be retained, keeping in mind that radiometry is not a mandatory measurement for a BIO-Argo float, just an optional one (see later and Table 5.1). Finally, it should be emphasized that a tilt sensor (x and y directions) will simultaneously register the vertical orientation of the float.

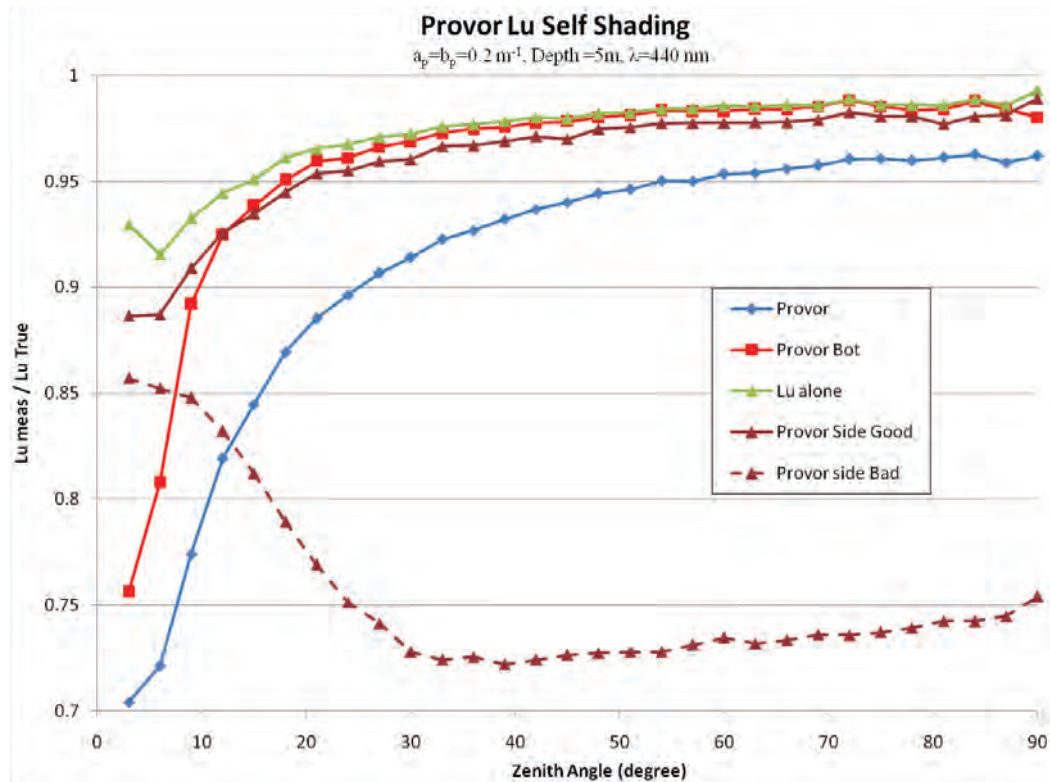


**Figure 5.1** Effect of sensor position with respect to the sun, on the accurate retrieval of  $L_u$ . For low sun zenith angles, errors due to self-shading are considerably reduced with respect to bottom/top positions for  $L_u$  when sensors are on the sunlit side of the float. The blue line corresponds to the  $L_u$  sensor positioned just below the float, the red line identifies the sensor placed one meter below the float bottom, the brown solid line is for a sensor on the sunlit side of the float, while the brown dashed line is for a sensor on the opposite side, and the green line corresponds to a sensor not affected by the float. These simulations of self shading were performed by using a Monte-Carlo method (SimulO program) for a depth of 5 meters. The optical parameters used were the optical parameters of pure water itself taken at 440 nm, both absorption and scattering coefficients equal to  $0.2 \text{ m}^{-1}$  and a volume scattering function with a backscattering ratio of 1.83% (Fournier-Forand). Image courtesy of Edouard Leymarie, Laboratoire d’Océanographie de Villefranche, France.

### 5.1.2.2 Backscattering coefficient

This measurement is essential for validating semi-analytical models e.g. general circulation models (GCM). One wavelength is sufficient for measuring  $b_b$ , preferably in a spectral domain not sensitive to absorption by biogenic substances. Thus 700 nm appears to be a reasonable choice. If the implementation of a second wavelength is feasible, then it is recommended that a near-IR wavelength be chosen (e.g. 810 or 870 nm) allowing the spectral dependency of backscattering to be determined from two sufficiently distinct wavelengths.

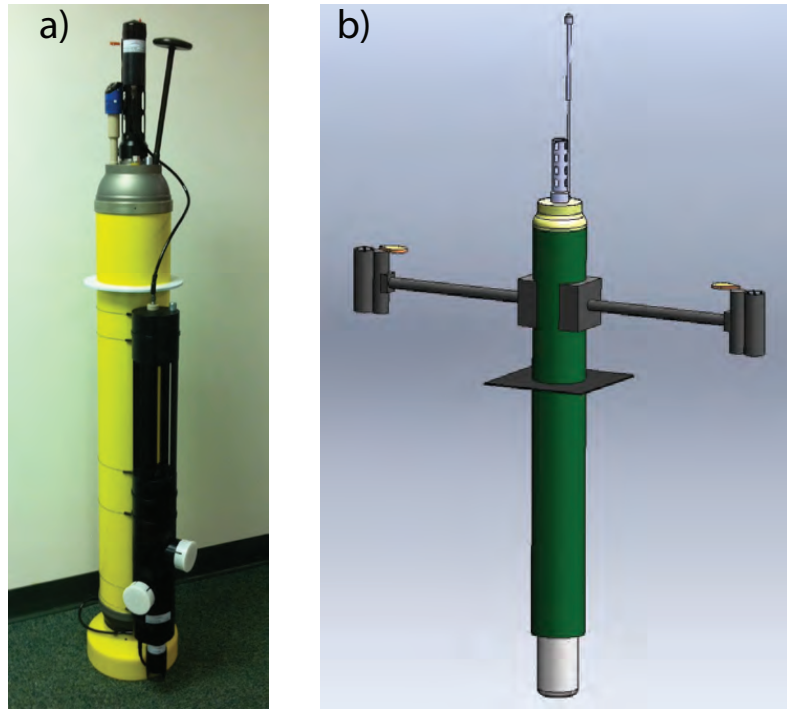


**Figure 5.2** Two examples of CAL/VAL floats: a) Apex cal/val float developed at the University of Maine (USA), and b) PROVOR cal/val float developed at the Laboratory of Oceanography in Villefranche-sur-mer (France).

### 5.1.2.3 Chla fluorescence

The primary biogeochemical product derived from ocean colour is [Chla] at the surface. Although Chla fluorescence is not the perfect estimator of [Chla] (see Section 3.4) it nevertheless remains the most widely used proxy.

### 5.1.3 Mission description and constraints

Whilst the data will offer considerably broader applications than direct satellite validation, maximizing validation matches will remain the principal mission driver. The following recommendations are thus proposed, taking into account the fact that no reference measurement of incident irradiance at the surface will be available and that the profiling speed is low ( $\sim 0.1 \text{ m s}^{-1}$  or even lower).

Two-way communication is essential for two reasons. First of all it will allow VAL-float match-ups to be optimized. It will indeed guarantee flexibility in sampling strategy that is essential to develop a cost-effective approach, i.e. performing the largest number of good match-ups during the float lifetime. In particular, taking into consideration forecasts of cloud cover conditions will allow for optimizing the sampling strategy. For expected cloud-free days, float-surfacing time will be phased with respect to the time of satellite overpasses and replicate or additional



measurements (see below) will be performed. For cloudy days, sampling could be relaxed. Iridium (or equivalent) telemetry is also essential for transmission of large amounts of data that will be acquired considering that high vertical resolution is required (~10 cm scale for radiometry) and multispectral (or hyperspectral) data will be acquired.

The surface layer (indicatively 0 - 200 m) should be sampled several times (at least three) around the satellite overpass on a match-up day. An additional series of at least three profiles in the very top layer (from 0 - 5 to 0 - 20 m, according to water optical status) would provide an estimation of the short-time variability of the irradiance impinging at the surface.

Sub-surface measurement,  $E_d(0^-)$  and  $L_u(0^-)$ , should also be performed over a ~15 min period while the float is drifting at the surface, and the mean and standard deviation of the spectra transferred, as an index of short-time variability at surface. Vertical sampling should get as close as possible to the water surface, for extrapolation of underwater quantities to the surface, and be performed with a high frequency to minimize the effect of waves. The corollary is that depth sensors should perform with a fine resolution at the scale of cm.

## 5.2 The BIO-Argo Mission

### 5.2.1 General objectives

The rationale for the development of such a float is to provide the biogeochemical community with an unprecedented quantity of (real-time) vertical profiles of a number of biological and bio-optical measurements. Obviously, this large bio-optical database would also satisfy the requirements of OCR satellite validation. This objective would be achieved by developing a generic, cheap, low consumption bio-optical/bio-geochemical payload that could be disseminated through the Argo network to take advantage of existing infrastructure. Besides providing data in chronically under-sampled time periods (e.g. winter, high latitudes) and/or locations (e.g. Southern Ocean), the dense and continuous data acquisition from a BIO-Argo network would support various scientific or operational topics, besides satellite validation, including:

1. The extension of the satellite signal to the ocean interior.
2. The validation of global circulation models coupled to global biogeochemical models with key variables.
3. The assimilation into (future) global biogeochemical operational models.
4. The extraction of statistical biogeochemical/bio-optical trends, with possible application in climate science, from the generated dense databases.
5. The identification of processes in the ocean interior not detected by ocean colour.

6. The validation of two main kinds of bio-optical models of primary production either based on Chla (Antoine et al., 1996; Behrenfeld and Falkowski, 1997) or on phytoplankton carbon (Behrenfeld et al., 2005).

### 5.2.2 Measurements and specific requirements

The bio-optical/bio-geochemical scientific payload recommended here has to correspond to a minimum set of "mandatory" measurements relevant to ocean bio-optics and biogeochemistry. Chla fluorescence and backscattering coefficients are the primary variables to be measured. Optionally, they could be complemented by other measurements (see later).

### 5.2.3 Mission description and constraints

A BIO-Argo float should adhere strictly to the standard Argo mission protocols with respect to frequency of cycles, depth range and resolution. Any deviation from these rules (e.g. sampling at meter-resolution rather than at fixed depths) should either correspond to an improvement for the Argo T/S acquisition, or have no impact. A number of improvements and nuances are therefore suggested.

Argos telemetry has been proven to be efficient in transferring fluorescence and backscattering measurements at the same time as T and S measurements, following the standard Argo depth resolution (Boss et al., 2008a). Yet Iridium communication satellites should also be considered for BIO-Argo floats because of the high-speed transfer rates. Firstly, a large amount of data can be transferred so that the vertical resolution of measurements can be increased (up to a resolution of meters), including that for T and S. Secondly, the time of transfer is very fast (tens of minutes) which has the advantage of limiting the sometimes high surfacing time of the float (hours to days for Argos). In addition, this can save a lot of energy, as transmission is energy consuming.

Because of fluorescence Chla quenching in certain oceanic areas during daytime, especially at noon, the measurement of Chla in the surface layer is sometimes biased. One way of circumventing this problem is to profile to the surface at night. If radiometric measurements are recorded by (some of) the BIO-Argo floats (optional measurement, see Table 5.1), the profiling should thus be performed at noon.

### 5.2.4 The BIO-Argo float in the context of Argo-related activities

These recommendations for BIO-Argo measurements are related to ocean-colour radiometry activities. Nevertheless they have to be considered as partial recommendations in the context of developing a more generic Argo-type float dedicated to biogeochemistry. Indeed, on going discussions with various communities (e.g. friends of oxygen of Argo) have converged on the identification of four primary variables to be implemented on autonomous platforms: Chla,  $b_b$ ,  $O_2$  and nitrate

are seen as essential variables to be measured (Claustre et al., 2010a). This recommendation results from a balance between scientific needs of the biogeochemical community on the one hand, and the maturity of the sensors vis-à-vis their integration onto autonomous platforms, on the other hand. Some important additional variables (e.g. pH) could be envisaged in the future as soon their measurements become operationally feasible. The development of a biogeochemical Argo-related float has to be undertaken in close interaction with the physical oceanographers of the Argo program. In particular, this would imply a strict conformation to Argo rules, which would thus limit the number of measured bio-optical variables, for energy budget reasons. Any additional cost linked to biogeochemical variables (e.g. cost of the equipment, additional consumption due to sensor, data management of new measurements) will have to be covered by additional resources from the ocean-colour and/or the biogeochemical communities.

## 5.3 The Carbon-Explorer Float Mission

### 5.3.1 General objectives

The entire ocean biomass turns over once per week and is responsive to the rapid changes of environmental variables (Bishop, 2009 and references therein). Particle concentrations exhibit large spatial and temporal variability over seasonal time scales or shorter (Boss et al., 2008b; Bishop and Wood, 2009). The mission of the Carbon Explorer (CE) float is thus to observe, optimally, carbon parameters and carbon-relevant parameters on time scale scales relevant to biological carbon productivity and carbon export processes. More specifically, the scientific outcomes of the Carbon Explorer float would be:

1. Development of physically-based parameterizations of carbon cycle processes. In other words, improvement of the predictive capability of ocean carbon simulations.
2. Measurement of diurnal changes in heat and stratification of the euphotic layer.
3. Definition of the diurnal variability of the light field experienced by phytoplankton.
4. Determination of current velocities in the upper thermocline (during drift periods).
5. Estimation of net community productivity for the entire photic zone.
6. Provision of PIC and POC concentration profiles to validate GCM-coupled global biogeochemical models.
7. Detection of the calcite saturation state of the water column.
8. Contribution to the validation of Level 3 satellite products (POC, PIC, NCP, export) for ocean-colour sensors.

### 5.3.2 Measurements and specific requirements

A prime requirement is to sample the diurnal (dawn-dusk) changes in carbon parameters. Sensors measuring IOPs thus form the primary payload. CE floats could be deployed within the Argo framework and mission profiling cycle (5 or 10 day) with a 10-15% mission cost for a pair of dawn/dusk profiles (by using a shallow parking depth between dawn and dusk) on each profiling cycle.

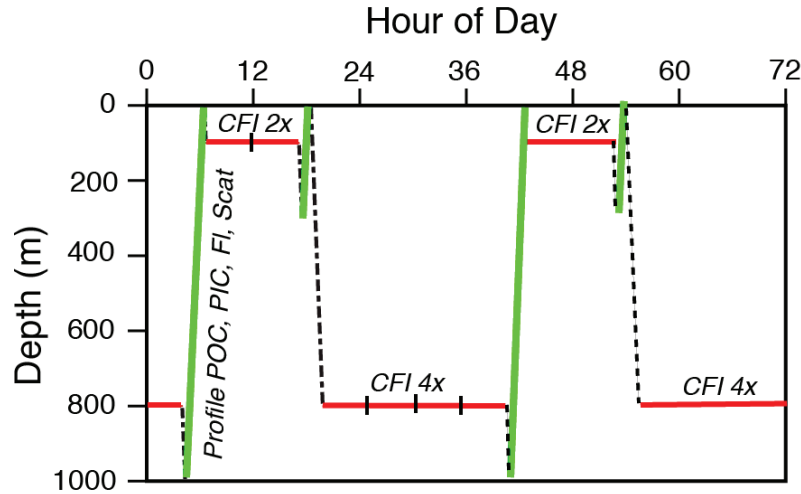


**Figure 5.3** Example of a typical Carbon-Explorer float mission allowing sampling of the vertical profile of relevant biogeochemical and bio-optical variables as well measurement of the carbon flux index during drifting periods.

### 5.3.3 Mission description and constraints

The Carbon-Explorer float will profile to the surface at local dawn and dusk measuring turbidity, (or  $b_{bp}(\lambda)$ ),  $c_p$  (660 nm), Chla fluorescence, and particle birefringence (PIC). The float should have the ability to ‘sleep’ at as many as three discrete depths for Carbon Flux Index (CFI) measurement. Derived products will be POC, PIC, and Chla concentration and possibly TSM (through combination of  $c_p$  and scattering measurements), and Carbon Flux Index. The float must have fast bidirectional satellite telemetry and ideally should have higher battery capacity than conventional Argo floats to permit missions lasting at least two years at higher frequency (double the current 400,000 m profiling capability of Carbon-Explorers and Argo Floats). Programming of the floats should be flexible and should allow control of the CTD pump for periodic CFI measurements at depth. Some CE floats should carry  $O_2$  sensors to test whether there is sufficient precision to track diurnal variations of  $O_2$  in the surface layer. The float design should anticipate the addition of sensors for dissolved carbon constituents as they become float ready. Mission protocols (e.g. Figure 5.3) and automated data reduction procedures have been developed as part

of the CE program (Bishop et al., 2002; 2004; Bishop and Wood, 2009).

### Technical Issues

---

#### 6.1 Life-Time, Bio-Fouling Deployment Issues

Upper ocean moorings have been used traditionally to support biogeochemical sensor deployments and have generated significant results at both the BATS and HOT time series sites (McGillicuddy et al., 1998; Emerson et al., 2002; Karl et al., 2003; Sakamoto et al., 2004). However, many sensors suffer from drift problems due to bio-fouling when they are held continuously in the euphotic zone. Consequently, there are relatively few multi-year time series observations of biogeochemical properties in the upper ocean that are based on autonomous sensors and which can be used to assess impacts of climate on biogeochemical processes.

Profiling floats have a significant advantage in that they can park the sensors in cold, dark, deep waters between each vertical profile. Minimal fouling is expected to occur under these conditions. Indeed, multi-year deployments of chlorophyll fluorometers, optical backscattering sensors, and oxygen sensors show only modest effects of fouling (Bishop et al., 2002; Kortzinger et al., 2004; Boss et al., 2008a; Riser and Johnson, 2008; Bishop, 2009). The recovery of a bio-optical float after two years of data acquisition in the Mediterranean Sea confirmed that bio-fouling is a relatively minor issue for fluorometers and backscattering sensors looking downwards, and even for downwelling radiometers (Claustre, unpublished results). Indeed, for the latter sensors, which are mounted on the upper part of the float, the surfacing of each float allows the sensor to be flushed when passing the ocean-air interface. Surface residence time, and hence bio-fouling risks, can be minimized by using high throughput telemetry (see next section), which is generally the case for such multi-sensor platforms.

The transmissometers, which are mounted vertically, are quite sensitive to the accumulation of sedimenting material on the upward-looking window, which can thus become a preferential site for bio-fouling. The use of the CTD exhaust to periodically 'blow off' particles from this window during parking periods and prior to the profile, is an interesting alternative that also provides a measure of sedimentation (CFI) (Bishop et al., 2004; Bishop and Wood, 2009). This procedure is recommended for Carbon-Explorer floats where the measure of sedimentation is also a target.

In summary, apart from transmissometry measurements, preliminary data sug-

gest that deployment of optical sensors on profiling floats is a highly effective mechanism for producing long-term records with little or no effect of bio-fouling. Despite this encouraging observation, it remains highly desirable to continue developing and testing procedures aimed at preventing or diminishing bio-fouling. This is especially relevant in light of the fact that longer lifetimes for floats, and hence sensors, are anticipated (see later). In particular, the use of copper plate/tape should become a standard. For the moment, active bio-fouling controls such as shutters, which are likely to have high energy consumption, have not yet been proven at depths greater than 300 m.

## 6.2 Communication

Argos, operated by CLS, is the main satellite operator for tracking and data transmission (about 95% of the Argo fleet are fitted with Argos transmitters). With respect to data transmission, a float equipped with a suite of optical sensors is obviously different from a classical Argo float which transmits three main variables (pressure, temperature and salinity) with a coarse vertical resolution ( $> 10$  m). It is highly desirable that a bio-optical sensor float acquires data with a high sampling rate, especially in the upper oceanic layer. The current Argos standard technology is not suitable for these sampling rates together with the acquisition of multiple variables. Despite being very reliable, Argos has a low transmission rate, which requires floats to stay at the surface for significant time, costing energy and possibly leading to more rapid fouling. Additionally, in certain areas such as the Mediterranean Sea, Argos transmission is extremely long ( $> 6$  hours to transmit TS data).

For multi-sensor floats with high spectral and spatial resolution (multi- or hyper-spectral, high vertical acquisition), alternative transmission to Argos is thus essential. The Iridium satellite constellation provides enhanced capabilities with high rates of data transfer and is now being used for multi-sensors floats. Iridium also presents the advantage of bi-directionality allowing commands to be sent to the floats. This is a crucial property that can be used to develop adaptive sampling, for example to optimize the VAL-float surfacing with respect to satellite overpass or even to meteorological conditions. Complementary to Iridium, Argos-3 now provides high data transmission rates and bi-directionality. The first Argos-3 satellites were launched in 2007 and 2009 and subsequent Argos-3 instruments are planned for 2011 and 2012. Argos 3 presents an interesting alternative for float data transmission, and prototype floats are being tested. These developments must be pursued further by float manufacturers.

### 6.3 Energy Constraints

In 2007, the "Friends of Oxygen on Argo" group dedicated a significant part of their report to issues related to energy consumption and float life-time. If energy constraints were a major issue at that time, it is much less critical nowadays. There have been, and still are, significant technology improvements that permit considerable energy savings and also foster longer float life-times, even with the additional sensors.

1. SeaBird, which is currently the sole manufacturer for CTD sensors, has improved its pump, rendering it more efficient with respect to energy consumption.
2. Lithium ion batteries are now becoming a standard, providing more power per unit of battery mass; these batteries are highly recommended for bio-optical floats. The technology of these batteries is regularly improving thanks to the development of clean vehicles. For example, in early 2011, Saft, one of the leading manufacturers, released a new generation of batteries with 15% extended capacity per unit mass.
3. Iridium transmission reduces transmission time with respect to Argos and consequently saves energy per unit of data transmitted.
4. The bio-optical sensors that are now mounted routinely on floats do not have high energy consumption (< 1 watt, see Chapter 4). Furthermore, bio-optical sensor manufacturers understand that bio-optical floats can represent a very interesting market, and as a consequence issues related to sensor consumption are now taken into consideration in the process of sensor development or improvement.

The addition of bio-optical sensors will have some impact on the float lifetime, but float technology, which is already cost effective, is improving and consequently profile costs are progressively decreasing, and will likely continue to do so in the near future. With such improvements, it is anticipated that a bio-optical float with a standard package can perform ~300 cycles at meter resolution. At the standard Argo temporal resolution (1 cycle every 10 days), this equates to a float life-time of ~8 years. Obviously, rather than using the float for such a long period, it would be better to increase the temporal resolution of measurements (through Iridium) which would also avoid potential problems with sensor drift or bio-fouling (see Section 6.1).

The establishment of energy budgets is essential for the bio-optical community (and more generally the biogeochemical community) wanting to integrate sensors on the Argo floats. Indeed, it is critical to address the impact of additional sensors on the life-time of a standard TS float. In other words, what is the cost of a TS profile for a bio-optical float compared to a standard TS Argo float? Any "parasitism" of Argo floats by biogeochemical sensors has to be accompanied by an accurate evaluation of additional resources. Currently, it is not easy to obtain this type of



budget information from the information provided by the float manufacturers (if at all). It is therefore strongly recommended that float manufacturers provide the community with software or Excel spreadsheets to quantify the energy budgets for standard and multi-sensor applications.

# Data Management Issues

---

## 7.1 Quality Control

### 7.1.1 General philosophy

Quality control (QC) is an essential step for any dataset and is crucial for data collected automatically from a "remote" instrument. Several examples of QC exist for oceanographic instruments on remote platforms (i.e. satellite instruments, moorings, gliders). For biogeochemical profiling floats, the QC procedure should be inspired by these existing systems and should have a common philosophy. In this regard, QC procedure should:

- ❖ assign different processing levels to the acquired data (a system of flags should be defined, to indicate quality of data);
- ❖ follow a unique method and run under a unique processor, regardless of the type of float and mission - in addition, the processor (i.e. the ensemble of algorithms and software processing data from acquisition to user delivery) should be relatively flexible so that it can be rapidly adapted to technological innovations or new parameters;
- ❖ be accurately documented and periodically revisited;
- ❖ be similar (as far as possible) to those used for other remote platforms/parameters, thus facilitating integration of data in a larger database.

Among the existing QC systems, the Argo program is the closest in terms of platform typology. This program established a very efficient QC protocol for the temperature and salinity parameters (ADMT, 2010). The Argo QC follows a three step procedure: the "Real Time" mode (RT), the "Adjusted Mode" (AM) and the "Delayed Mode" (DM). Each Argo QC mode identifies a specific level of data quality, but also a maximum time delay for data availability to end-users:

- ❖ RT is a totally automatic QC, required to deliver data with only one-day delay; human operator is not required; flags are assigned on the basis of 19 successive tests, determining the RT quality of data;
- ❖ AM is an intermediate data quality level; it is used retrospectively on the Argo QC to re-adjust RT data using correction factors determined in the framework of the DM;
- ❖ DM is the final product delivered by the Argo system; it is composed of a set of semi-automatic algorithms checking drift and bias on the acquired data and

by visual inspection carried out by a scientific officer; generally, DM data are delivered with a 0.5 to 1 year delay after acquisition.

The Argo QC is continuously updated, according to decisions undertaken by a specific and dedicated working group (the Argo QC Data Management Team). The success of the Argo program, in terms of scientific applications as well as operational use of data, is directly related to the efficiency of this three step QC procedure. We recommend the adoption of the Argo QC philosophy to process and qualify data acquired for the three missions described here (BIO-Argo, VAL and Carbon-Explorer).

In the following section, the, BIO-Argo QC procedure will be presented first, as it should be used by all three float missions (the detailed, real-time QC procedure for Chla acquired by a BIO-Argo float, currently operated by the Coriolis data center, is presented in Appendix B) and the QC procedures for the VAL and Carbon-Explorer Argo missions will be described next.

## 7.1.2 BIO-Argo mission

### 7.1.2.1 General Considerations

All sensors need to be factory-calibrated in physical units or relative to a standard (e.g. Quinine Sulphate (QS) for CDOM fluorescence). If possible, calibration should be checked prior to deployment (at least for dark currents). During the float life-time, attempts should be made to cross-reference sensor measurements to other data sources (climatologies, remote sensing, local measurements) to insure the highest confidence in the data. Every effort should be made to provide an honest account of the likely uncertainties (better a large error bar than a false sense of certainty).

The RT QC assumes that sensors are well calibrated and that algorithms are accurate. In a first approximation (i.e. RT), this assumption could be considered realistic. For DM, visual inspection should be performed and tests should be applied to verify temporal consistency of observations and to identify bias or drifts of the sensors. If required, automatic corrections could be applied on the RT data, within the framework of AM.

### 7.1.2.2 Real-time mode (RT)

The Argo RT QC mode is based on 19 successive tests, which automatically assess the quality of the observations. The results of these tests are summarized by assigning a QC flag, ranging from 1 (good data) to 4 (bad data). A value of 0 is assigned if RT QC is not performed.

Most of the Argo QC RT tests are performed to identify problems related to bad geo-localisation, erroneous timing, wrong platform identification, pressure errors etc. For these tests, the Argo procedure should be strictly adopted for the RT of the BIO-Argo mission (see Appendix B for Chla example). Three of these tests require modifications to adapt to the BIO-Argo variables:

- ❖ Test 6 - Global Range Test: This test is a first rough assessment to identify spurious or erroneous data. The rationale is that, outside a specific range, data cannot be considered to be reliable because the values have never been observed in natural conditions. The application of such a test on BIO-Argo data is, however, complicated by the extremely high variability often observed for biological variables.
- ❖ Test 9 - Spike Test: Argo test number 9 is primarily devoted to the identification of spikes, defined as "measurement quite different from adjacent ones" (ADMT, 2010). The simple adaptation of the Argo Spike Test to the BIO-Argo variables is not straightforward because of the specificity in the vertical distribution of biological variables (increase or decrease with depth not uniform, presence of sharp sub-surface maxima, high noise, especially at depth).
- ❖ Test 11 - Gradient Test: Argo gradient test is introduced to identify vertically adjacent data points having very sharp differences. Although this is relevant for temperature and salinity profiles that vary relatively slowly with depth, this test is less appropriate for BIO-Argo variables which can increase or decrease rapidly within few meters. This test should nevertheless be maintained to flag suspect points, which, for some reason, have passed the spike test.

To apply these tests on BIO-Argo variables, the threshold values should be defined, on the basis of statistics on existing data sets (see also Appendix B).

#### 7.1.2.3 Adjusted mode (AM)

Possible bias and drifts in the data, identified in the DM, could be corrected automatically on the RT data. For example, a constant bias could be systematically added or removed to the RT data, if clearly identified in the DM. Adjusted Mode (AM) data correspond to RT data for which automatic corrections defined in the DM (if applicable) have been applied. The AM allows the quality of the RT data to be corrected while maintaining the unmodified RT observations (i.e. raw data). AM is very useful to verify calibration performances.

#### 7.1.2.4 Delayed mode (DM)

The DM allows a more precise assessment of the data set accuracy, as statistics and tests can be applied to long time series. The DM should identify data problems that passed all the automatic RT tests. Similar to the Argo system, DM QC from BIO-Argo should be performed according to a two-phase approach: a semi-automatic DM and a final DM.

The semi-automatic DM (SDM) should be composed of a set of automatic algorithms, which verify data accuracy, by using methods requiring long time series. For the BIO-Argo QC, SDM should examine the occurrence of obvious deviations in time series, which could concern a single profile, a series of profiles, or the entire

database obtained by a specific sensor. Remote sensing or climatologies should be used to verify the accuracy of the float data (see Appendix B for an example of Chla). Trends in the time series should be identified by routine (i.e. 6 months) match-up comparisons between profiling floats and satellite-derived ocean-colour products (see Boss et al., 2008a). Offsets in float data could be identified by the analysis of time series of satellite/floats match-ups. Match-up algorithms should be adapted to float specificities and particular attention should be devoted to the temporal and spatial windows used to compute satellite match-ups (see discussion in Boss et al., 2008b; also Section 7.3). However, the use of remote sensing in the SDM QC should be limited to identification of error trends (Guinehut et al., 2009), and not to the re-adjustment of float data, which should be supervised by human intervention in the final DM.

The final DM QC procedure aims to produce the "best" set of data for a specific BIO-Argo float. It should be based on a comparison with ancillary data and on visual inspection. The ancillary data can include the other variables acquired by the float (e.g. T, S, irradiance, or  $b_b$  for Chla QC) or data from external sources (i.e. remote sensing, calibration profile at deployment, climatologies). The visual inspection should be performed by researchers involved in the scientific analysis of the data and not by the data center.

### 7.1.3 The VAL mission

#### 7.1.3.1 Real-time mode

The standard BIO-Argo QC procedure for temperature, salinity, Chla fluorescence or  $b_b$  can be used for VAL-floats. The following is a list of elements which can be implemented easily into an operational, real-time, quality control procedure for radiometric measurements:

- ❖ dark values (measurements performed at depth) are below a pre-defined threshold;
- ❖ no negative values (or values below a pre-defined threshold) at any wavelength after conversion of raw data into calibrated data;
- ❖ vertical tilt values lower than a pre-defined threshold (usually from 5 to 10 degrees);
- ❖ in the case of a unique  $L_u$  sensor placed on one side of the float, the azimuth angle of the  $L_u$  sensor with respect to sun azimuth should be within a pre-defined range in order to reject profiles potentially affected by a strong float shadowing effect.

#### 7.1.3.2 Adjusted mode

Possible drifts or bias in the data could be corrected automatically in the RT data after identification in DM through post-deployment sensor calibration or inter-

comparison with "match-up" measurements from other floats or ship campaigns, which is discussed in the next section.

### 7.1.3.3 Delayed mode

The delayed mode allows for automatic objective filtration schemes (possibly requiring ancillary data) as well as for more subjective analyses made by an expert user, usually the scientist responsible for the float. The following list of elements and tests should be included in a delayed analysis:

- ❖ When a post-deployment calibration is available, a correction for a possible drift is applicable to the data (note that imposing a maximum value for the calibration drift can also be used for rejecting profiles). Absolute calibrations should be performed using NIST traceable sources, by one unique laboratory (possibly the manufacturer) or by "inter-calibrated" laboratories;
- ❖ Instrument self-shading correction below a pre-defined threshold;
- ❖ Derived products (e.g.  $K$ ,  $nL_w$ ,  $R$ ) below or above a pre-defined threshold (e.g. below the pure seawater coefficients for  $K_d$  or  $K_u$ );
- ❖ Consistency of the derived AOPs (possibly combined into spectral ratios) across a series of "close in time" successive profiles (preferentially three) near the surface, to evaluate the variability of the irradiance impinging at the sea surface;
- ❖ Stability of the downward irradiance at the surface measured continuously when the float is at the surface (once the high frequency variations due to waves have been subtracted). To be statistically valid such a qualitative analysis implies that the float remains at the surface for a sufficient time after profiling (in the order of 10-30 minutes). Both this point and the previous one aims at compensating for the absence of a reference downward irradiance sensor at the surface during the vertical profile;
- ❖ Consistency of the spectral shape of the derived products (e.g.  $K$ ,  $nL_w$ ,  $R$ ) with respect to *a priori* spectral shapes for the area and season under investigation. Such an analysis is generally based on a statistical approach but can also give rise to a more subjective visual analysis by an expert user (D'Alimonte and Zibordi, 2006);
- ❖ Consistency of the derived AOPs (possibly combined into spectral ratios) with other variables measured in parallel on the float (Chla fluorescence, CDOM fluorescence, beam attenuation coefficient);
- ❖ Consistency of the derived AOPs verified through inter-comparison with "match-up" measurements from other floats or ship campaigns.

The data processing scheme should allow for an interactive definition of the surface "extrapolation" layer (i.e. the layer for which the hypothesis of a linear decrease of the log of radiometric quantities as a function of depth, is respected). Such a definition, essential for the derivation of  $K$  coefficients and of AOPs extrapolated at

the sea surface ("0+"), could be roughly estimated or computed in the RT mode and refined in the DM.

#### 7.1.4 Carbon-Explorer mission

Codes for automated data processing of transmissometer and scattering sensor data (including quality flags) have been developed and implemented operationally for the Carbon-Explorer program. The data transmitted are binned over the observing depth intervals and mean and standard deviation (s.d.) of binned results transmitted. The performance of untreated IOP sensors of particulates can be tracked in the deep waters where particle concentrations are low and nearly constant (Figure 7.1). Although raw transmissometer  $c_p$  values rise as high as 0.8 (loss of transmission = 20%) after 400 days of operation, the known near consistency and low value of deep water  $c_p$  ( $0.012 \text{ m}^{-1}$ ) validates the use of 900 - 1000 m  $c_p$  values in a scheme to compensate for bio-fouling effects. Real time adjustment of data is then possible.

## 7.2 Archiving and Data Distribution

The following is a description of what has been developed for Argo data. The data flow within BIO-Argo should be carried out in a similar fashion through three organizational entities, i.e. the Principal Investigator (PI), the Data Assembly Center (DAC) and the Global Data Assembly Center (GDAC). The PI, typically a scientist at a research institution, maintains the observing platform and the sensors that deliver the data. This PI is responsible for providing the data and all auxiliary information to a DAC, which assembles the files in a standardized format (NetCDF) and delivers them to one of two GDACs, where they are made publicly available. The user can then access the data at either GDAC.

### 7.2.1 Standardization of the format

As for the Argo data management group, the BIO-Argo group is creating a unique data format for internet distribution to users, and for data exchange between national data centers (DACs) and global data centers (GDACs). This has resulted in a concerted effort to define the various bio-parameters in the metadata and technical attributes (names, definitions, units). Profile data, metadata, trajectories and technical data are included in this standardization effort. The data in the GDACs are held in NetCDF format that contains profile and trajectory data and associated metadata and quality control flags. BIO-Argo data formats are based on NetCDF and are divided into four sections. For example, for the profile data file, the four sections are organized as follows (see also the Argo User's Manual to get further information on the files <http://www.argodatamgt.org/Media/Argo-Data-Management/Argo-Documentation/General-documentation/Data-format/Argo-User-s-manual>):

900-1000 m  $c_p$  and scattering statistics from Bishop and Wood (2009) data.

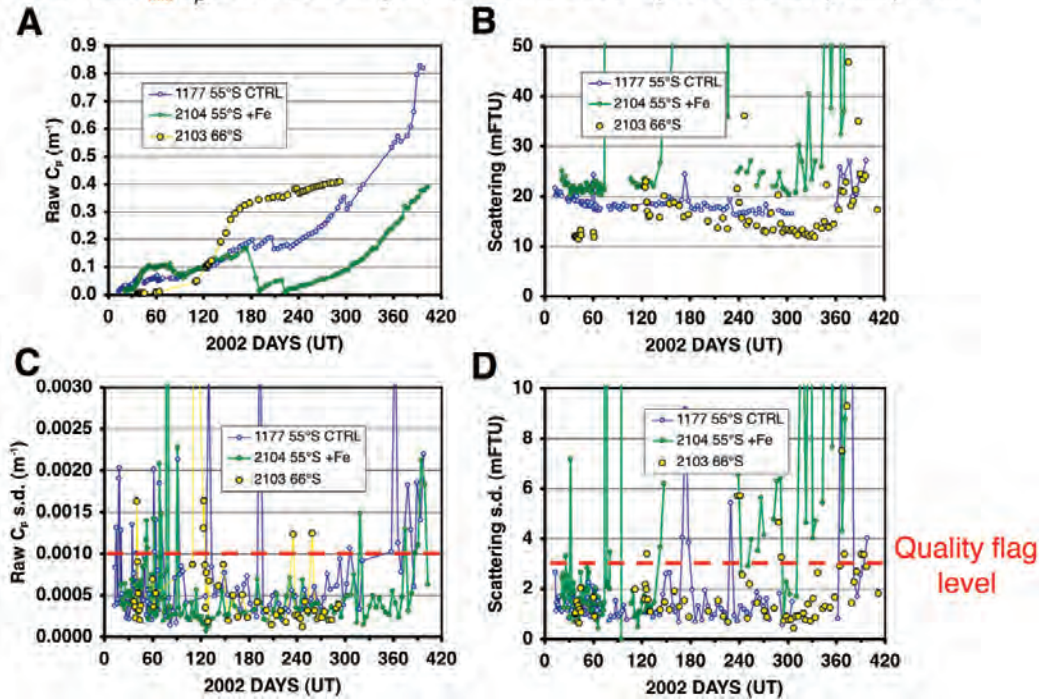


**Figure 7.1** Examination of transmissometer and turbidity data quality over a long term float deployment (data from Bishop and Wood, 2009). The rate of fouling of untreated sensors rose as profiling frequency was decreased. More frequent washes of the upward looking transmissometer window (CFI procedures) at drift depth would lessen fouling effects. Shown also are records for 900-1000 m scattering. One sensor (float 2104) became obviously fouled (see flag criteria). Floats 1177 and 2104 deployed within 10 km of each other demonstrate that turbidity can be determined to  $\pm 2$  mFTU. Unlike transmissometer data, it is impossible to quantify the fouling effects on scattering sensors unless fouled by filamentous material. From these observations, we would put a quality flag on the  $c_p$  or turbidity profile, based on their 900-1000 m standard deviation (s.d.), for  $c_p$  s.d.  $> 0.001 \text{ m}^{-1}$  and turbidity s.d.  $> 3$  mFTU. As part of a delayed mode quality control, an operator would inspect the flagged profiles and release if profiles are judged to be real.

- ❖ The first section provides information about the number of profiles, parameters, levels, string dimensions, etc.
- ❖ The second section contains information about the whole file, such as version of the file format (defined by the Argo Data Management Team), version number of the data handbook, date of reference for Julian days etc. This section also contains general information on each profile - each item has a N\_PROF (number of profiles) dimension. The STATION\_PARAMETERS lists the parameters contained in the profile; each parameter should be defined according to a convention (for instance TEMP for temperature, PSAL for salinity), then the bio-parameters have to be strictly defined. In this sec-



tion, a variable named DATA\_MODE indicates if the profile contains only real time data (DATA\_MODE=R) or real time and adjusted data in delayed mode (DATA\_MODE=D).

- ❖ The third section contains information on each level of each profile. Each variable in this section has a N\_PROF (number of profiles) and N\_LEVELS (number of pressure levels) dimension. The raw data received from the float and examined by real-time quality control should be placed in the <PARAM> field and flags in the <PARAM\_QC> field. Each parameter can be adjusted (in delayed-mode) and in that case, the adjusted values are set to <PARAM\_ADJUSTED> field.
- ❖ The fourth section contains history information for each action performed on each profile. A history record is created whenever an action is performed on a profile. For instance, reference of the software used to process delayed mode data, step of the quality control (according to codes defined in the Argo framework), date of the action, etc.

For the meta-data file, the data section is replaced by the characteristics of the float, float deployment and mission information, float sensor information and float cycle information. This section contains the main characteristics of the float such as system of transmission, positioning system, model of the float, type of sensor and associated resolution. For the technical information format, the number and the type of technical information can be different from one float model to another. For the bio-parameters, efforts should be made to fill in all the information about the technical data.

## 7.2.2 Data status

As for Argo, two versions of the data will have to be considered, both in the same NetCDF file: the real time data in <PARAM> and delayed mode data in <PARAM\_ADJUSTED>.

### 7.2.2.1 Real time data

The data are subjected to initial quality control at national DACs. This data should be free from gross errors in position, temperature, salinity and pressure. These files are available on the GDAC FTP sites. In general, this data should be consistent with ocean climatologies even though no climatology tests have been performed at this stage.

### 7.2.2.2 Delayed mode data

These data profiles have been subjected to detailed scrutiny by oceanographic experts and the adjusted bio-optical parameters have been estimated by the different methods, some of which have been discussed above.

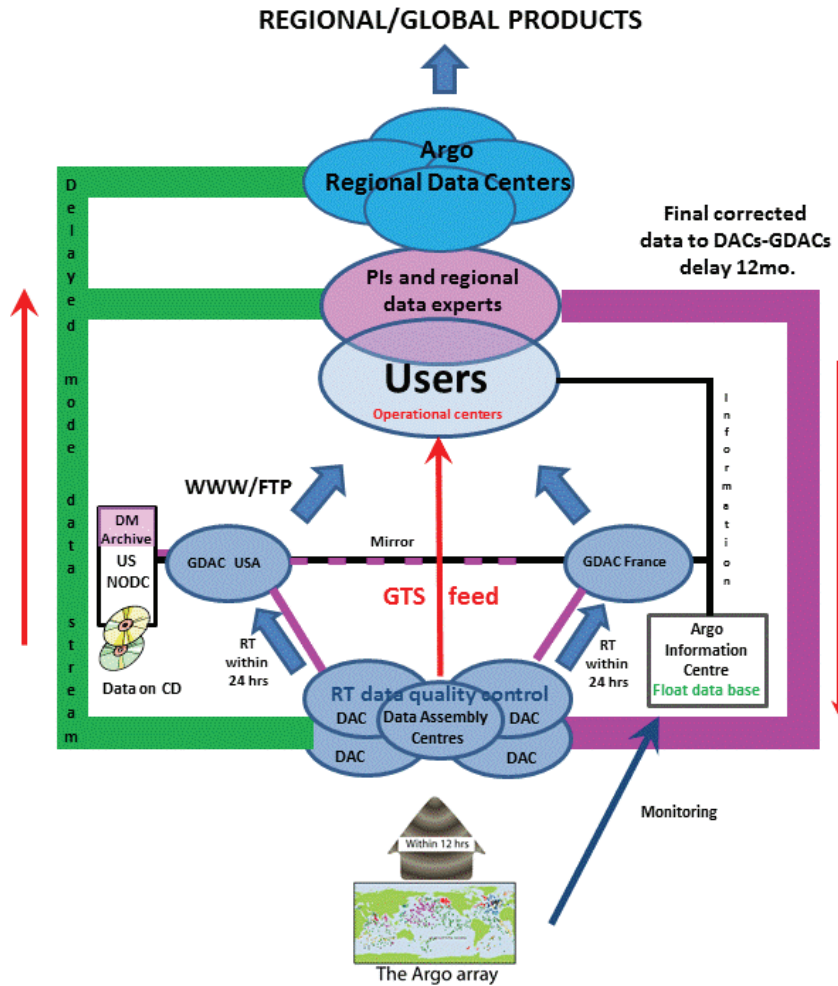


**Figure 7.2** The structure of data flow for real-time and delayed-mode distribution as part of the Argo program. The same framework is suggested for data of the BIO-Argo type. The data are available to users through 3 routes: (i) Through operational centers via TESAC messages on the GTS; (ii) Via ftp, http, LAS downloads from two Global Data Assembly Centers; and (iii) From an archived data set at the US NODC (see [http://www-argo.ucsd.edu/FrArgo\\_data\\_and.html](http://www-argo.ucsd.edu/FrArgo_data_and.html)).

### 7.2.2.3 Data distribution

The pathway of data flow from the floats to the data centers and users is illustrated in Figure 7.2. First, the data are sent to the two GDACs which is the first time the data are publicly available. The BIO-Argo data distribution will be provided within an integrated access from Global GDACs to datasets in BIO-Argo format using ftp servers (plus OpenDap technology, if necessary). Data are freely available from the GDACs to all users, and the data will also reach operational ocean and climate forecast/analysis centers via the Global Telecommunications System (GTS).

### 7.3 Matching Float and OCR Satellite Measurements

It is not possible for a float to cover the spatial scale measured by an ocean-colour satellite ( $\sim 1 \text{ km} \times 1 \text{ km}$ ), and hence spatial variability may affect the quality of match-ups between the two (note that this problem is inherent for all current CAL/VAL activities). In addition, cloud cover may mask the pixel above the float but not another adjacent pixel. For various reasons (e.g. attempting to avoid fluorescence quenching by profiling at night) it is also possible that the time of measurement may not coincide with the satellite overpass.

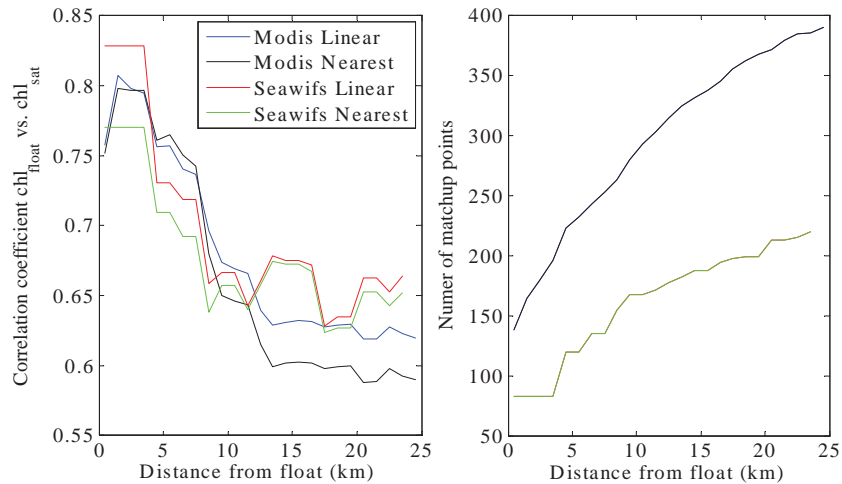


**Figure 7.3** Example of spatial correlation between float Chla and satellite Chla in the North Atlantic and impact on the number of match-ups. Left panel: MODIS (1-km pixel) and SeaWIFS (4-km pixel) data are used with two different interpolation methods with time (linear and nearest neighbor). Right panel: Number of float-satellite match-ups as function of the horizontal scale of averaging around the float's location (based on the float data used in Boss et al. 2008b).

A question then arises regarding the effect of these mismatches in time/space on the ability and usefulness of attempting to match up ocean-colour satellite data with Argo float data. Fortunately, optical data exhibit spatial and temporal correlations making it useful for match up beyond the exact location and time of sampling. For example, Boss et al. (2008a) compared the correlation between match-up data collected within 24 h and with various distances from the float (Figure 7.3). They found that the correlation degraded slowly to a distance of 7.5 km and then degraded more rapidly (Figure 7.3). On the other hand, the number of match-ups increased significantly ( $\sim 50\%$ ) as the distance increased to 7.5 km. This spatial scale matched the local internal deformation radius, suggesting physical stirring by mesoscale eddies dominated the spatial variability. Temporal de-correlation between successive profiles was about two weeks (Figure 5 in Boss et al., 2008a) suggesting match-ups with the closest satellite pass was most appropriate. Thus, depending on

the application (e.g. CAL, VAL, sensor checkup) it is recommended that a similar scale analysis be performed so that match-up numbers can be maximized without a significant (application dependent) sacrifice in accuracy.



# Towards the Implementation of Float Arrays

---

Three classes of bio-optical floats are presented in this report. They have various degrees of maturity, are designed for specific scientific applications and are generally quite costly. These characteristics put some constraints on the short- and middle-term implementation plans and the tentative sizing of the future arrays.

The Carbon-Explorer is a mature and operational float dedicated to carbon cycle measurements (Bishop et al., 2002; 2004; Bishop, 2009; Bishop and Wood, 2009). Its flexibility to accommodate a suite of up-to-date and developing laboratory sensors as well as its mission capability to sample at high frequency (e.g. diel cycle for primary production measurements) makes it especially dedicated for specific processes or targeted regional studies. It is not targeted for large global dissemination in the classic Argo mode. Sensors proven on the Carbon-Explorer platform (e.g. PIC or other carbon parameters) would be expected to migrate to the BIO-Argo mission. In this section we will focus on the other two classes of floats: the VAL-float and the BIO-Argo float. These are based on commercially-available sensors and are directly relevant to remote sensing activities, thus they can readily become components of existing arrays.

## 8.1 VAL-floats: Preparatory Phase Before an Operational Array

The technology (sensor, float, transmission) is available and has already been tested elsewhere. The VAL-float requires an optimal integration of the various elements, especially the radiometers, with respect to the required highest quality measurements. Except for a few floats equipped with  $E_d$  sensors (Mitchell, 2003), no optimized radiometric measurement has been made to date. Currently, there are on-going developments aimed at building VAL-floats by integrating a suite of  $E_d$  and  $L_u$  sensors, as well as a suite of IOP and other biogeochemical sensors onto various float platforms (APEX and PROVOR). The prototypes of these floats will be tested over the 2011–2012 period, preferably in oceanic areas with well-characterized bio-optical properties. The close vicinity of the permanent MOBY (Hawaii) and BOUSSOLE (Western Mediterranean Sea) optical moorings are the appropriate sites to conduct these float performance evaluations.

After this preparatory phase, and if the concept of a VAL-float appears scientifically valid and cost-effective, the implementation of an operational VAL-float array will be envisaged. The specifics of the VAL-float with respect to sensors and mission requirements (energy costs) prevents it from being part of the regular Argo program. A dedicated VAL-float array will have to be developed independently. Claustre et al. (2010b) suggested that, over a 5 year-term, an array of 20 - 40 floats deployed in various trophic areas (covering the range of [Chla] detected by ocean-colour satellites) is a reasonable target. Prior to development, specific locations and periods for maximizing the efficiency with respect to VAL activities will have to be identified. The total annual cost is estimated to be ~\$0.4 - \$0.8M. Deployment is straightforward and the cost is negligible when using ships of opportunity. Two full-time employees will be required for data management and quality control procedures.

## **8.2 BIO-Argo Floats: Pilot and Regional Studies Before Global Dissemination**

The rationale for the development of an array of BIO-Argo floats is to provide the biogeochemical community with an unprecedented quantity of real-time vertical profiles of key biogeochemical and bio-optical variables. This objective will be achieved by developing a generic, low cost, low consumption bio-optical/biogeochemical payload that would be disseminated through the Argo network and would take advantage of the existing infrastructure. The present Argo array with ~3,000 operational floats provides a horizontal resolution (average distance between floats) of around 300 km, assuming the floats are evenly distributed. This is adequate to derive mean quantities such as the average heat content or temperature, on a monthly time scale (Testor et al., 2010). The same large-scale properties could be derived from a globally-resolved BIO-Argo network. However, from the analysis of BIO-Argo float data (Boss et al., 2008a), it has been clearly shown that the space and time correlation of biological variables are much shorter than that of physical variables (Figure 7.3). Additionally, implementing bio-optical measurement capabilities on the whole Argo array would represent a (prohibitive) additional cost of ~\$800M.

Rather than a global network, it might be more efficient to first implement regional approaches. It has thus been proposed (Johnson et al., 2009; Claustre et al., 2010a) that pilot studies could be conducted at regional scales in some biogeochemically-relevant "hotspots". There are indeed regional "hot-spots" that are natural laboratories for addressing key scientific questions of global relevance, and which would benefit from being tackled in a highly integrated way. These pilot studies could serve as test cases for evaluating the design and efficiency of a BIO-Argo array, in particular with respect to data management and dissemination. In particular, the BIO-Argo float density could be much higher than the standard Argo float density, to address biogeochemical processes important at specific scales

(e.g. sub- and mesoscales; event scales such as storms). Among these regional hotspots, the North Pacific, the North Atlantic sub-polar gyre and oxygen minimum zones associated with upwelling areas are potential target areas (Johnson et al., 2009; Whitmire et al., 2009; Claustre et al., 2010a). For all these areas, the potential link and synergy with OCR is obvious. Currently, the biogeochemical community is organizing itself at an international level to design these pilot studies. These funded floats could begin to contribute to a BIO-Argo program.

Within 3–4 years, we should benefit from the experience of these pilot studies and it should be possible to establish a more global dissemination of BIO-Argo floats. In the meantime, and to prepare for this next step, the biogeochemical and bio-optical community has to establish a close link with the Argo program with the objective of developing a well-identified, biogeochemical component which is fully integrated within Argo. It should be emphasized that the concerns relevant to float life-time reduction due to additional biogeochemical sensors (assuming this is a real issue), is now much less critical than before. The life-time of standard T/S Argo floats is improving, with some floats reaching life-time of >5 years with standard Argo mission rules. In this case, the main concern could be sensor performance rather than float life-time. With respect to cost-effective acquisition of high quality oceanographic data, it is thus not efficient to focus on reaching the longest float life-time with only T/S sensors. Rather, it might be more judicious to define a good compromise for the simultaneous acquisition of biological and physical variables on the same float, over reasonable life-time (e.g. 4–5 years).



## **Acknowledgments**

We thank Antoine Poteau and Xiaogang Xing for data treatment and the production of certain figures. Discussions with Norm Nelson with respect to CDOM fluorescence measurements in open ocean waters were greatly appreciated. Stephanie Dutkiewicz is acknowledged for helpful suggestions that significantly improved some sections of the report.

## Appendix A

### Symbols and Acronyms

Symbols, acronyms and associated units (wavelength dependency omitted for optical variables)

Symbol	Description	Units
$a$	Absorption coefficient	$\text{m}^{-1}$
$a_{ph}$	Absorption coefficient of pigmented particulate matter	$\text{m}^{-1}$
$a^*$	Chla specific absorption coefficient	$\text{m}^{-2} \text{mg Chla}^{-1}$
$a_{CDM}$	Absorption coefficient of coloured detrital matter	$\text{m}^{-1}$
$b$	Total scattering coefficient	$\text{m}^{-1}$
$b_b$	Total backscattering coefficient	$\text{m}^{-1}$
$b_{bp}$	Backscattering coefficient of particles	$\text{m}^{-1}$
$b_{bw}$	Backscattering coefficient of water	$\text{m}^{-1}$
$c$	Beam attenuation coefficient	$\text{m}^{-1}$
$c_p$	Beam attenuation coefficient of particles	$\text{m}^{-1}$
CDOM	Coloured dissolved organic matter	
[Chla]	Chlorophyll- <i>a</i> concentration	$\text{mg m}^{-3}$
$E$	Irradiance	$\text{W m}^{-2}$
$E_d$	Downward irradiance	$\text{W m}^{-2}$
$E_u$	Upward irradiance	$\text{W m}^{-2}$
$E_s$	Extra-atmospheric sun irradiance	$\text{W m}^{-2}$
$F$	Chla fluorescence	$\text{mole Quanta m}^{-3} \text{s}^{-1}$
$FCDOM$	CDOM fluorescence	$\text{mole Quanta m}^{-3} \text{s}^{-1}$
$K_d$	Diffuse attenuation coefficient for downward irradiance	$\text{m}^{-1}$
$K_{Lu}$	Diffuse attenuation coefficient for upward radiance	$\text{m}^{-1}$

$K_u$	Diffuse attenuation coefficient for upward irradiance	$\text{m}^{-1}$
$L$	Radiance	$\text{W m}^{-2} \text{sr}^{-1}$
$L_u$	Upwelling radiance	$\text{W m}^{-2} \text{sr}^{-1}$
$L_w$	Water-leaving radiance	$\text{W m}^{-2} \text{sr}^{-1}$
$nL_w$	Normalized water-leaving radiance	$\text{W m}^{-2} \text{sr}^{-1}$
PAR	Photosynthetically available radiation	$\text{mole quanta m}^{-2} \text{d}^{-1}$
[POC]	Particulate organic carbon concentration	$\text{mg m}^{-3}$
[PIC]	Particulate inorganic carbon concentration	$\text{mg m}^{-3}$
$R_{rs}$	Remote sensing reflectance	$\text{sr}^{-1}$
S	Salinity	
T	Temperature	$^{\circ}\text{C}$
Z	Depth	m
$Z_e$	Euphotic depth	m
$\phi_f$	Fluorescence yield	$\text{mole quanta emitted (mole quanta absorbed)}^{-1}$
$\lambda$	Wavelength	nm

## Appendix B

### Example of Quality Control for Chla Fluorescence

---

The following data quality control is a first version of a prototype, which was developed by LOV laboratory in collaboration with the Coriolis Data Center. It was based on the analysis of the fluorescence signal from 8 PROVIBIO floats deployed in a variety of open ocean waters. This part is modified from the PABIM white book (D'Ortenzio et al. 2010).

#### B.1 Real Time Mode

The following Argo tests are strictly followed for the RT QC for Chla fluorescence:

- ❖ Test 1: Platform identification
- ❖ Test 2: Impossible date test
- ❖ Test 3: Impossible location test
- ❖ Test 4: Position on land test
- ❖ Test 5: Impossible speed test
- ❖ Test 8: Pressure increasing test
- ❖ Test 13: Stuck value test
- ❖ Test 15: Grey list
- ❖ Test 17: Visual QC
- ❖ Test 19: Deepest pressure test

Four RT Argo tests require modifications to be adapted for Chla:

- ❖ Test 6: Global range. The application of a global range test for [Chla] is complicated by: i) its extremely high temporal and horizontal variability, and ii) the specificity of its vertical distribution (not uniform with depth, recurrent presence of a deep chlorophyll maximum up to one order of magnitude greater than surface values, deep concentrations close to zero). Negative values can be also recorded and are likely the result of instrumental and electronic noise as well as fluorometer calibration issues (i.e. "dark" variable of the calibration equation). Negative values are generally of two different types: i) large negative values ( $\sim -1 \text{ mg m}^{-3}$ ), can be obtained at all depths along a vertical profile (no depth dependence) and are flagged as bad data; ii) very low negative values are exclusively recorded at depths where fluorescence vanishes. The lower limit for the global range is set at  $-0.1 \text{ mg m}^{-3}$ , and data in the  $-0.1$  to  $0.0 \text{ mg m}^{-3}$

interval are thus flagged with flag "3", as they are potentially correctable in the Adjusted Mode QC. The global range for [Chla] for valid RT data is thus fixed at 0.00 - 50.00 mg m<sup>-3</sup>.

- ❖ Test 9: Spike test. The Argo spike test for temperature and salinity is implemented by computing a "test value" defined as:

$$Argo\_Test\_value = |V2 - (V3 + V1)/2|$$

where  $V1$ ,  $V2$  and  $V3$  are as in the spike test. Observations with *Argo\_test\_value* exceeding a fixed threshold value are flagged as bad data. This test is *a priori* less suitable for [Chla], which can rapidly increase or decrease within a few meters (see spike test discussion). It is nevertheless maintained in its present form for [Chla] QC, but with an elevated threshold value of 3 mg m<sup>-3</sup>. The (limited) objective of this test is to flag really bad points, which, for some reasons, could have passed the spike test.

- ❖ Test 18: Frozen profile test - not applicable here.

Finally, four Argo tests are not applicable to Chla:

- ❖ Test 7: Regional test. Chla concentration is much more variable in space (vertically and horizontally) and time than temperature and salinity. This variability occurs over 2 to 3 orders of magnitude. A regional test, which should check the [Chla] profile in areas with specific characteristics, is not yet applicable because of lack of a reference dataset. However, with increasing *in situ* data collection and the unavoidable development of 4D Chla climatologies (that will likely be derived from remote sensing of surface properties) the test could be more easily implemented in the future.
- ❖ Test 12: Digit rollover test. The platforms dedicated to the measurement of [Chla] have been developed to take advantage of increased data storage capacity. Therefore no data storage related problems are expected.
- ❖ Test 14: Density inversion. Not applicable.
- ❖ Test 16: Gross salinity or temperature sensor drift. This test is based on the analysis of deep values between two consecutive profiles. In principle, this test could be adapted to check the stability of the fluorescence sensors. However, in the first version of the RT QC for Chla, this test is not recommended because "deep" (e.g. 1,000 m) fluorescence values are preferably analyzed in the Adjusted Mode.

## B.2 Adjusted Mode

The Adjusted Mode (AM) should be used to verify and possibly correct the fluorescence vs chlorophyll calibration. *Chla\_AM*, the corrected [Chla] after the AM correction is defined as:

$$Chl\_AM = bias\_AM + Chl\_RT$$

where  $ChL_{RT}$  is the RT controlled [Chla] (i.e. factory calibrated fluorescence + RT tests) and  $bias_{AM}$  is the correction offset computed by averaging deep values in a layer between a predefined depth  $Z_m$  and the last observed point. Considering the general vertical distribution of [Chla] in the ocean, two cases are distinguished:

1. In the case of stratified waters, [Chla] at depth should always be equal to zero. Deep points ( $Z_m > 400$  m) are used to calculate  $bias_{AM}$  without limitations.
2. In the case of mixed waters, [Chla] at depth could not systematically be equal to zero.  $bias_{AM}$  should be computed by averaging data from depths greater than the mixed layer depth (MLD).  $Z_m$  is thus fixed at the MLD.

In summary:

$$bias_{AM} = MEAN(ChL_{RT}(Z_m, last\_point))$$

$$Z_m = MAX(400, MLD(T,S))$$

The *semi automatic delayed mode (SDM)* is devoted to check the occurrence of important deviations in the time series of float observations, and might concern a single profile as well as a series of profiles. The deviations can be ascribed to two main categories:

1. A temporary failure of the fluorescence vs [Chla] calibration: The relationship between [Chla] and fluorescence is dependent on phytoplankton community structure as well as the nutrient and light history. Even an *a priori* well-calibrated fluorometer (factory calibrated using cultures) could produce inaccurate [Chla] in some specific biological situations (e.g. a bloom), or environmental conditions (e.g. heavy cloud cover).
2. A degradation of the sensor performance.

In the SDM phase of the [Chla] QC, it is recommended that ocean-colour satellite observations of surface [Chla] be used to check routinely (i.e. every 6 months) the stability of float data. Satellite/float match-ups will be automatically computed, and the time series of the differences will be analyzed.

$$Sat\_offset = |Chl_{sat} - ChL_{AM}(Z=0)|$$

$Sat\_offset$ , although not zero, should be constant over a long time period (i.e. 6 months). Any temporally rapid change in  $Sat\_offset$  (checked with statistical methods) should indicate a possible drift in the fluorometer calibration or response. The corresponding profiles will be flagged automatically as uncertain, and listed in a "grey list" for further controls. However, no adjustments based on satellite data should be applied to float [Chla] in the SDM phase.

### B.3 Delayed Mode

For [Chla] QC, DM should be based mainly on visual inspection, to identify erroneous data or profiles. Particular attention must be paid to:

1. Data flagged by the RT Spike Test. If a sharp gradient exists, in particular on the deep sub-surface maximum, the spike test could flag good data;
2. Surface and sub-surface data affected by fluorescence quenching, which acts to decrease the [Chla]. Cross-checking of the fluorescence profile with the corresponding physical profiles or, when present, with other bio-optical properties such as  $b_{bp}$  (see Sackmann and Perry, 2008) might allow identification of such a profile. The assumption that the fluorescence profile is constant within the mixed layer or that the  $b_{bp}/[\text{Chla}]$  ratio is constant in the upper layer, can be a basis for profile correction (note that profiling at night avoids the quenching problem).

Different methods can then be applied to improve the fluorescence vs [Chla] relationship and hence the retrieval of accurate [Chla]. The general form for the delayed mode Chla ( $Chl_{DM}$ ) is:

$$Chl_{DM} = bias_{DM} + Chl_{RT} * offset_{DM}$$

The choice of the method for the retrieval of  $Bias_{DM}$  and  $offset_{DM}$  depends on the availability of associated measurements. If no such data are available, no corrections are applied and  $offset_{DM}$  will be set to 1 and  $bias_{DM}$  will be set to  $bias_{AM}$ .

#### B.3.1 Radiometry-based correction

If radiometry is concomitant to the fluorescence measurement, a bio-optical correction relying on relationships linking  $K_d$  and [Chla] (e.g. Morel and Maritorena, 2001) could be used to refine the fluorescence vs [Chla] relationship. Recently this type of method has been proposed by Xing et al. (2011). They present the advantages of taking into consideration natural and instrumental variations in the [Chla] vs fluorescence relationship over the whole float life-time.

#### B.3.2 HPLC correction

If radiometry is not concomitant with the fluorescence measurement, and if HPLC Chla samples were taken as part of the deployment cruise (generally for the first profile),  $bias_{DM}$  and  $offset_{DM}$  should be re-evaluated by linear regression using routinely employed methods (e.g. Morel and Maritorena, 2001).

#### B.3.3 Satellite correction

This correction should be applied when neither radiometry nor HPLC data are available. As described in Boss et al. (2008a), spatially and temporally collocated

ocean-colour [Chla] estimates could be used to re-calibrate float fluorescence profiles. The rationale is to calculate *bias\_DM* and *offset\_DM* on the basis of mean chlorophyll estimations obtained from space. A key point is the selection of the temporal and spatial boxes used to average satellite observations around the location and the time of the float profile. Here, a temporal window of 6 hours and a spatial box of 7.5 km are proposed, following the indications of the correlation tests performed by Boss et al. (2008a). However, a more detailed study is required, as variability of the surface chlorophyll field could be regionally dependent (Uz and Yoder, 2004).





## References

---

- Abbott MR, Richerson PJ, Powell TM (1982) *In situ* response of phytoplankton fluorescence to rapid variations in light. *Limnology and Oceanography* 27:218-225
- ADMT (2010) Argo quality control manual. Available online at: <http://www.argodatamgt.org/content/download/341/2650/file/argo-quality-control-manual-V2.6.pdf> (accessed 6 July, 2011)
- Ahn YH, Bricaud A, Morel A (1992) Light backscattering efficiency and related properties of some phytoplankters. *Deep-Sea Research* 39:1835-1855
- Alvain S, Moulin C, Dandonneau Y, Breon FM (2005) Remote sensing of phytoplankton groups in Case 1 waters from global SeaWiFS imagery. *Deep-Sea Research Part I-Oceanographic Research Papers* 52:1989-2004
- Antoine D, André JM, Morel A (1996) Oceanic primary production 2. Estimation at global scale from satellite (coastal zone color scanner) chlorophyll. *Global Biogeochemical Cycles* 10:57-69
- Antoine D, D'Ortenzio F, Hooker SB, Bécu G, Gentili B, Tailliez D, Scott AJ (2008) Assessment of uncertainty in the ocean reflectance determined by three satellite ocean color sensors (MERIS, SeaWiFS and MODIS-A) at an offshore site in the Mediterranean Sea (BOUSSOLE project). *Journal of Geophysical Research* 113: C07013, doi:10.1029/2007JC004472
- Babin M (2008) Phytoplankton fluorescence: theory, current literature and *in situ* measurements. In: Babin M, Roesler C, Cullen JJ (eds) *Real-time coastal observing systems for marine ecosystem dynamics and harmful algal blooms*. Unesco, Paris, p 237-280
- Baker ET, Lavelle JW (1984) The effect of particle-size on the light attenuation coefficient of natural suspensions. *Journal of Geophysical Research-Oceans* 89:8197-8203
- Balch WM, Gordon HR, Bowler BC, Drapeau DT, Booth EC (2005) Calcium carbonate measurements in the surface global ocean based on Moderate-Resolution Imaging Spectroradiometer data. *Journal of Geophysical Research* 110:C07001, doi:07010.01029/02004JC002560
- Behrenfeld MJ, Boss E (2006) Beam attenuation and chlorophyll concentration as alternative optical indices of phytoplankton biomass. *Journal of Marine Research* 64:431-451
- Behrenfeld MJ, Boss E, Siegel DA, Shea DM (2005) Carbon-based ocean productivity and phytoplankton physiology from space. *Global Biogeochemical Cycles* 19: GB1006, doi:10.1029/2004GB002299
- Behrenfeld MJ, Falkowski PG (1997) Photosynthetic rates derived from satellite-based chlorophyll concentration. *Limnology and Oceanography* 42:1-20
- Bishop JKB (1999) Transmissometer measurement of POC. *Deep-Sea Research I* 46:353-369
- Bishop JKB (2009) Autonomous observations of the ocean biological carbon pump. *Oceanography* 22:182-193
- Bishop JKB, Calvert SE, Soon MYS (1999) Spatial and temporal variability of POC in the northeast Subarctic Pacific. *46:2699-2733*
- Bishop JKB, Davis RE, Sherman JT (2002) Robotic observation of dust storm enhancement of carbon biomass in the North Pacific. *Science* 298:817-821
- Bishop JKB, Wood TJ (2008) Particulate matter chemistry and dynamics in the twilight zone at VERTIGO ALOHA and K2 sites. *Deep-Sea Research Part I-Oceanographic Research Papers* 55:1684-1706
- Bishop JKB, Wood TJ (2009) Year-round observations of carbon biomass and flux variability in the Southern Ocean. *Global Biogeochemical Cycles* 23: doi:10.1029/2008GB003206.
- Bishop JKB, Wood TJ, Davis RE, Sherman JT (2004) Robotic Observations of Enhanced Carbon Biomass and Export at 55°S During SOFeX. *Science* 304:417-420
- Boss E, Behrenfeld M (2010) *In situ* evaluation of the initiation of the North Atlantic phytoplankton bloom. *Geophysical Research Letters* 37: L18603, doi:10.1029/2010GL044174
- Boss E, Pegau WS (2001) Relationship of light scattering at an angle in the backward direction to the backscattering coefficient. *Applied Optics* 40:5503-5507
- Boss E, Perry MJ, Swift D, Taylor L, Brickley P, Zaneveld JRV, Riser S (2008b) Three years of ocean data from a bio-optical profiling float. *Eos Trans AGU* 89(23), doi:10.1029/2008EO230001

- Boss E, Slade W, Hill P (2009a) Effect of particulate aggregation in aquatic environments on the beam attenuation and its utility as a proxy for particulate mass. *Optics Express* 17:9408-9420
- Boss E, Slade WH, Behrenfeld M, Dall'Olmo G (2009b) Acceptance angle effects on the beam attenuation in the ocean. *Optics Express* 17:1535-1550
- Boss E, Swift D, Taylor L, Brickley P, Zaneveld R, Riser S, Perry MJ, Stratton PG (2008a) Observations of pigment and particle distributions in the western North Atlantic from an autonomous float and ocean color satellite. *Limnology and Oceanography* 53:2112-2122
- Boss E, Taylor L, Gilbert S, Gundersen K, Hawley N, Janzen C, Johengen T, Purcell H, Robertson C, Schar DWH, Smith GJ, Tamburri MN (2009c) Comparison of inherent optical properties as a surrogate for particulate matter concentration in coastal waters. *Limnology and Oceanography-Methods* 7:803-810
- Brasseur P, Gruber N, Barciela R, Brander K, Doron M et al. (2009) Integrating Biogeochemistry and ecology into ocean data assimilation systems. *Oceanography* 22:206-215
- Bricaud A, Babin M, Morel A, Claustre H (1995) Variability in the chlorophyll-specific absorption coefficients of natural phytoplankton: Analysis and parameterization. *Journal of Geophysical Research* 100:13,321-313,332
- Bricaud A, Claustre H, Ras J, Oubelkheir K (2004) Natural variability of phytoplanktonic absorption in oceanic waters: Influence of the size structure of algal populations. *Journal of Geophysical Research-Oceans* 109: C11010, doi:10.1029/2004JC002419
- Bricaud A, Roesler CS, Parslow JS, Ishizaka J (2002) Bio-optical studies during the JGOFS-equatorial Pacific program: a contribution to the knowledge of the equatorial system. *Deep Sea Research Part II: Topical Studies in Oceanography* 49:2583-2599
- Brown CW, Huot Y, Purcell MJ, Cullen JB, Lewis MR (2004) Mapping coastal optical and biogeochemical variability using an autonomous underwater vehicle and a new bio-optical inversion algorithm. *Limnology and Oceanography methods* 2:262-281
- Claustre H, Antoine D, Boehme L, Boss E, D'Ortenzio F et al. (2010a) Guidelines towards an integrated ocean observation system for ecosystems and biogeochemical cycles. In: Hall J, Harrison D.E. and Stammer, D. (ed) Proceedings of the "OceanObs'09: Sustained Ocean Observations and Information for Society" Conference Venice, Italy, 21-25 September 2009, Vol 1. ESA Publication WPP-306
- Claustre H, Bishop J, Boss E, Stewart B, Berthon J-F et al. (2010b) Bio-optical profiling floats as new observational tools for biogeochemical and ecosystem studies. In: Hall J, Harrison D.E. and Stammer, D. (ed) Proceedings of the "OceanObs'09: Sustained Ocean Observations and Information for Society" Conference, Vol 1. ESA Publication WPP-306
- Claustre H, Bricaud A, Babin M, Bruyant F, Guillou L, Le Gall F, Marie D, Partensky F (2002) Diel variations in *Prochlorococcus* optical properties. *Limnology and Oceanography* 47:1637-1647
- Claustre H, Huot Y, Obernosterer I, Gentili B, Tailliez D, Lewis MR (2008) Gross community production and metabolic balance in the South Pacific Gyre, using a non intrusive bio-optical method. *Biogeosciences* 4:463-474
- Claustre H, Maritorena S (2003) The many shades of ocean blue. *Science* 302:1514-1515
- Claustre H, Morel A, Babin M, Cailliau C, Marie D, Marty JC, Tailliez D, Vaultot D (1999) Variability in particle attenuation and chlorophyll fluorescence in the Tropical Pacific: Scales, patterns, and biogeochemical implications. *Journal of Geophysical Research* 104:3401-3422
- Coble PG (1996) Characterization of marine and terrestrial DOM in seawater using excitation emission matrix spectroscopy. *Marine Chemistry* 51:325-346
- Conte MH, Dickey TD, Weber JC, Johnson RJ, Knap AH (2003) Transient physical forcing of pulsed export of bioreactive material to the deep Sargasso Sea. *Deep-Sea Research Part I-Oceanographic Research Papers* 50:1157-1187
- Corbiere A, Metzl N, Reverdin G, Brunet C, Takahashi A (2007) Interannual and decadal variability of the oceanic carbon sink in the North Atlantic subpolar gyre. *Tellus Series B-Chemical and Physical Meteorology* 59:168-178
- Cullen JJ, Lewis MR (1995) Biological processes and optical measurements near the sea surface: Some issues relevant to remote sensing. *Journal of Geophysical Research* 100:13255-13266

- Cullen JJ, Lewis MR, Davis CO, Barber RT (1992) Photosynthetic characteristics and estimated growth rates indicate grazing is the proximate control of primary production in the Equatorial Pacific. *Journal of Geophysical Research* 97:639-654
- D'Alimonte D, Zibordi G (2006) Statistical assessment of radiometric measurements from autonomous systems. *IEEE Transactions on Geoscience and Remote Sensing* 44:719-728
- D'Ortenzio F, Marullo S, Ragni M, Ribera d'Alcala M, Santoleri R (2002) Validation of empirical SeaWiFS algorithms for chlorophyll-a retrieval in the Mediterranean Sea; A case study for oligotrophic seas. *Remote Sensing of Environment* 82:79-94
- D'Ortenzio F, Thierry V, Eldin G, Claustre H, Testor P, Coatanoan C et al. (2010). Oceanic autonomous platforms for biogeochemical studies : instrumentation and measure (PABIM). Available online at [http://projets.ifremer.fr/coriolis/content/download/3150/23513/file/2009\\_PABIM\\_white\\_book\\_version1.3.pdf](http://projets.ifremer.fr/coriolis/content/download/3150/23513/file/2009_PABIM_white_book_version1.3.pdf) (accessed 6 July, 2011)
- Dall'Olmo G, Westberry TK, Behrenfeld MJ, Boss E, Slade WH (2009) Direct contribution of phytoplankton-sized particles to optical backscattering in the open ocean. *Biogeosciences Discuss* 6:291-340
- Davis RF, Moore CC, Zaneveld JRV, and Nap JM (1997) Reducing the effects of fouling on chlorophyll estimates derived from long-term deployments of optical instruments. *Journal of Geophysical Research* 102(C3): 5851-5855
- Dickey T (2003) Emerging ocean observations for interdisciplinary data assimilation systems. *Journal of Marine Systems* 40-41: 5-48
- Doney SC, Lima I, Moore JK, Lindsay K, Behrenfeld MJ, Westberry TK, Mahowald N, Glover DM, Takahashi T (2009) Skill metrics for confronting global upper ocean ecosystem-biogeochemistry models against field and remote sensing data. *Journal of Marine Systems* 76:95-112
- DuRand MD, Olson RJ (1998) Diel patterns in optical properties of the chlorophyte *Nannochloris* sp.: Relating individual-cell to bulk measurements. *Limnology and Oceanography* 43:1107-1118
- Emerson S, Stump C, Johnson B, Karl DM (2002) *In situ* determination of oxygen and nitrogen dynamics in the upper ocean. *Deep-Sea Research Part I-Oceanographic Research Papers* 49:941-952
- Forget G, Ferron B, Mercier H (2008a) Combining Argo profiles with a general circulation model in the North Atlantic. Part 1: Estimation of hydrographic and circulation anomalies from synthetic profiles, over a year. *Ocean Modelling* 20:1-16
- Forget G, Mercier H, Ferron B (2008b) Combining Argo profiles with a general circulation model in the North Atlantic. Part 2: Realistic transports and improved hydrography, between spring 2002 and spring 2003. *Ocean Modelling* 20:17-34
- Freeland H, Roemmich D, Garzoli S, Le Traon P-Y, Ravichandran M et al. (2010) Argo - A Decade of Progress. In: Hall J, Harrison D.E. and Stammer, D (eds) *Proceedings of OceanObs'09: Sustained Ocean Observations and Information for Society*, Vol 2. ESA Publication WPP-306, Venice, Italy
- Gardner WD, Walsh ID, Richardson MJ (1993) Biophysical forcing of particle production and distribution during a spring bloom in the North Atlantic. *Deep Sea Research Part II: Topical Studies in Oceanography* 40:171-195
- Gernez P, Antoine D, Huot Y (2011) Diel cycles of the particulate beam attenuation coefficient under varying trophic conditions in the northwestern Mediterranean Sea: Observations and modeling. *Limnology and Oceanography* 56:17-36
- Gordon HR, Ding KY (1992) Self-shading of in-water optical-instruments. *Limnology and Oceanography* 37:491-500
- Gordon HP, Lewis MR, McLean SD, Twardowski MS, Freeman SA, Voss KJ, and Boynton GC (2009) Spectra of particulate backscattering in natural waters. *Optics Express* 17:16192-16208
- Gregg WW (2008) Assimilation of SeaWiFS ocean chlorophyll data into a three-dimensional global ocean model. *Journal of Marine Systems* 69:205-225
- Gregg WW, Friedrichs MAM, Robinson AR, Rose KA, Schlitzer R, Thompson KR, Doney SC (2009) Skill assessment in ocean biological data assimilation. *Journal of Marine Systems* 76:16-33
- Gruber N, Doney S, Emerson S, Gilbert D, Kobayashi T, Körtzinger A, Johnson G, Johnson K, Riser S, Ulloa O (2007) The Argo-oxygen program: A white paper to promote the addition of oxygen sensors to the international Argo float program. Available online at [http://ioc-unesco.org/index.php?option=com\\_oe&task=viewDocumentRecord&docID=700](http://ioc-unesco.org/index.php?option=com_oe&task=viewDocumentRecord&docID=700) (accessed 6 July, 2011)

- Guay CKH, Bishop JKB (2002) A rapid birefringence method for measuring suspended  $\text{CaCO}_3$  concentrations in seawater. *Deep Sea Research Part I: Oceanographic Research Papers* 49:197-210
- Guinehut S, Coatanoan C, Dhomps AL, Le Traon PY, Larnicol G (2009) On the use of satellite altimeter data in Argo quality control. *Journal of Atmospheric and Oceanic Technology* 26:395-402
- Hooker SB, Zibordi G, Berthon JF, Brown JW (2004) Above-water radiometry in shallow coastal waters. *Appl Optics* 43:4254-4268
- Huot Y, Morel A, Twardowski MS, Stramski D, Reynolds RA (2008) Particle optical backscattering along a chlorophyll gradient in the upper layer of the eastern South Pacific Ocean. *Biogeosciences* 5:495-507
- IOCCG (2000) Remote Sensing of Ocean Colour in Coastal, and Other Optically-Complex, Waters. Sathyendranath S (ed) Reports of the International Ocean-Colour Coordinating Group, N°3, IOCCG, Dartmouth, Canada
- IOCCG (2006) Remote Sensing of Inherent Optical Properties: Fundamentals, Tests of Algorithms, and Applications. Lee Z-P (ed) Reports of the International Ocean-Colour Coordinating Group, N°6, IOCCG, Dartmouth, Canada
- Johnson KS, Berelson WM, Boss ES, Chase Z, Claustre H, Emerson SR, Gruber N, Körtzinger A, Perry MJ, Riser SC (2009) Observing biogeochemical cycles at global scales with profiling floats and gliders: prospects for a global array. *Oceanography* 22:216-225
- Johnson KS, Coletti LJ (2002) *In situ* ultraviolet spectrophotometry for high resolution and long-term monitoring of nitrate, bromide and bisulfide in the Ocean. *Deep-Sea Research I* 49:1291-1305
- Johnson KS, Riser SC, Karl DM (2010) Nitrate supply from deep to near-surface waters of the North Pacific subtropical gyre. *Nature* 465:1062-1065
- Karl D, Laws EA, Morris P, Williams PJI, Emerson S (2003) Metabolic balance of the open sea. *Nature* 426:32
- Kirk JTO (1994) *Light and Photosynthesis in Aquatic Ecosystems*. Cambridge University Press, Second edition
- Körtzinger A, Schimanski J, Send U, Wallace D (2004) The ocean takes a deep breath. *Science* 306(5700):1337
- Kostadinov TS, Siegel DA, Maritorena S (2009) Retrieval of the particle size distribution from satellite ocean color observations. *Journal of Geophysical Research-Oceans* 114: C09015, doi: 10.1029/2009JC005303
- Kostadinov TS, Siegel DA, Maritorena S (2010) Global variability of phytoplankton functional types from space: assessment via the particle size distribution. *Biogeosciences* 7:3239-3257
- Lee T, Lee T, Stammer D, Awaji T, Balmaseda M, Behringer B (2010) Ocean state estimation for climate research. In: Hall J, Harrison D.E. and Stammer, D. (eds) *Proceedings of the "OceanObs'09: Sustained Ocean Observations and Information for Society" Conference, Vol 1*. ESA Publication WPP-306
- Lee ZP, Carder KL, Arnone RA (2002) Deriving inherent optical properties from water color: a multiband quasi-analytical algorithm for optically deep waters. *Applied Optics* 41:5755-5772
- Lequéré C, Harrison SP, Prentice IC, Buitenhuis ET, Aumont O, et al. (2005) Ecosystem dynamics based on plankton functional types for global ocean biogeochemistry models. *Global Change Biology* 11: DOI: 10.1111/j.1365-2486.2005.1004.x
- Loisel H, Bosc E, Stramski D, Oubelkheir K, Deschamps PY (2001) Seasonal variability of the backscattering coefficient in the Mediterranean Sea based on satellite SeaWiFS imagery. *Geophysical Research Letters* 28:4203-4206
- Loisel H, Morel A (1998) Light scattering and chlorophyll concentration in Case 1 waters: A re-examination. *Limnology and Oceanography* 43:847-858
- Loisel H, Nicolas JM, Sciandra A, Stramski D, Poteau A (2006) Spectral dependency of optical backscattering by marine particles from satellite remote sensing of the global ocean. *Journal of Geophysical Research* 111, C09024:doi:10.1029/2005JC003367
- Lynch DR, McGillicuddy DJ, Werner FE (2009) Skill assessment for coupled biological/physical models of marine systems. *Journal of Marine Systems* 76:1-3
- MacCready P, Quay P (2001) Biological export flux in the Southern Ocean estimated from a climatological nitrate budget. *Deep-Sea Research II* 48:4299-4322

- Maffione RA, Dana DR (1997) Instruments and methods for measuring the backward-scattering coefficient of ocean waters. *Applied Optics* 36:6057-6067
- Maritorena S, Siegel DA, Peterson AR (2002) Optimization of a semianalytical ocean color model for global-scale applications. *Applied Optics* 41:2705-2714
- Martz TR, Johnson KS, Riser SC (2008) Ocean metabolism observed with oxygen sensors on profiling floats in the South Pacific. *Limnology and Oceanography* 53:2094-2111
- McClain C, Signorini S, Christian JR (2004) Subtropical gyre variability observed by ocean-color satellites. *Deep Sea Research II* 51:281-301
- McGillicuddy DJ, Johnson R, Siegel DA, Michaels AF, Bates NR, Knap AH (1999) Mesoscale variations of biogeochemical properties in the Sargasso Sea. *Journal of Geophysical Research* 104:13,381-313,394
- McGillicuddy DJ, Robinson AR, Siegel DA, Jannasch HW, Johnson R, Dickey T, McNeil J, Michaels AF, Knap AH (1998) Influence of mesoscale eddies on new production in the Sargasso Sea. *Nature* 394:263-266
- McNeil JD, Jannasch HW, Dickey T, McGillicuddy D, Brzezinski M, Sakamoto CM (1999) New chemical, bio-optical and physical observations of upper ocean response to the passage of a mesoscale eddy off Bermuda. *Journal of Geophysical Research* 104:15,537-15,548
- Metzl N, Corbière A, Reverdin G, Lenton A, Takahashi T, Olsen A, et al. (2010) Recent acceleration of the sea surface  $f\text{CO}_2$  growth rate in the North Atlantic subpolar gyre (1993,2008) revealed by winter observations. *Global Biogeochemical Cycles* 24:GB4004, doi:10.1029/2009GB003658
- Mitchell BG (2003) Resolving spring bloom dynamics in the Sea of Japan. In: Rudnick DL, Perry MJ, (eds) *ALPS: Autonomous and Lagrangian Platforms and Sensors*, Workshop Report, ([http://www.geo-prose.com/ALPS/alps\\_rpt\\_12.16.03.pdf](http://www.geo-prose.com/ALPS/alps_rpt_12.16.03.pdf)), 26-27
- Mobley CD (1994) *Light and Water: Radiative Transfer in Natural Waters*, Academic Press, San Diego, 592 pp
- Morel A (1973) Diffusion de la lumière par les eaux de mer; résultats expérimentaux et approche théorique. In: *AGARD Lect Ser*, 63: 3.1.1.-3.1.76
- Morel A (1988) Optical modeling of the upper ocean in relation to its biogenous matter content (Case 1 waters). *Journal of Geophysical Research* 93:10,749-10,768
- Morel A, Ahn YH (1991) Optics of heterotrophic nanoflagellates and ciliates - a tentative assessment of their scattering role in oceanic waters compared to those of bacterial and algal cells. *Journal of Marine Research* 49:177-202
- Morel A, Antoine D (1994) Heating rate within the upper ocean in relation to its bio-optical state. *Journal of Physical Oceanography* 24:1652-1665
- Morel A, Berthon JF (1989) Surface pigments, algal biomass profiles, and potential production of the euphotic layer: Relationships reinvestigated in view of remote-sensing applications. *Limnology and Oceanography* 34:1545-1562
- Morel A, Claustre H, Antoine D, Gentili B (2007a) Natural variability of bio-optical properties in Case 1 waters: attenuation and reflectance within the visible and near-UV spectral domains, as observed in South Pacific and Mediterranean waters. *Biogeosciences* 4:913-925
- Morel A, Claustre H, Gentili B (2010) The most oligotrophic subtropical zones of the global ocean: similarities and differences in terms of chlorophyll and yellow substance. *Biogeosciences Discussions* 7:5047-5079
- Morel A, Gentili B (2004) Radiation transport within oceanic (Case 1) waters. *Journal of Geophysical Research* 109: doi:10.1029/2003JC002259
- Morel A, Gentili B (2009) A simple band ratio technique to quantify the colored dissolved and detrital organic material from ocean color remotely sensed data. *Remote Sensing of Environment*:doi:101016/j.rse.102009.101001.101008
- Morel A, Gentili B, Claustre H, Babin M, Bricaud A, Ras J, Tieche F (2007b) Optical properties of the "clearest" natural waters. *Limnology and Oceanography* 52:217-229
- Morel A, Maritorena S (2001) Bio-optical properties of oceanic waters: A reappraisal. *Journal of Geophysical Research* 106:7163-7180
- Mueller JL, Austin RW (1992) *Ocean Optics protocols for SeaWiFS validation*. NASA Tech. Memo. 104566, Vol 5. SeaWiFS Tech. Report Series, Goddard Space Flight Center, Greenbelt, Maryland,

45 pp

- Mueller JL, Austin RW (1995) Ocean Optics protocols for SeaWiFS validation. NASA Tech. Memo. 104566, Vol 25. SeaWiFS Tech. Report Series, Goddard Space Flight Center, Greenbelt, Maryland, 67 pp
- Niewiadomska K, Claustre H, Prieur L, d'Ortenzio F (2008) Submesoscale physical-biogeochemical coupling across the Ligurian current (northwestern Mediterranean) using a bio-optical glider. *Limnology and Oceanography* 53:2210-2225
- Pegau WS, Zaneveld JRV, Voss KJ (1995) Toward closure of the inherent optical properties of natural waters. *Journal of Geophysical Research-Oceans* 100:13,193-13,199
- Riser SC, Johnson KS (2008) Net production of oxygen in the subtropical ocean. *Nature* 451:323-325
- Roemmich D, Boebel O, Freeland H, King B, LeTraon P-Y et al. (1999) On the design and Implementation of Argo - An initial plan for a global array of profiling floats. International CLIVAR project Office ICPO Report No21 GODAE Report No 5 Published by the GODAE International Project office, c/o Bureau of Meteorology, Melbourne, Australia, 32pp
- Roemmich D and the Argo Steering Team (2009) Argo: the challenge of continuing 10 years of progress. *Oceanography* 22(3):45-55
- Rossi BB (1957) Optics. Addison-Wesley Publishing Company, Reading, MA, 510 pp.
- Rubin SI (2003) Carbon and nutrient cycling in the upper water column across the Polar Frontal Zone and Antarctic Circumpolar Current along 170°W. *Global Biogeochemical Cycles* 17: 1087, doi:10.1029/2002GB001900
- Sackmann BS, Perry MJ (2008) Seaglider observations of variability in daytime fluorescence quenching of chlorophyll-a in Northeastern Pacific coastal waters. *Biogeosciences Discussions* 5:2839-2865
- Sakamoto CM, Karl DM, Jannasch HW, Bidigare RR, Letelier RM, Walz PM, Ryan JP, Polito PS, Johnson KS (2004) Influence of Rossby waves on nutrient dynamics and the plankton community structure in the North Pacific subtropical gyre. *Journal of Geophysical Research-Oceans* 109: C05032, doi:10.1029/2003JC001976
- Sathyendranath S, Cota GF, Stuart V, Maass H, Platt T (2001) Remote sensing of phytoplankton pigments: a comparison of empirical and theoretical approaches. *International Journal of Remote Sensing* 22:249-273
- Siegel DA, Dickey TD, Washburn L, Hamilton MK, Mitchell BG (1989) Optical determination of particulate abundance and production variations in the oligotrophic ocean. *Deep-Sea Research* 36:211-222
- Siegel DA, Doney SC, Yoder JA (2002a) The North Atlantic spring phytoplankton bloom and Sverdrup's critical depth hypothesis. *Science* 296:730-733
- Siegel DA, Maritorena S, Nelson NB, Hansell DA, and Lorenzi-Kaiser M (2002b) Global distribution and dynamics of colored dissolved and detrital organic materials. *Journal of Geophysical Research* 107(C12): 3228, doi:3210,1029/2001JC000965
- Siegel DA, McGillicuddy DJ, Jr., Fields EA (1999) Mesoscale eddies, satellite altimetry, and new production in the Sargasso Sea. *Journal of Geophysical Research* 104:13,359-313,379
- Stramski D, Boss E, Bogucki D, Voss KJ (2004) The role of seawater constituents in light backscattering in the ocean. *Progress in Oceanography* 61:27-56
- Stramski D, Kiefer DA (1991) Light scattering by microorganisms in the open ocean. *Progress in Oceanography* 28:343-383
- Stramski D, Reynolds RA (1993) Diel variations in the optical properties of a marine diatom. *Limnology and Oceanography* 38:1347-1364
- Stramski D, Reynolds RA, Babin M, Kaczmarek S, Lewis MR, Rottgers R, Sciandra A, Stramska M, Twardowski MS, Franz BA, Claustre H (2008) Relationships between the surface concentration of particulate organic carbon and optical properties in the eastern South Pacific and eastern Atlantic Oceans. *Biogeosciences* 5:171-201
- Stramski D, Reynolds RA, Kahru M, Mitchell BG (1999) Estimation of particulate organic carbon in the ocean from satellite remote sensing. *Science* 285:239-242
- Stramski D, Wozniak SB (2005) On the role of colloidal particles in light scattering in the ocean. *Limnology and Oceanography* 50:1581-1591
- Sverdrup HU (1953) On conditions for the vernal blooming of phytoplankton. *Journal du Conseil*, 18(3): 287-295.

- Talagrand O (1997) Assimilation of observations, an introduction. *Journal of the Meteorological Society of Japan* 75:191-209
- Testor P, Meyers G, Pattiaratchi C, Bachmayer R, Hayes et al. (2010) Gliders as a component of future observing systems. In: Hall J, Harrison D.E. and Stammer, D. (eds) Proceedings of the "OceanObs'09: Sustained Ocean Observations and Information for Society" Conference Venice, Italy, 21-25 September 2009, Vol 2. ESA Publication WPP-306
- Tjiputra JF, Polzin D, Winguth AME (2007) Assimilation of seasonal chlorophyll and nutrient data into an adjoint three-dimensional ocean carbon cycle model: Sensitivity analysis and ecosystem parameter optimization. *Global Biogeochemical Cycles* 21: GB1001, doi:10.1029/2006GB002745
- Twardowski MS, Claustre H, Freeman SA, Stramski D, Huot Y (2007) Optical backscattering properties of the 'clearest' natural waters. *Biogeosciences* 4:1041-1058
- Uitz J, Claustre H, Morel A, Hooker S (2006) Vertical distribution of phytoplankton communities in open ocean: an assessment based on surface chlorophyll. *Journal of Geophysical Research* 111:doi:10.1029/2005JC003207
- Uz BM, Yoder JA (2004) High frequency and mesoscale variability in SeaWiFS chlorophyll imagery and its relation to other remotely sensed oceanographic variables. *Deep-Sea Research Part II* 51:1001-1017
- Walsh ID, Chung SP, Richardson MJ, Gardner WD (1995) The diel cycle in the integrated particle load in the Equatorial Pacific: A comparison with primary production. *Deep-Sea Research* 42:465-477
- Werdell PJ, Bailey SW (2005) An improved *in-situ* bio-optical data set for ocean color algorithm development and satellite data product validation. *Remote Sensing of Environment* 98:122-140
- Westberry T, Behrenfeld MJ, Siegel DA, Boss E (2008) Carbon-based primary productivity modeling with vertically resolved photoacclimation. *Global Biogeochemical Cycles* 22: GB2024, doi:10.1029/2007GB003078
- White AE, Spitz YH, Letelier RM (2007) What factors are driving summer phytoplankton blooms in the North Pacific Subtropical Gyre? *Journal of Geophysical Research-Oceans* 112: C12006, doi:10.1029/2007JC004129
- Whitmire AL, Letelier RM, Villagrán V, Ulloa O (2009) Autonomous observations of *in vivo* fluorescence and particle backscattering in an oceanic oxygen minimum zone. *Optics Express* 17(24):21,992-22,004
- Whitmire AL, Pegau WS, Karp-Boss L, Boss E, Cowles TJ (2010) Spectral backscattering properties of marine phytoplankton cultures. *Optics Express* 18:15,073-15,093
- Wong CS, Whitney FA, Matear RJ, Iseki K (1998) Enhancement of new production in the northeast subarctic Pacific Ocean during negative North Pacific index events. *Limnology and Oceanography* 43:1418-1426
- Wunsch C (1996) *The Ocean Circulation and Inverse Problem*, Cambridge University Press, 442 p
- Xing X, Morel A, Claustre H, Antoine D, D'Ortenzio F, Poteau A, Mignot A (2011) Combined processing and mutual interpretation of radiometry and fluorimetry from autonomous profiling Bio-Argo Floats: I. Chlorophyll a retrieval. *Journal of Geophysical Research* 116: C06020, doi:10.1029/2010JC006899
- Xing X, Morel A, Claustre H, D'Ortenzio F, Poteau A (submitted) Combined processing and mutual interpretation of radiometry and fluorimetry from autonomous profiling Bio-Argo floats: II. CDOM retrieval. *Journal of Geophysical Research*
- Zibordi G, D'Alimonte D, Berthon JF (2004) An evaluation of depth resolution requirements for optical profiling in coastal waters. *Journal of Atmospheric and Oceanic Technology* 21:1059-1073
- Zibordi G, Ferrari GM (1995) Instruments self-shading in underwater optical measurements - experimental data. I. *Applied Optics* 34:2750-2754